PRODUCTION OF RECOMBINANT ANTIBODY FRAGMENTS IN BACTERIA AND THEIR DEVELOPMENT TOWARDS MEDICAL DIAGNOSIS

REKOMBİNANT ANTİKOR FRAGMANLARININ BAKTERİLERDE ÜRETİMİ VE TIBBİ TANIYA YÖNELİK GELİŞTİRİLMESİ

İLKAY KOÇER KULOĞLU

ASSOC. PROF. DR. EDA ÇELİK AKDUR

Supervisor

PROF. DR. MATTHEW P. DELISA

Co-Supervisor

Submitted to
Graduate School of Science and Engineering of Hacettepe University
as a Partial Fulfillment to the Requirements
for the Award of the Degree of Doctor of Philosophy
in Chemical Engineering.

2021

To my family…

ABSTRACT

PRODUCTION OF RECOMBINANT ANTIBODY FRAGMENTS IN BACTERIA AND THEIR DEVELOPMENT TOWARDS MEDICAL DIAGNOSIS

İlkay KOÇER KULOĞLU

Doctor of Philosophy, Department of Chemical Engineering

Supervisor: Assoc. Prof. Dr. Eda ÇELİK AKDUR

Co-Supervisor: Prof. Dr. Matthew P. DELISA

August 2021, 159 pages

Antibodies and antibody derivatives have been widely used in diagnostic and therapeutic applications as well as in biotechnological research tools. Since their application in these areas requires for their production with a high yield, recombinant protein technology has been used to meet the increasing demand in the global market and to reduce production costs. Single-chain variable fragment (scFv), which is one of the most widely used recombinant antibody fragments, is formed by linking heavy and light units of variable domains with a flexible linker peptide. Successful construction of scFvs is based on composition, length and flexibility of linker peptides in addition to variable domain order.

In this thesis, the production of model scFvs, that are highly soluble, active and correctly folded in *Escherichia coli* was proposed and the effects of linker peptides to properties of scFvs towards immobilization for diagnostic applications were investigated. For this purpose, anti-HER2 scFv against human epidermal growth

receptor 2 (HER2) and scFv13R4 against β-galactosidase were selected as model antibody fragments. Firstly, scFv version of the full-length antibody targeting HER2 glycoprotein, which overexpresses in breast cancer patients, was constructed via splicing by overlap extension polymerase chain reaction (SOE-PCR). Anti-HER2 scFv was expressed in the cytoplasm of *E. coli* strains BL21(DE3) and SHuffle T7 Express cells, the latter of which has more oxidizing conditions for disulfide bond formation, to determine the suitable strain for functional production of the scFv. Evaluation of the host strains revealed significantly higher solubility and up to four-fold higher antigen-binding activity of anti-HER2 scFv expressed in SHuffle T7 Express versus BL21(DE3). Hence, subsequent productions of scFvs were performed in SHuffle T7 Express. Thereafter, anti-HER2 scFvs were designed in two different domain orientations, which were V_H-linker-V_L or V_L-linker-V_H, to determine the optimum domain orientation for this scFv. They were expressed in SHuffle cells to compare their properties in terms of solubility, monomer/dimer formation, binding activity and affinity. Soluble production was characterized by Western blot analysis, and *in vitro* immunological characterization of anti-HER2-scFv was performed with enzyme-linked immunosorbent assay (ELISA) and surface plasmon resonance (SPR). Consequently, domain orientation of anti-HER2 scFv was investigated for the first time, and each scFv showed high binding activity and selectivity against HER2, regardless of the variable domain orientation. In addition, effects of bioprocess operation parameters such as induction temperature, inducer concentration, duration of induction and medium composition on expression of scFvs were investigated. It was found that IPTG concentration did not significantly affect the anti-HER2 scFv expression, higher amount of soluble anti-HER2 scFvs were observed between 16-20 h after induction and ratio of soluble expression increased at temperatures lower than 30°C. Overexpression of anti-HER2 scFv was also observed when produced in chemically defined minimal medium in SHuffle cells. In the second part of the study, anti-HER2 scFv in V_L-linker-V_H orientation was used, owing to its relatively higher expression. ScFvs were re-designed by adding linkers with different amino acid composition, towards immobilization onto polystyrene (PS) surfaces and characteristics of the new scFvs were investigated. Direct, indirect and

sandwich ELISA was performed for determination of immobilization, antigen-binding properties and detection of HER2, respectively. It was observed that the immobilization activities of scFvs with different linkers changed in relation to PS plate type, and absence or presence of Tween 20 in coating buffer. Additionally, the same linkers were cloned into the other model antibody fragment, scFv13R4, to investigate the versatility of the effects of linkers and similar results were observed. Lastly, *in silico* analysis was performed to observe the effect of linkers on stability and functionality of anti-HER2 scFvs with homology modelling and molecular dynamics (MD) simulation. Based on the experimental results and MD simulations, one of the designed linkers was found to be an appropriate substitution for the standard linker within the scFvs for immunoassay applications. Overall, the model scFvs constructed in this study hold great potential as biorecognition elements in immunoassays or diagnostic tools owing to their highly soluble expression and biologically active forms with nM range dissociation constants (K_d).

Keywords: recombinant antibody, scFv, *Escherichia coli*, V_L/V_H, linker peptide, immobilization, *in silico*.

ÖZET

REKOMBİNANT ANTİKOR FRAGMANLARININ BAKTERİLERDE ÜRETİMİ VE TIBBİ TANIYA YÖNELİK GELİŞTİRİLMESİ

İlkay KOÇER KULOĞLU

Doktora, Kimya Mühendisliği Bölümü

Tez Danışmanı: Doç. Dr. Eda ÇELİK AKDUR

Eş Danışman: Prof. Dr. Matthew P. DELISA

Ağustos 2021, 159 sayfa

Antikorlar ve antikor türevleri, teşhis ve tedavi edici uygulamalar ile biyoteknolojik araştırmalarda geniş bir kullanım alanına sahiptir. Bu alanlardaki uygulamaları yüksek verimle üretimlerini gerektirmesinden dolayı, antikorların küresel pazarda artan taleplerini karşılamak ve üretim maliyetlerini azaltmak için rekombinant protein teknolojisi kullanılmaktadır. En yaygın olarak kullanılan rekombinant antikor fragmanlarından biri olan tek zincirli değişken fragman (scFv), ağır ve hafif değişken bölgelerin esnek bir bağlayıcı peptit ile bağlanmasıyla oluşturulur. Scfv yapılarının özellikleri, değişken bölgelerin bağlanma sırası ile bağlayıcı peptitlerin içeriğine, uzunluğuna ve esnekliğine bağlı olarak değişmektedir.

Bu tez çalışmasında, çözünür, aktif ve doğru katlanmış scFv'lerin *Escherichia coli* bakterisinde üretimleri önerilmiş, bağlayıcı peptitlerin scFv'lerin diagnostik uygulamalarda immobilizasyonuna yönelik etkileri araştırılmıştır. Bu amaçla, insan epidermal büyüme reseptörü 2 (HER2)'ye karşı anti-HER2 scFv ve β-galaktosidaza

karşı scFv13R4, model antikor fragmanları olarak seçilmiştir. İlk olarak, meme kanseri hastalarında normalden fazla üretilen HER2 glikoproteinini hedefleyen tam uzunluktaki antikorun scFv versiyonu, örtüşme uzantısı ile ekleme polimeraz zincir reaksiyonu (SOE-PCR) ile oluşturulmuştur. Anti-HER2 scFv, fonksiyonel üretimi için uygun hücrenin belirlenebilmesi amacıyla *E. coli* BL21(DE3) ve disülfid bağı oluşumu için sitoplazmasında daha fazla oksitleyici koşullara sahip *E. coli* SHuffle T7 Express hücrelerinin sitoplazmalarında üretilmiştir. Hücrelerin karşılaştırılması, BL21(DE3)'e karşı SHuffle T7 Express'te üretilen anti-HER scFv'nin önemli ölçüde daha yüksek çözünürlük ve dört kata kadar daha yüksek antijen bağlama aktivitesi ile sonuçlanmıştır. Bu nedenle, scFv'lerin ilerleyen çalışmalardaki üretimleri SHuffle T7 Express ile gerçekleştirilmiştir. Daha sonra anti-HER2 scFv, özellikleri açısından en uygun bağlanma sırasının belirlenebilmesi için V_H-bağlayıcı-V_L ve V_L-bağlayıcı-V_H olarak tasarlanmıştır. Çözünürlük, monomer/dimer oluşumu, bağlanma aktivitesi ve afinite özelliklerinin karşılaştırılması amacı ile SHuffle hücrelerinde üretilmiştir. Çözünür üretimleri Western blot analizi ile karakterize edilirken, anti-HER2 scFv'nin *in vitro* immünolojik karakterizasyonu enzim bağlı immünosorbent analizi (ELISA) ve yüzey plazmon rezonans (SPR) analizi ile yapılmıştır. Sonuç olarak, anti-HER2 scFv'nin oluşturulmasında değişken alanların bağlanma sırası ilk defa bu çalışma ile araştırılmış; anti-HER2 scFv, değişken alanların bağlanma sırasından bağımsız olarak, her iki yapıda da HER2'ye karşı yüksek bağlanma aktivitesi ve seçicilik göstermiştir. Ayrıca, indükleme sıcaklığı, indükleyici (IPTG) derişimi, indükleme süresi ve ortam bileşimi gibi biyoproses işletim koşullarının scFv üretimine etkileri de araştırılmıştır. IPTG derişiminin anti-HER2 scFv üretimini önemli ölçüde etkilemediği, indükleme sonrası 16-20 sa aralığında daha yüksek miktarda çözünür scFv üretildiği ve 30°C'den düşük sıcaklıklarda çözünür protein oranının arttığı sonucuna varılmıştır. SHuffle hücrelerinde kimyasal olarak tanımlanmış minimal ortamda da anti-HER2 scFv üretimi gözlenmiştir. Çalışmanın ikinci bölümünde, daha yüksek protein üretimi sebebiyle V_L-bağlayıcı-V_H yapısında anti-HER2 scFv kullanılmıştır. ScFv'ler polistiren (PS) yüzeylere immobilizasyona yönelik farklı amino asit bileşimine sahip bağlayıcılar ile yeniden tasarlanmış ve yeni scFv'lerin özellikleri incelenmiştir. İmmobilizasyonun, antijene bağlanma özelliklerinin ve

HER2'nin tespit edilebilirliğinin belirlenmesi için sırasıyla direkt, indirekt ve sandviç ELISA yöntemleri uygulanmıştır. Farklı bağlayıcılara sahip scFv'lerin immobilizasyon aktivitelerinin PS plaka tipine ve scFv kaplama çözeltisinin Tween 20 içerip içermemesine bağlı olarak değiştiği gözlenmiştir. Ayrıca, bağlayıcıların başka scFv'lerde etkisini anlamak için aynı bağlayıcılar bir diğer model antikor fragmanı scFv13R4 yapısına da eklenmiş ve benzer sonuçlar elde edilmiştir. Son olarak, bağlayıcı peptitlerin anti-HER2 scFv'lerin stabilitesi ve işlevselliği üzerindeki etkilerini gözlemlemek için homoloji modelleme ve moleküler dinamik (MD) simülasyonu yöntemleri ile *in silico* analiz yapılmıştır. Deneysel sonuçlar ve MD simülasyonlarına dayanarak, tasarlanan bağlayıcılardan birinin immünoanaliz uygulamaları için standart bağlayıcıya uygun bir alternatif olabileceği sonucuna varılmıştır. Genel olarak, bu çalışmada oluşturulan model scFv'ler çözünebilir ve biyolojik olarak aktif üretilebilmeleri ile nM düzeyde ayrışma sabitlerine (K_d) sahip olmaları nedeniyle, immünoanalizlerde veya tanı araçlarında biyolojik tanıma elemanları olarak kullanım potansiyeline sahiptir.

Anahtar Kelimeler: rekombinant antikor, scFv, *Escherichia coli*, V_L/V_H, bağlayıcı peptit, immobilizasyon, *in silico*.

ACKNOWLEDGEMENTS

I would like to express my sincere gratitude and special thanks to my supervisor Assoc. Prof. Dr. Eda Çelik Akdur for her guidance, valuable support and motivation throughout all my graduate journey. She always encouraged me to carry out my PhD studies successfully.

I would like to specially thank my co-supervisor Prof. Dr. Matthew P. DeLisa giving me the opportunity to work as a fellow PhD student in his laboratory in Cornell University for a year, and sharing his invaluable time and supporting me all the time. I have learned a lot in his group.

I am also thankful to Prof. Dr. Ali Tuncel and Prof. Dr. Pınar Çalık for accepting to be a member of my progress jury and for all their enlightening comments and directions.

I sincerely acknowledge The Scientific and Technological Research Council of Turkey (TÜBİTAK) for the national and international scholarships (TÜBİTAK-BİDEB; 2211-A and 2214-A) which encouraged me and provided financial support during my PhD studies. I sincerely acknowledge Hacettepe University Scientific Research Projects Coordination Unit (BAP-FBA-2021-18857) which supported a part of my thesis study.

I would like to sincerely thank my lab mates, Emine Altun, Dilek Şahinbaş, Selen Cilasun, Dr. Murat Akdoğan, Batuhan Doğan and Khaliunsarnai Tsogtbaatar for supporting me with a nice working environment and their great friendship. Special thanks to my Cornell friends: Tommy, May, Emily, Ty, Xiaolu, Sean and Kevin for their valuable support, hospitality and not making me feel alone abroad.

I am grateful to Dr. Özge Yüksel Orhan, Dr. Gökçe Dicle Kalaycıoğlu, Dr. Hande Günan Yücel, Dr. Yasemin Günaydın, Dr. Hande Ünsal Hunter, Dr. Gökçe Alp, Dr. Özlem Hamaloğlu, Dr. Çiğdem Kip, Dr. Aslıhan Gökaltun and Neslişah Cihan for always being with me and their friendship.

I would like to thank to all academic, administrative and technical staff of Hacettepe University, Department of Chemical Engineering, for their help and support throughout my education. I would like to express my thanks to Assoc. Prof. Dr. Emre Taşcı for his help on computational studies.

I would like to deeply thank to my whole family for loving, supporting and encouraging me all through my life. I would like to thank my husband Eray Kuloğlu for his patience at all times, continuing support and his great encouragement.

TABLE OF CONTENTS

LIST OF TABLES

LIST OF FIGURES

SYMBOLS AND ABBREVIATIONS

Symbols

K_d	Equilibrium dissociation constant
K_a	Affinity constant
k_a	Association constant
k_d	Dissociation constant

Abbreviations

Amp	Ampicillin
β-gal	β-galactosidase
Bp	Base pair
BSA	Bovine serum albumin
CIAP	Calf intestinal alkaline phosphate
dH_2O	Distilled water
DNA	Deoxyribonucleic acid
EB	Elution Buffer
EDTA	Ethylenediaminetetraacetic acid
ELISA	Enzyme linked immunosorbent assay
Escherichia coli	*E. coli*
Fab	Antigen binding region
Fc	Crystallizable region
HER2	Human epidermal growth receptor 2
HRP	Horseradish peroxidase
IB	Inclusion body
IgG	Immunoglobulin G
IPTG	Isopropyl β-D-1-thiogalactopyranoside
Kan	Kanamycin

Kb	Kilo base
LB-Broth	Luria Bertani broth
mAb	Monoclonal antibody
MD	Molecular dynamics
OD	Optical density
PBS	Phosphate buffer saline
PCR	Polymerase chain reaction
PolySia	Polysialic acid
PS	Polystyrene
Rg	Radius of gyration
RMSD	Root mean square deviation
RMSF	Root mean square fluctuation
RT	Room temperature
SASA	Solvent accessible surface area
ScFv	Single-chain variable fragment
SDS-PAGE	Sodium dodecyl sulfate-polyacrylamide gel electrophoresis
SOB	Super optimal broth
Spec	Spectinomycin
SPR	Surface plasmon resonance
SD	Standard deviation
TB	Terrific broth
TBE	Tris Borate EDTA
TBS	Tris buffer saline

1. INTRODUCTION

Since the first recombinant antibody (Orthoclone OKT3) was launched to the market in 1986, antibody and antibody derivatives have become the largest market of biopharmaceuticals owing to their flexibility, specificity and diversity characteristics [1]. Until December 2019, 79 antibodies have been marketed or approved by the US Food and Drug Administration (FDA). It is predicted that the annual global sales of monoclonal antibodies in 2020 will be over 125 billion USD and this value will reach 138.6 billion USD in 2024, thus having a significant growth potential [1, 2].

An IgG molecule, the predominant serum antibody, consists of two light and two heavy chains, which are held together by disulfide bonds. Each IgG molecule is composed of three domains that form a Y-shaped structure: two antigen-binding fragments (Fab) and one fragment crystallizable (Fc). Antibodies can be produced in polyclonal, monoclonal and recombinant forms. Polyclonal antibodies that recognize different epitopes on the single antigen are composed of antibodies produced by different B cells. Monoclonal antibodies (mAb) are molecules synthesized from a single B cell clone that can specifically bind to a particular region of the antigen [3]. In addition to full-length antibodies, native antibody fragments can be isolated or new antibody derivatives which are classified as recombinant antibody fragments could be engineered. Single-chain variable fragments (scFvs), which are one of the most frequently used type of recombinant antibodies, are formed by linking heavy (V_H) and light (V_L) units of variable domains with a flexible linker peptide, varying from 10 to 25 amino acids in length [4]. The length and composition of the linkers as well as orientation of V_H and V_L regions could influence thermostability, production efficiency and antigen-binding affinity of scFvs [5, 6].

Antibodies and antibody fragments are extensively used in therapeutic, medical diagnostic and biotechnological research applications. Because of the high demand for antibodies in many of these tools, there has been an increasing interest in studies on the development of bioprocesses to meet the growing need in the global market and reduce production costs [7]. The scFv is an active component of the whole antibody which could maintain comparable specificity and affinity to a target antigen [8]. Therefore, scFv antibodies could be used as a substitute for whole antibodies. Compared with the conventional antibodies, the scFv antibody: (i) can be produced in microbial systems with lower costs owing to its smaller size (ii) can be engineered to enhance selectivity and affinity, and (iii) shows better tumor penetration [9].

In literature, there are numerous studies on the production and development of scFv molecules using microbial systems [10]. *Escherichia coli* is one of the most preferred microorganisms for expression of recombinant proteins with regard to its fast growth, lower production costs, well understood genetic structure and ease of genetic manipulation [11]. However, soluble expression of scFvs in *E. coli* could be difficult because of the two intrachain disulfide bonds, which need oxidizing environment for formation. ScFvs are secreted to the periplasmic or extracellular compartments of *E. coli,* which have an oxidizing environment; however, periplasmic expression can limit the expression yield due to its low capacity [12-14]. Although the cytoplasm has larger space, reducing conditions cause misfolding and aggregation due to hindrance of disulfide bond formation and extra protein recovery methods are required for misfolded proteins expressed in the cytoplasm. Thus, current investigations are mainly focused on soluble production of scFvs with high yields in *E. coli* [15-17].

The principle of the immunosensors is based on the specific recognition of the antigen/antibodies in the analyte by the immobilized antibody/antigens to the sensor surface and the generation of signals depending on the concentration of the analyte. While antibodies are considered to be excellent probes in biosensor applications owing to their high specificity and affinity toward their targets, using these molecules can cause some problems such as difficulties in oriented immobilization and loss of specificity. Hence, protein and genetic engineering techniques allow the use of small antibody formats to eliminate these problems. ScFv antibodies have much potential to be used as biorecognition elements in various types of biosensors, optical biosensors and immunological assays due to their production and modification easily, lower molecular weight and high customizability with a wide variety of immobilization techniques [18].

Several approaches have been used for engineering scFvs during their production to immobilize them to a solid surface without denaturation. For example, the scFv linker peptides may be designed to have the metal binding cysteine (Cys) or histidine (His) amino acids in the sequence for the attachment on gold sensor surfaces, with enhanced orientation, or linkers may contain positively charged amino acids for immobilization to negatively charged surfaces via electrostatic and non-covalent interactions [19]. Additionally, material-binding peptides that have the ability of specifically recognizing the target materials such as hydrophilic polystyrene [20], silicon [21] and gold surfaces [22] were developed to increase the oriented immobilization. However, there is no study about the effects of these peptides on scFvs immobilization, when included within the linker region, which is usually 15 amino acids long.

Successful construction of scFvs is based on composition, length and flexibility of linker peptides, which can influence stability and structure as well as antigen-binding activities and expression levels of scFvs. Therefore, selecting a functional linker among various linkers is one of the crucial steps for designing an optimal scFv [23, 24]. On the other hand, computational approaches could offer molecular insight without experimental studies. *In silico* studies including molecular docking and molecular dynamics (MD) simulation are important tools to understand structure-function relationships of the protein-ligand, protein-surface and protein-protein complexes [25].

In this thesis study, the production of model scFvs with soluble, active and correctly folded properties in *E. coli*, and engineering the linker region of antibody fragments to attain well-oriented immobilization to polystyrene surfaces was proposed. Anti-HER2 scFv against human epidermal growth receptor 2 (HER2) and scFv13R4 against β-galactosidase [26] was selected as model antibody fragments. Since scFv13R4 was mutated to be produced folded and functional in the cytoplasm in a previous study [27], it was used in linker engineering part of the study. In the first part, scFv version of the full-length antibody of Herceptin [28] targeting HER2 glycoprotein, which overexpresses in breast cancer patients, was constructed via splicing by overlap extension (SOE) polymerase chain reaction. For selection of the appropriate strain, anti-HER2 scFv was expressed in cytoplasm of *E.coli* BL21(DE3) and SHuffle T7 Express cells, the latter of which has more oxidizing conditions. Anti-HER2 scFvs were designed in two different domain orientations, which were V_H-linker-V_L or V_L-linker-V_H. Considering the results obtained from other studies, the effects of variable domain orientation were compared in terms of solubility, monomer/dimer formation, binding activity and affinity. In addition, the effects of bioprocess parameters such as induction temperature, inducer concentration, duration of induction and medium composition on expression of scFvs were investigated. Soluble production was shown using SDS-PAGE and Western blot; *in vitro* immunological characterization of anti-HER2-scFv was performed with enzyme-linked immunosorbent assay (ELISA) and surface plasmon resonance (SPR). In the second part of the study, anti-HER2 scFvs were developed by adding linkers with different amino acid composition towards immobilization onto polystyrene (PS) surfaces and characteristics of the new scFvs were investigated. Direct, indirect and sandwich ELISA were performed for determination of immobilization, antigen-binding activity/affinity, and HER2 detection attached on the PS surface, respectively. Additionally, the same linkers were added in to the other model antibody fragment, scFv13R4, to investigate the versatility of the effects of linkers. Lastly, the effect of linkers on stability and functionality of anti-HER2 scFvs were analyzed with homology modelling and MD simulation methods via GROMACS [29]. Overall, the model scFvs constructed in this study hold great potential as biorecognition elements in immunoassays or diagnostic tools owing to their highly soluble expression and biologically active forms.

2. LITERATURE SURVEY

2.1. Antibody and Antibody Fragments

Antibodies (immunoglobulins) are one of the glycoprotein structures of the immune system with their high affinity and specific recognition capacity towards antigens. Immunoglobulins are divided into five classes by their heavy chains (IgA, IgG, IgM, IgD and IgE) and IgG is the predominant class in the blood.

A full-legth IgG antibody molecule consists of two heavy (H) chains with 50 kDa and two light (L) chains with 25 kDa molecular weight, and these chains which have constant (C) and variable (V) regions are held together by disulfide bonds (Figure 2.1). Whereas the H chain contains three constant regions (C_{H1}, C_{H2} and C_{H3}) and one variable region (V_H), the L chain has one constant region (C_L) and one variable region (V_L) [30].

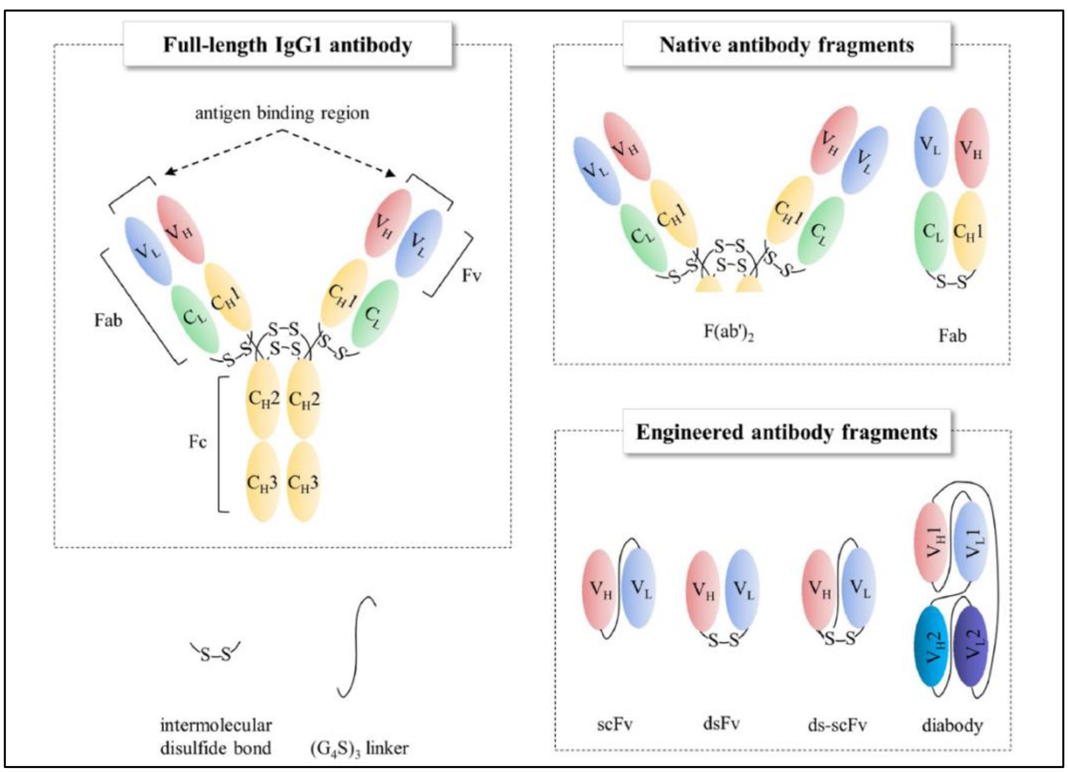

Figure 2.1. Representative structure of antibody and antibody fragments [31]

IgG antibody is composed of two main functional parts, the fragment crystallizable (Fc) and the antigen-binding fragment (Fab). The Fab region consists of the V and C regions of the heavy (V_H and C_{H1}) and light (V_L and C_L) chains. Two Fab domains having identical antigen-binding sites for a target antigen are connected to the Fc at the hinge region, which provides a high degree of flexibility for Fabs compared to Fc (Figure 2.1). While the Fc region composed of C domains of two heavy chains binds to various effector molecules and cells for activation of the immune system, variable regions (F_v) play role in antigen binding [32]. Wu and Kabat reported that six loop regions, three from L and three from H variable domains, are responsible for specifically recognizing and binding to its antigen by forming a unique surface and they called them as "complementarity determining regions (CDRs)" [33]. It was reported that constant domains of antibody exhibit only small changes in sequence when examined in the different antibody classes, while the CDRs show a high degree of sequence variability [34].

In addition to Fabs, smaller antibody fragments such as the single-chain variable fragments (scFv), diabodies, single-domain antibodies and disulfide-stabilized Fv (dsFv) can be generated from antibodies using antibody engineering and molecular cloning techniques. These antibody fragments can also be modified to bispecific, multi-specific, multimeric or multifunctional forms by linking them to other molecules or fragments [35].

Antibodies and antibody fragments, which have the largest market among pharmaceutical proteins, are the most valuable proteins that can be used as a therapeutic, for medical diagnosis and biological research (immunoblotting, flow cytometry, etc.) tools [1]. Since the first recombinant antibody (Orthoclone OKT3) was launched to the market in 1986, 79 monoclonal antibodies (mAb) or antibody fragments have been approved by the US FDA and more than 570 therapeutic monoclonal antibodies have been used in clinical studies around the world [36]. Until March 2020, eight antibody fragments were approved as drugs by the US FDA. Six of them including blinatumomab, ranibizumab, caplacizumab, certolizumab pegol, moxetumomab pasudotox and brolucizumab were obtained from *Escherichia coli,* whereas abciximab and idarucizumab were produced by mammalian hosts, based on the data reported by “The Antibody Society” [37].

2.1.1. Monoclonal Antibodies

Antibodies are classified into three primary groups based on production technology: polyclonal antibodies, monoclonal antibodies and recombinant antibodies. Polyclonal antibodies are characterized by a heterogeneous mixture of immunoglobulin molecules secreted by different B-cell lineages and recognize multiple epitopes on the same antigen. These types of antibodies are produced by injecting the antigen of interest into an animal to obtain high levels of antibodies and then antibodies are harvested through blood draws. The polyclonal antibodies can be used directly in serum, which are separated from leukocytes and erythrocytes, or antibodies can be purified from the serum using affinity column chromatography methods [38]. Monoclonal antibodies are produced using hybridoma technology, which was invented in 1975 by Georges Kohler and Cesar Milstein [39]. In this technology, a myeloma cell becomes drug-sensitive by mutation of hypoxanthine guanine phosphoribosyl transferase (HGPRT) gene. Then, it is chemically fused with B-cells from an animal exposed to the antigen of interest and fused cells are incubated in a medium having the selective drug. Consequently, only the fused cells which have functional HGPRT gene obtained from B-cells survive, because unfused B-cells having short life span and unfused myeloma cells which lack HGPR die off. Thus, fused cells are immortal and carry the antibody gene of B-cells and this brings growing continuously and producing antibody. Since resulting antibodies are secreted by the same B-cells, they bind to a single epitope of the antigen [40].

The technology used for monoclonal antibodies have several advantages over the polyclonal antibodies: (i) the hybridoma technology provides an endless supply for production of antibody owing to immortality of the hybridoma cell lines; (ii) generation of monoclonal antibodies becomes simple and effective after the hybridoma clones are established; (iii) since the target antibody is principally detected based on the selection strategy, impurity of the antigen can be tolerated; (iv) antibodies having selective properties for specific structures could be produced [41, 42].

2.1.2. Recombinant Antibody Technology

Although monoclonal antibodies produced by hybridoma technology have been widely utilized as diagnostic and therapeutic agents, the emergence of recombinant antibody technology and studies towards understanding of structure and action of antibodies have paved the way for developments in novel production strategies of antibodies. Antibody fragments which retain their specificity and stability could be produced via recombinant antibody technology.

Fab fragments that were only obtained by proteolytic cleavage of the antibody using enzymes such as papain and pepsin in the past could also be produced by recombinant synthesis [34]. In the late 1980s, Pluckthun and Skerra showed that correctly folded antibody fragments could be produced by using vectors in bacterial systems [43]. Afterwards, recombinant antibody fragments have been generated in various host systems including mammalian [44], plant [45], insect [46], yeast [47] cells and cell-free systems [48].

The Fv fragment contains variable domains of H and L chains linked via a disulfide bond. A flexible linker peptide is introduced into the Fv fragment to overcome stability issues and this structure is named as a single-chain Fv or scFv. Single-chain antibody fragment (scAb) can be generated by incorporating a light chain constant domain into an scFv [49]. Diabody is formed from the V_H and V_L domains of two scFvs as two polypeptide chains. These domains are linked by a short glycine-rich linker to lead intrachain dimerization of the two chains. Single-domain antibodies, which are another type of antibody fragment, are unpaired variable domains (V_L or V_H). These domains that are easy to engineer maintain the antigen binding specificities of a full-length antibody [50].

2.2. Single-chain Variable Fragments (scFvs)

The scFv antibody was developed recombinantly for the first time in 1988 by Huston et al. [51] and Bird et al. [4] independently from each other, and contains the functional V_H - V_L regions required for high affinity binding against the target antigen. These fragments with a molecular weight of about 28 kDa are formed by linking V_H and V_L units with a flexible linker peptide (10-25 amino acids) and can be produced synthetically by genetic engineering techniques with only suitable vector and host cell combinations.

The most frequently used linkers for the production of scFvs are composed of repeats of glycine and serine stretches of 15 or 20 aa having sequences of $(GGGGS)_3$ or $(GGGGS)_4$, respectively. Besides minimization of oligomerization, these linkers are also crucial for correct folding of protein structure and the antigen binding site formation [51, 52]. It has been estimated that the distance between C-terminus (carboxyl terminus) of one V domain and N-terminus (amino terminus) of the other V domain must be at least 3.5 nm to form an antigen binding site [51]. Furthermore, studies have shown that length of the linker have an effect on the oligomeric state of scFvs. Linker chains greater than 15 amino acids tend to generate scFvs in monomeric behaviour. While linkers of 6-15 residues results in the formation of dimeric or trimeric structures, higher order multimeric molecules are produced with linker chains less than five residues [8, 53]. Linkers less than 15 residues hinder the correct rotation and pairing of complimentary V domains and this effects the formation of the proper interface. As a result of this configuration, variable domains of two, three or four scFvs swap with intermolecular association and diabodies, triabodies or tetrabodies are formed, respectively [54].

The length and amino acid composition of the linker that offer optimum thermostability and affinity for the target antigen can show differences among scFvs. The order of V_L and V_H domains with the same linker can also have an effect on expression efficiency, stability and monomer/dimer formation of scFvs. Linker sequences could be engineered to improve functionalities of scFvs, when the produced scFvs show low affinity or poor stability compared to the parental antibody [6]. In literature, there are some studies investigating linkers with regard to their length and sequences to improve the solubility and activity of scFvs [55, 56]. Furthermore, the binding order of V_L and V_H domains to construct the scFvs show differences throughout the literature. Whereas V_L-linker-V_H orientation showed favorable biophysical properties in one study [57], another study reported that the V_H-linker-V_L was more favorable in terms of characteristics of scFvs [58]. It was also reported that the two orientations showed the same binding activities [59]. Therefore, it could be concluded that there is no common rule for the construction of scFv structure which gives the optimum expression level, stability and activity. Each scFv requires to be investigated individually to determine the optimum format for expression.

2.2.1. Expression of ScFvs

Type of antibody fragments, the size and sequence of protein, occurrence of post-translational modifications and the number of disulfide bonds have an effect on the expression of antibodies. Recombinant antibody fragments are mostly composed of antigen binding unit of full-IgG structure and this unit is influenced by the conformational changes and selected expression conditions may cause aggregation of the produced antibodies, which renders them inappropriate for applications [60]. Thus, determination of optimum functional expression conditions is important for the applications of antibodies.

Conventional IgGs are mostly expressed in mammalian cell lines including human embryonic kidney (HEK), Chinese hamster ovary (CHO) cells since CH_2 domain of full-length antibodies comprises an *N*-linked glycosylation site [61]. In contrast to antibodies, most antibody fragments are not glycosylated and this provides amenability for production in microbial systems, which are cheaper, faster and easier to cultivate and modify [62].

The scFvs have several advantages over full-antibodies with Fab and Fc region: (i) they can be ideal structures for large scale production in microbial systems owing to their small size and lack of glycosylation [47]; (ii) sequences that code V_L and V_H domains are combined in a single transcript and therefore, scFvs could be generated faster, in higher yields at lower costs, since balancing the expression of the L and H chains is not required [62]; (iii) they can be easily modified to improve selectivity and affinity [34]; (iv) they show better tumor penetration in cancer immunotherapy due to their smaller size [63]; (v) the scFvs do not show effector functions and immune cell activation due to lack of an Fc region and this allows the scFv molecules to react with their target antigens without an effect on the immune system of the host [64]. The lack of an Fc region that causes lower thermostability than parental antibody and tendency to formation of aggregates could be sometimes disadvantageous based on the usage purpose. This situation leads to a shorter half-life and increment on the risk of the immunogenicity [35, 65]. This disadvantage could be eliminated by combination of the scFv with albumin or polyethylene glycol to increase their half-life. However, these attempts could cause an increment in the size of scFvs and extra cost, and this could offset the advantages of scFvs over full-antibodies [66].

Despite the advantages of expression in microbial systems, scFvs obtained from bacteria do not have a comparable stability to whole antibodies or an expression yield from mammalian hosts, which have yields greater than 10 g/L in CHO cells [67]. Therefore, recent investigations have been focused on increasing protein stability as well as expression yield in bacteria with various vector systems, and engineered strains have been developed for this purpose [31].

2.2.2. *Escherichia coli* for ScFv Production

Selection of a suitable expression host is the first step for recombinant antibody fragment production. In the literature, there are studies on the expression of recombinant antibody fragments in various bacterial hosts such as *Escherichia coli* [54], *Pseudomonas putidas* [68], *Bacillus megaterium* [69, 70] and *Bacillus subtilis* [69, 71]. *Escherichia coli* is one of the most preferred organisms in recombinant protein production owing to its high growth rates, ease of genetic manipulation, well understood genetic structure and lower production costs [11, 72].

E. coli is composed of three compartments for protein production: cytoplasm, periplasm and extracellular medium. Expression of scFvs in *E. coli* could be difficult because of the intrachain disulfide bonds, which are crucial for structural stability and correct folding. To address this challenge, there are various approaches based on the expression compartment. The first approach is development of vector systems targeting scFvs to the oxidizing periplasm or extracellular medium by adding signal peptides [12, 73]. The second one is the expression of scFvs in reducing cytoplasm of *E. coli*. Although high yields of protein can be obtained from this compartment, the reducing condition of the cytoplasm which hampers the disulfide formation is not suitable for functional antibody fragments [74]. As a result, antibody fragments produced in the cytoplasm show tendencies for instability and insoluble aggregation, which is known as “inclusion body”. This situation requires the application of refolding processes after purification that consume extra time, labor and cost [75]. Another approach is altering of the reduction-oxidation pathways in cytoplasm with mutations in the *E. coli* strains [16, 76].

Figure 2.2 summarizes the compartments of *E. coli* for the expression of recombinant antibody fragments.

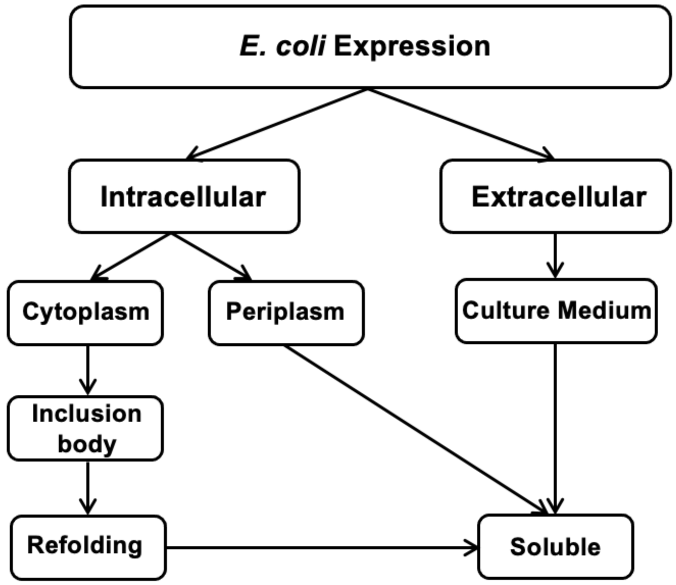

Figure 2.2. Compartments for the recombinant protein expression in *E. coli*. Figure modified from [54]

2.2.2.1. Periplasmic Expression

Proteins are firstly produced in the cytoplasm of *E. coli* and directed to the secretion pathways at the inner membrane owing to specific N-terminal sequences. The periplasmic compartment of *E. coli* allows for disulfide bond formation via specific chaperones, enzymes and foldases [77].

Since the scFv molecule requires two disulfide bonds for structural stability and correct folding, periplasm is the most preferred compartment for antibody fragments [78, 79]. Secretion of recombinant proteins to the periplasm in *E. coli* occurs via (i) signal peptides such as LamB, OmpA, MalE, PelB or PhoA that use the inner membrane secretion (Sec) pathway, which transports unfolded proteins; (ii) signal peptides such as TorA or Pac using the twin-arginine transport (Tat) pathway that transports fully folded proteins or (iii) signal peptides such as DsbA or TolB using the signal recognition molecule system (SRP) pathway that transports unfolded proteins [80].

There are numerous reports about the effects of different signal peptides on the expression and features of the scFvs [13, 81-83]. For instance, Karyolaimos and coworkers have screened four signal peptides (DsbA, Hbp, OmpA and PhoA) fused to an scFv and a recombinant protein with disulfide bonds to increase the production yield in the periplasm of *E. coli*. The main finding of this study was that the signal peptide which gave the highest production differed for each protein, and the construct having the OmpA signal peptide provided the highest production yield for the scFv [13]. Kasli and coworkers have investigated the effects of PelB and DsbA signal peptides on the production of periplasmic scFv and they showed that the PelB signal sequence resulted in higher scFv solubility and better cell physiology [81]. In another study, expression of anti-HER2 scFv fused with the PelB signal peptide was compared for the cytoplasm, periplasm and extracellular regions, and anti-HER2 scFv accumulated in the periplasm as expected, and its accumulation occurred in the extracellular region after 17 hours as a result of cell lysis [14].

Despite mentioned benefits, the capacity of the periplasm which is less than 20% of the total cell volume can limit overall expression yield, depending on the protein of interest, expression host and the type of signal peptide. Another disadvantage of this compartment is based on the leakage of antibody fragments into the medium. Antibody fragments accumulate in the periplasm due to metabolic stress. This situation leads to more permeable membrane structure, which causes a higher diffusivity of the accumulated proteins from the periplasm to the extracellular medium [84].

2.2.2.2. Cytoplasmic Expression

Since the cytoplasm has larger space than the periplasmic region, this compartment has a potential to produce recombinant protein almost 1.5 times the total amount of intracellular protein [74]. However, reducing conditions of the cytoplasm and absence of appropriate molecular chaperons result in the partial expression of disulfide bonds. This reducing environment causes the interaction of partially folded proteins with each other and also inhibits the intrachain disulfide bond formation capability, which result in aggregation and inclusion body formation. Protein recovery strategies could be applied by *in vitro* refolding and solubilization processes for preparation of soluble and functional scFvs from misfolded inclusion bodies. Since these applications are laborious, time-consuming and can cause poor recovery yields, the need for different strategies regarding solubility of protein, correct folding and expression efficiency of antibody fragments in *E. coli* cytoplasm has arisen [85].

Several studies have suggested that the use of tags or hydrophilic proteins such as glutathione S-transferase (GST) [86], maltose-binding protein [87] and green fluorescent protein (GFP) [88] fused to scFvs can enhance yields of soluble and functional proteins. However, the fusion tags are needed to be cleaved due to possibility of interference with the protein activity or folding. Removal of tags is also laborious and needs extra cost. In addition, maintenance of solubility and functionality of scFv can be difficult without a tag in some situations [89].

The cytoplasm of *E. coli,* which is occupied by the thioredoxin-thioredoxin reductase (*trxB*) and the glutaredoxin-glutaredoxin reductase (*gor*) systems, has a negative redox potential. To overcome the limitations due to reducing conditions of cytoplasm, strains of *E. coli* such as Origami [90] and SHuffle [91], which are genetically mutated by the reduction-oxidation mechanisms in the cytoplasm, have been developed to produce disulfide bonded proteins. Engineering of these *E. coli* strains was achieved by deleting *trxB* and *gor* genes to provide an oxidative cytoplasmic environment. Mutant cells become nonviable in the lack of thioredoxin and glutaredoxin pathways since essential proteins cannot be cycled back to their active reduced states. Screening of suppressors of Δ*trxB* Δ*gor* lethality results in the generation of a strain whose mutant peroxidase AhpC* has capacity to reduce Grx1 that provides growing cells [92], while the thioredoxins stay in their oxidized state. Disulfide bond formation could be catalyzed by oxidized Trx1 and this mutant *E. coli* strain is named as Origami. SHuffle strain also has *trxB* and *gor* mutations as the Origami, besides the overexpression of cytoplasmic disulfide isomerase (DsbC) proteins that provide correctly folded proteins [93].

There have been a growing number of reports related to expression of a variety of proteins in SHuffle cells, including full-length IgG expression for the first time [28]. Ahmadzadeh and colleagues have reported that solubility and production yield of scFv against HER2 increased when expressed in SHuffle at 30°C [17]. In another study, Liu and coworkers expressed soluble and active scFvs by the combination of SHuffle strain and cytoplasmic chaperone optimization [16]. In the referred study, plasmids containing scFv fragments were transformed in SHuffle strains comprising different chaperone combinations. As a result of a systematic screening of chaperones, it was found that GroEL-GroES system was the best in terms of increasing the expression yield of soluble antibody fragments. Results of the study also showed that scFvs obtained from this system had a stable tertiary structure as well as binding activity. In addition to genetically engineered strains, the CyDisCo (Cytoplasmic Disulphide bond formation in *E. coli*) system has been used to screen cytoplasmic expression of Fab and scFv antibodies generated from different organisms and from various classes of antibodies [94]. This study resulted in approximately 50% higher soluble expression yield of anti-HER2 scFv with CyDisCo in EnPresso B media than without CyDisCo.

Collectively, studies emphasize that SHuffle strains have a vast potential for the expression of active and soluble antibody derivatives in the cytoplasm of *E. coli*. Furthermore, combination of SHuffle with cytoplasmic chaperones or tags, as well as with media for high cell density cultures makes possible the production of proteins in high amounts on a lab scale [93].

2.2.2.3. Extracellular Expression

Another option for production of scFvs is their direct secretion into the *E. coli* culture medium. Generally, protein of interest fused to an N-terminal signal peptide could be transferred to the periplasm by the Sec machinery. However, it can further pass to the extracellular medium. Secretion into the extracellular medium has numerous advantages such as correct protein folding due to more oxidative and ample space, higher yield of protein expression and ease of purification processes [95].

Recombinant proteins can also be harvested directly from the culture supernatant in the case of extracellular expression and this reduces the impurities related to cell lysis. Additionally, accumulation of inclusion bodies in the intracellular compartments and toxic effects arisen from some recombinant proteins when expressed intracellularly can be eliminated in the extracellular secretion.

There are studies that accomplished the extracellular expression by optimization of the optical density for initiation of induction and by addition of chemical agents such as Triton X-100 that have increased the permeability of the outer cell membrane [96, 97]. It was reported that the active form of scFv against Aflatoxin B1 with PelB signal peptide was not found in the periplasmic region, while it was observed in the extracellular environment with the addition of 0.25% Triton X-100 [12]. There are also studies that performed extracellular secretin using different signal peptides such as YebF [95, 98] and OsmY [99] as well as HlyA signal peptide coupled at the C-terminal and using the hemolysin transport system [100].

2.2.3. Optimization of Expression Parameters

Since a universal methodology giving high functional yield of recombinant antibody fragments is not found, the expression conditions are required to be optimized for each antibody individually. Culture media, induction temperature, inducer concentration, aeration rate, pH, feeding strategies and host/vector systems influence the production efficiency of the target protein. Studies on optimization of these parameters have observed a major increment in the yield of antibody fragments by enhancing solubility, folding, expression and secretion of the proteins [7].

Nadkarni and colleagues investigated different media compositions and induction strategies and showed that higher Fab yields could be obtained by Studier's lactose autoinduction medium when compared with glucose or glycerol based medium [101]. Other studies reported that L-arginine, sucrose and glutathione addition to culture media improved the folding or the disulfide bond formation of scFvs, thus increased the yields of scFvs [102, 103]. In another study, combination of SHuffle strain with high cell density cultivation media was reported to increase intracellular single domain antibody production [104].

Multiple parameters such as inducer, media, aeration and temperature are sometimes required to be investigated simultaneously for optimization because changing a single factor each time could be laborious. For this purpose, statistical design of experiments (DoE) can be applied by detecting a correlation between multiple parameters and determining the optimum conditions to achieve ideal expression [7]. Akbari and coworkers optimized the temperature, inducer concentration and duration after induction for expression of scFv against HER2 by performing DoE and they obtained 3-fold increase in scFv yield [105].

2.3. Human Epidermal Growth Receptor 2 (HER2) in Cancers

Breast cancer is the second most leading cancer type worldwide, and it is the most frequent in women with an estimated 2.3 million new cases diagnosed in 2020. It ranks the fourth for mortality from cancer overall and is the primary cause of cancer related deaths in women [106].

Subtypes of breast cancer are categorized according to the presence of intracellular and transmembrane receptors which are estrogen (ER), progesterone (PR) and the human epidermal growth receptor 2 (HER2, also known as ERBB2). The human epidermal growth factor receptor family, which has four members (HER1, HER2, HER3 and HER4), is crucial for controlling cell growth and signaling. The expression level of its members changes related to the type of cancer cells. HER2, a 185 kDa transmembrane glycoprotein, is composed of three domains: a transmembrane lipophilic segment, the intracellular tyrosine kinase domain, and an extracellular domain. Although HER2 lacks a ligand binding domain as distinct from other HER family members, this receptor is activated upon forming heterodimers with other receptor family members [107]. Studies showed that heterodimerization among receptors triggered the cell growth and transformation [108]. Previous studies also reported that amplification and overexpression of the gene encoding was observed in approximately 20% of breast carcinomas and overexpression of HER2 caused poor prognosis [109]. As a result of these properties, HER2 has ben identified as a significant biomarker for diagnostic and therapeutic applications related to breast cancer [110].

2.3.1. Anti-HER2 Antibody and Antibody Fragments

The development of monoclonal antibodies targeting the extracellular domain of the HER2 protein was reported as a breakthrough for breast cancer therapy. Antibodies against HER2 inhibit the biological activity of protein by (i) hindering receptor heterodimerization, (ii) reducing receptor on cell surface and (iii) binding to the Fc-gamma receptors on effector cells to kill tumor cells [111].

Trastuzumab, which was approved by the FDA of the USA in 1998 and also European Medicines Agency (EMA) in 2000, was developed as the first humanized monoclonal antibody (mAb) to treat HER2 overexpressing breast cancer [110, 112]. After that, novel therapeutic agents against HER2 have been developed to advance breast cancer treatment [112]. Pertuzumab, a novel humanized mAb, was approved by FDA in 2012 and it was used in combination with trastuzumab and a chemotherapy drug called docetaxel to treat metastatic breast cancer patients that could not be treated with either trastuzumab or chemotherapy [113]. Franklin and coworkers showed that pertuzumab could bind to HER2 and sterically inhibit its dimerization with other HER members [114]. In addition to full-length antibodies, other studies reported that smaller fragments of trastuzumab and pertuzumab could inhibit tumor growth [115-117]. The results obtained from studies indicate that the Fc region is not essential to inhibit the growth of tumor cells. Consequently, the targeting abilities of scFvs allow them to be utilized in various therapeutic and diagnostic applications. There have been studies reporting the usage of antibody fragments against HER2 applied in immunotoxins [118, 119] and immunoliposomes [120] as breast cancers therapeutics.

2.4. Antibody-Based Biosensors

The first biosensor introduced by Leland C. Clark in 1956 was invented to determine the amount of glucose in serum samples [121]. Since then, several types of biosensors have been developed for detection of a broad range of substrates comprising proteins, oligonucleotides, small molecules, cells and viruses.

A biosensor contains three parts: a biorecognition element, a transducer and a signal processing unit. As biosensors are applied to obtain reliable and rapid analyses, choice of the biorecognition element is an important step for optimization of a biosensor [122]. Immunosensors, i.e. antibody-based biosensors, are analytic devices that generate a measurable signal in response to antigen-antibody interactions. Some key parameters are effective on the performance of an immunosensor: (i) ability to immobilize biorecognition elements while keeping up their activity; (ii) selectivity of biorecognition element to a specific analyte in solution; (iii) minimum level of non-specific adsorption to the solid surface; (iv) sensitive detection of biorecognition element; (v) stability of biorecognition element [34, 123].

2.4.1. Antibodies in Biosensor Applications

Polyclonal and monoclonal antibody-based immunoassays have been applied as important diagnostic tools for more than 40 years. Some problems may arise from usage of polyclonal antibodies as probe in biosensors because of varying affinity and specificity to more than one target, and batch related differences [124]. On the contrary, monoclonal antibodies can be more desirable due to specificity to a unique epitope on the target analyte and reproducibly endless production owing to immortality of the hybridoma cell lines [125].

The general working principle of an immunosensor is based on the specificity of the antibody against the antigen in the analyte, and the signal generation depending on the concentration of the sample. For this purpose, proper immobilization of the antibody to the sensor surface is significant for an immunosensor design. An immobilized full-length antibody can be oriented to the surface in different ways: side-on (one Fc and one Fab domain bound to the surface), tail-on (Fc domain bound to the surface), head-on (two Fab domains bound to the surface), and flat-on (with three domains bound to the surface). If the antigen binding sites of antibodies are available for interaction with the target protein, maximum performance could be obtained from the biosensor. Attachment of antibodies through the antigen binding sites (side-on, head-on and flat-on) causes a decrease or elimination of antigen-binding activity [126]. Therefore, controlling the orientations of antibodies is important for improved biosensor sensitivity.

Despite the advantages of monoclonal antibodies, there is the possibility to lose their function within the biosensor because of unpredictable conformation changes on solid support or undesirable reactivities occurred by their Fc domain. For this reason, various recombinant antibody fragments have been optimized in terms of stability and affinity to increase their usage as antibody-based probes in biosensor applications [127]. Recombinant antibody fragments have numerous preferable properties comprising low molecular weight, high flexibility, high customizability and easy access to the target protein that make them a strong alternative for full-length antibodies [49].

2.4.2. Immobilization Techniques of Antibody Fragments

Techniques used for immobilization can result in oriented or random attachment on to solid supports. Immobilization methods should be mild since binding of antibodies onto the surfaces is required to not affect their binding activity and specificity. Gold [128], glass [129], copper [128], silicon [130], polystyrene [131] and polymethyl methacrylate (PMMA) [132] surfaces or magnetic beads [133] can be given as examples of selected solid supports for the development of antibody-based biosensors.

Immobilization of antibody fragments could be performed via non-covalent and covalent attachment methods. Noncovalent binding of antibodies on surfaces is executed by physical adsorption occurring with electrostatic, ionic bonds, hydrophobic and hydrophilic interactions, van der Waals forces between antibodies and the surface. However, this technique does not allow control in terms of orientation and often results in poor binding and denaturation [134].

To enhance the antibody binding and reduce the quantity of denatured protein, modification techniques such as chemical modification or plasma treatment are applied to increase the hydrophilicity of surfaces [135]. Covalent immobilization of antibodies to chemically-activated solid surfaces, which are treated to contain hydroxy, thiol, amino or carboxyl groups for the attachment of antibodies by their free amino groups, is another method for immobilization. This robust method can increase the density and orientation outcomes at the surface. Since this method can also cause conformation changes or denaturation, protein engineering techniques provide alternative methods to ensure site-directed antibody immobilization. Directional immobilization provides easy access to the analyte and more uniform antigen-binding kinetics, which increase the biosensor sensitivity [127]. Affinity immobilization techniques including material binding peptides, biotin-streptavidin interactions, DNA directed immobilization and metal affinity can be used to obtain enhanced protein orientation. Peptide sequences used in these techniques can be incorporated as tags into the antibody fragments by chemical conjugation or genetic fusion [135].

There are studies that generated polypeptides which could bind to the metal surface with strong binding affinity [128, 136]. In a study, scFv against hepatitis B virus antigen was fused with gold binding peptide and high binding affinity towards a gold surface was obtained with this structure. In addition, recognition site of scFv was observed as oriented towards the sample containing antigen after immobilization to the gold surface [137]. In another study, scFv antibodies were constructed with a C-terminal cutinase fusion protein to improve the binding of scFvs towards phosphonate groups on gold surface plasmon resonance (SPR) surfaces [138]. Similarly, Hu and coworkers designed an scFv by incorporating a glycan tag in C-terminal of protein for oriented immobilization on aminated supports and functional activity increased 4-fold relative to ionically adsorbed scFvs [139].

2.4.3. ScFv Immunosensors and Immunoassays

There are numerous groups of biosensors in which scFv antibodies are used as biorecognition elements: immunoassays, optical, piezoelectric and electrochemical biosensors [18]. Mechaly and coworkers expressed an scFv targeting *B. anthracis* spores and showed its successful application as a biorecognition element in enzyme-linked immunosorbent assay (ELISA), immunofluorescence assay and flow cytometry [140]. Hu and colleagues developed an scFv antibody against domoic acid and successfully immobilized it on a mesoporous silica surface towards potential immunodetection and immunopurification applications [141]. In another study, recombinant scFv microarrays were used to classify the metastatic breast cancer patients by examining the serum protein expression profile for the first time [142]. Finally, Lee and coworkers developed an scFv sensor chip combined with SPR system to detect heavy metal contamination of marine organisms [143]. Collectively, these studies show how the recombinant antibody technology can contribute to effective development of next generation immunosensors and immunoassays.

2.5. Engineering scFvs for Sensor Surface Immobilization

A wide variety of immunosensor applications have been performed by using recombinant antibody fragments instead of full-length antibodies, as mentioned earlier. In general, directional immobilization methods are applied based on the Fc part or carbohydrate moiety of whole antibodies while these methods are not suitable for antibody fragments like scFv or scAbs, because of the lack of the glycosylated Fc domain [49]. Therefore, linker engineering techniques can be used for directed immobilization of scFvs towards biosensor surface, in addition to affinity and stability engineering methods that provide increased assay sensitivity, avidity and stability.

2.5.1. Linker Engineering

There have been several approaches on engineering of scFvs, regarding their expression plasmid design and production strategy, to achieve immobilization onto the sensor surface without denaturation. Antibody fragments can be engineered to comprise metal-binding amino acids such as cysteine (Cys) and histidine (His) in the flexible linker to allow scFvs to attach at high density onto metal surfaces. Linkers of scFvs can also be constructed to include positively charged amino acids such as arginine (Arg) for effective immobilization onto negatively charged surfaces via electrostatic interactions. Shen and coworkes designed a MUA/A10B scFv against 11-mercaptoundecanoic acid (MUA) containing a 15 aa linker peptide with arginine (RGRGRGRGRSRGGGS) to improve adsorption efficiency on anionic charged surface and obtained 42-fold increase in detection limits when compared to A10B Fab antibody [144]. A 6xHis sequence fused to C-terminus of scFv can be applied for immobilization by non-covalent interactions to nickel-nitrilotriacetic acid (Ni-NTA) surfaces. Furthermore, bioaffinity techniques can also be applied by conjugating scFvs with biotin via free amines on the scFv for immobilization to streptavidin coated surfaces [49]. A summary of methods used for engineering of scFvs towards effective immobilization is given in Figure 2.3.

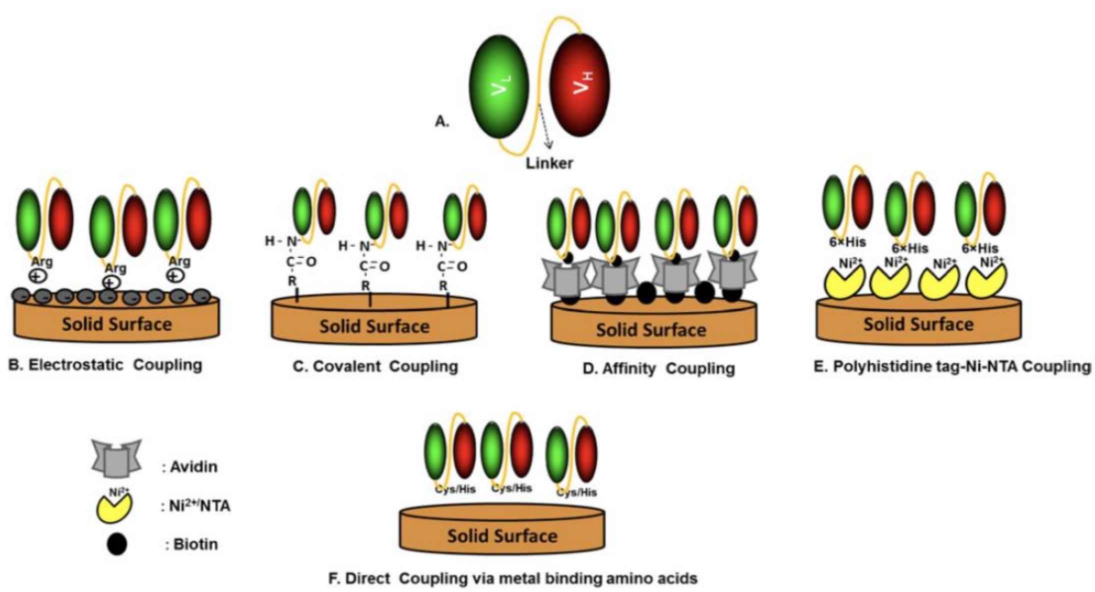

Figure 2.3. Types of immobilization approaches used for scFvs [49]

Material binding peptides can also be used for enhanced protein orientation. Phage screening methods have been developed to generate peptides having specificity to a variety range of materials such as polystyrene [145], polymethyl methacrylate [146], polycarbonate [147] and gold [148]. Polystyrene (PS), which is a relatively inexpensive material, has been widely used as a solid surface in ELISA, biochips and animal cell culture applications. Therefore, a PS-tag can be a potential peptide for research in diagnosis, immunoassay applications and drug screening [149-151]. If proteins fused with PS-tag peptides are used as capture reagents in ELISA, adsorption to polystyrene surfaces and overall capture ability increase [152]. Polystyrene binding peptides have been isolated and optimized in different studies and Table 2.1 gives amino acid sequences of the various peptides reported.

Table 2.1. Amino acid sequences of PS binding peptides

PS Affinity Peptide	**Amino Acid Sequence**	**Reference**
PS19	RAFIASRRIKRP	[153]
PS18	VRSWEEQARVTT	[153]
KPS19R	KRAFIASRRIRRP	[154]
PS19-6	RIIIRRIRR	[155]
PS19-4	RAIARRIRR	[155]
PS19-6L	RLLLRRLRR	[20]
PS23	AGLRLKKAAIHR	[153]
Lig1	FKFWLYEHVIRG	[145]
PB-TUP	VHWDFRQWWQPS	[156]

Peptides given in the table include several basic amino acids (K, R and H) that interact with the negative charges on polystyrene surfaces. Also, the presence of aliphatic amino acid residues (A, V, L and I) provides strong hydrophobic interactions with benzene ring structure of polystyrene. When binding of these peptides to a hydrophilic polystyrene was investigated, PS19 and PS19-6 exhibited maximum binding capacity, which were 81 mg/m^2 and 86 mg/m^2, respectively [20]. Studies related to site-specific immobilization of enzymes or antibody fragments to polystyrene surfaces typically were focused on adding these PS-tags to the C-terminal or N-terminal of proteins. Kumada and coworkers developed a solid-phase refolding strategy in which PS-tag fused scFvs expressed as inclusion bodies could immobilize onto hydrophilic polystyrene plate directly, and antigen-binding activities of scFvs in denatured form were recovered while washing the surface of plate. In this study, sensitivity of PS-tag fused scFvs attached on the polystyrene surface increased 25-fold against C-reactive protein (CRP) [157]. In another study, an scFv fused with PS-tag was used as capture antibody to detect *Listeria monocytogenes* in a sandwich ELISA, and improved detection sensitivity was obtained when compared with the assay using non-oriented scFv [158].

2.5.2. Affinity Engineering

Affinity determines the strength of the interaction between a specific paratope of an antibody and an epitope of its antigen. Antibodies which have high affinity to a target protein bind faster and release the protein more slowly when compared with low-affinity antibodies. High affinity antibodies are also more appropriate to utilize in immunoassays detecting low concentrations of the antigen. Avidity indicates total binding strength that occurs from multiple binding interactions.

If a monomeric scFv antibody, which contains only one antigen-binding site has low affinity in spite of high specificity, it would not be appropriate for applications detecting trace amounts of antigen since it cannot bind rapidly to an antigen in a sample solution. Conversely, if monomeric scFvs are assembled together by engineering to form multimer structures or attached as a layer of scFv on a solid support, increased sensitivity and avidity towards an antigen can be obtained [19].

Since high affinity is an important factor for the development of sensitive biosensors, there are methods to improve the interaction between the antibody and its antigen. These techniques including random mutagenesis, ribosome display, directed evolution and computational approaches are applied for optimization of antibody fragments to have more suitable affinity values for the intended applications [31, 159].

2.5.3. Stability Engineering

Besides long-term storage and reusability of antibody-based chips, stability of antibodies during manufacturing is also considered to be a significant factor. Therefore, studies towards increasing stability of antibody fragments have been attractive for the development of biosensors [127].

Generally, scAb and scFv antibodies show lower stability under thermal stress relative to whole antibodies. This result requires the suitable combination of antibody fragment design and selection of bacterial host, perhaps with a robust chaperone function [31]. Stabilization of antibody fragments can be applied by (i) isolation and screening of variants showing high stability using display systems [160, 161], (ii) creating non-native disulfide bond between V_L and V_H domains (dsFv) instead of a linker peptide [162, 163], (iii) rational design of V_L-V_H pair by point mutations [164, 165], and (iv) computational approaches [166].

2.6. Computational Approaches for Engineering of ScFvs

Proteins are composed of long chains of amino acids which have a particular three-dimensional structure in their native medium. Proteins carry out their biochemical functions relative to this structure. Therefore, knowledge about the mechanism which provides folding of proteins into their functional three-dimensional structures is important for further research. Amino acid sequence and the surrounding medium of a protein are effective on its folding [167]. To obtain a functionally active protein,

protein structures having the minimum free energy values are required to be determined and optimized [168].

In silico protein modelling is useful for predicting the three dimensional structures of proteins and their active sites [169]. To evaluate the conformational tendency of proteins, molecular dynamics (MD) simulations could be applied. MD simulations can be also performed at different temperatures to investigate thermostable nature of proteins [170]. Moreover, binding interactions of complexes such as protein-protein, protein-ligand can be investigated [171, 172]. Analyses used in protein modelling are summarized in Figure 2.4.

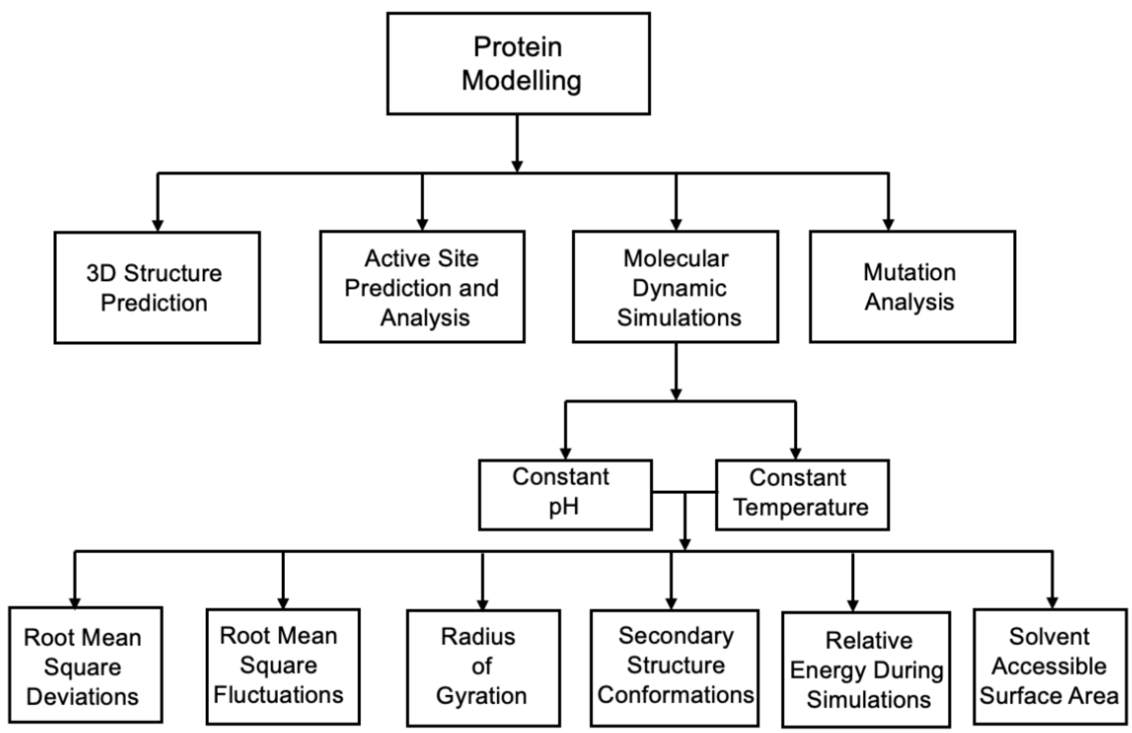

Figure 2.4. A classical workflow for protein modeling. Figure modified from [25]

2.6.1. Structure Prediction Analysis

A protein is made up several levels of structure. The linear amino acid sequence of the protein is considered as the primary structure. Secondary structure of the protein is defined by the local folded structures. The most common forms of this structure are α-helices and β-sheets which are linked by hydrogen bonds. Lastly, actively folded three-dimensional structure is described as the tertiary structure.

The availability of protein structure obtained from experimental methods has paved the way for development of computational structure prediction strategies. Homolog and "*ab* initio" methods can be applied to predict the structure of a protein. In homology modeling, the aim is to construct a suitable three-dimensional model for the protein with an unknown structure by utilizing from a template structure whose sequence shows similarity to the target protein [173]. There are two factors important for reliable model building. First, template structure and sequence of the target protein show a detectable similarity. Secondly, correct alignment between the sequence of target protein and the template structure is required to be computed [174]. The studies showed that the overall accuracy range obtained by homology methods were compatible with physical methods such as nuclear magnetic resonance (NMR) spectroscopy or X-ray crystallography [175].

Homology modelling can be applied via some software programs such as MODELLER [176], PHYRE 2 [177] and SWISS-MODEL [178]. If the resulting model shows low sequence similarity, less than 25% with the template structure, *ab* initio protocols are applied, which are based only on sequence information. Servers such as ROBETTA [179] and I-TASSER [180] are utilized for *ab initio* methods.

Homology modelling methods used in software programs are based on four steps, given in Figure 2.5. Briefly, related protein structures to target sequences are obtained from the protein data bank (PDB) and then, the templates appropriate for modelling are selected. In this step, template showing similarity greater than 25% is accepted as the reliable homolog and also accuracy of the template with regard to NMR data and resolution of the crystallographic structure is critical for selection of the template. Secondly, full-length template sequence is aligned with the target sequence. If similarity is observed greater than 40%, the alignment is accepted.

Then, a three-dimensional model is generated for each selected template. Lastly, scores calculated by the software are analyzed to choose the model. Alignment and model building steps are repeated if analyzing score of the model is not satisfactory [181].

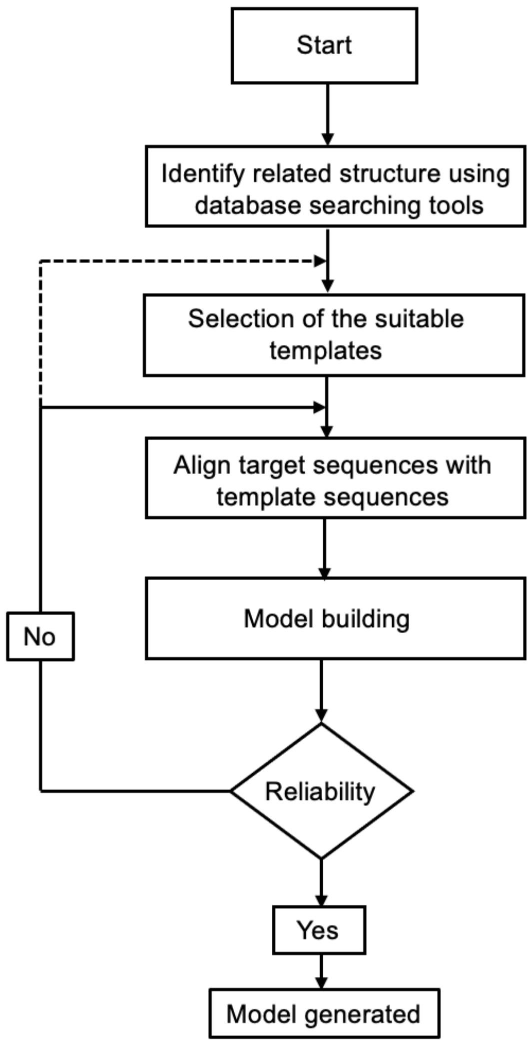

Figure 2.5. Steps used for homology modeling. Figure modified from [25]

2.6.2. Molecular Docking

Prediction of the desired orientation of the complex, obtained from binding a molecule to a second molecule to form a stable structure, is applied by molecular docking which is a computational technique [182, 183]. Binding sites on the protein surfaces are important factors for functions of proteins. The determination of these binding sites is often performed as a first step for studies on protein functions and drug design. Molecular docking and binding sites prediction can be applied by using various bioinformatics tools [25]. Web servers such as ClusPro [184], HADDOCK [185] and SwarmDock [186] have been used for prediction of the structure of protein-protein complexes.

There have been studies on prediction of antibody fragment structures docked with their target antigens. For example, Bandehpour and coworkers investigated the binding mechanism of scFvs and ESAT-6 antigen using ClusPro [171]. In another study, protein-protein docking was applied using HADDOCK server to investigate binding structures of scFv and its target protein Pep27, and to predict the epitopes on Pep27 [187].

2.6.3. Molecular Dynamics Simulations

MD simulation plays an important role in the field of the computational analysis of biomolecules. Behavior of a molecular system changing with time can be computed by using MD simulations. This gives knowledge about variations in protein conformation. In addition, determination of protein structures from experimental analyses is applied with MD simulations. Hence, this method can be defined as a kind of computer simulation that gives imitation of the motion of a system by observing interaction of molecules and atoms for a specific time period. This method has been generally used for complex dynamic processes comprising protein stability, protein folding, changes in conformation of system, drug design and prediction of three-dimensional structures [188, 189].

MD simulations of biomolecules can be applied using various softwares such as AMBER (Assisted Model Building and Energy Refinement), CHARMM (Chemistry at HARvard Macromolecular Mechanics), NAMD (Nanoscale Molecular Dynamics), and GROMACS (Groningen Machine for Chemical Simulations) [25]. Among them, GROMACS is a high-performance software that provides different topologies and parameters for the dynamic simulations of biomolecules [29]. This method is comprised of five main steps. Firstly, the proteins are added in a box with varying geometries and desired dimensions to create boundary conditions. Then, proteins are solvated in water molecules. Secondly, Na^+ or Cl^- ions are added to the system to neutralize the charges on the protein. Then, minimization of the system is performed. In the equilibration step, the temperature is increased from 0 K to a target temperature at a constant volume. Two phases which are NVT ensemble (constant number of particles, volume, and temperature) and NPT ensemble (constant number of particles, pressure, and temperature) are applied in the equilibration. Lastly, simulation is applied at the desired temperature. Defined codes are used for analyzing the resulting trajectories and observation of the behaviours of the atoms and molecules.

Analysis of the GROMACS trajectories gives information about the stability, flexibility and structure of the proteins by calculating radius of gyration (Rg), root mean square fluctuation (RMSF), root mean square deviation (RMSD) and the solvent accessible surface area (SASA). Rg measures compactness of the protein. If steady value of Rg is observed, it shows folding of the protein is in stable configuration. RMSF is graphed in relation to residue number to indicate the fluctuation of all residues. RMSD is used to understand stability of protein and closeness to the experimental structure. RMSD is also plotted, and fluctuations between 1-3 Angstroms are suitable for small proteins, whereas larger changes show a possibility of misbehaving of the protein. SASA indicates the interaction surface area of protein with its solvent molecules. If the temperature increases, SASA also increases related to the nature of the protein. Proteins denature with the increasing temperature, thus the hydrophobic region exposes to the solvent due to unfolding [170].

2.6.4. Computational Approaches for Estimation of Binding Free Energies

Binding free energy indicates the strength of the biomolecular interactions. A range of computational approaches such as thermodynamic integration (TI), free energy perturbation (FEP), or molecular mechanics Poisson-Boltzmann surface area (MM-PBSA) could be applied for estimation of binding free energies. Among these approaches, the MM-PBSA is the most commonly used method to calculate interaction energies for biomolecular complexes [190].

In MM-PBSA, binding free energy (ΔG_{bind}) of two proteins forming a complex is calculated using equation (2.1):

$$\Delta G_{bind}=G_{complex}-(G_{protein}+G_{protein}) \tag{2.1}$$

Equation 2.1 can also be used for other complexes such as protein-DNA, protein-ligand interactions. The free energy for each protein could be written as:

$$G_x=E_{MM}-TS+G_{solvation} \tag{2.2}$$

where x refers to complex or protein. E_{MM} is the average molecular mechanics potential energy in a vacuum. T refers to temperature and S refers to entropy, hence TS indicates the entropic contribution. $G_{solvation}$ term denotes the free energy of solvation.

E_{MM} is calculated by the summation of bonded and non-bonded interactions, as given in Equation 2.3. Angle, bond and dihedral energies are given by E_{bonded}, whereas electrostatic and van der Waals energies are given by $E_{non\text{-}bonded}$.

$$E_{MM}=E_{bonded}+E_{non\text{-}bonded}=E_{bonded}+(E_{vdW}+E_{elec}) \tag{2.3}$$

The contribution from the solvent is calculated by the summation of electrostatic (G_{polar}) and non-electrostatic ($G_{non\text{-}polar}$) terms as given below:

$$G_{solvation}=G_{polar}+G_{non\text{-}polar} \tag{2.4}$$

Collectively, each energy term is calculated individually and binding free energy of the complex is determined by using Equation 2.1

The relationship between binding energy and equilibrium dissociation constant (K_d) is given by:

$$\Delta G=RT\ln K_d \tag{2.5}$$

where, R and T refers to gas constant and the temperature, respectively [190].

2.7. Experimental Methods for Determination of Antibody Affinity

The affinity for an antigen is one of the most important factors that characterizes antibody molecules. To calculate the equilibrium constant accurately, the concentrations of the complex and free antigen or antibody in solution are needed to be determined in a such condition that does not disturb the equilibrium [191].

Affinity constant of an antibody can be calculated by using various methods. One of the most reliable and easier techniques is ELISA [192]. The methods applied by specialized equipment comprise (i) fluorescence quenching in which antibodies bind to fluorescent antigens and quench the fluorescence, (ii) isothermal titration microcalorimetry in which enthalpy and equilibrium constant as well as binding entropy can be determined [193], (iii) flow cytometry, which can be applied for recombinant antibodies displayed on the microbial cell surface [194], and (iv) surface plasmon resonance (SPR) [195].

2.7.1. Enzyme Linked Immunosorbent Assay (ELISA)

Enzyme-linked immunosorbent assay (ELISA) is a labeled immunological test which is applied for sensitively detection and quantification of substances such as proteins, glycoproteins, antibodies and antigens. This detection is achieved by complexing antigens and antibodies for production of a measurable signal [196].

For determination of equilibrium affinity constants of antibodies, Friquet and coworkers described a competitive ELISA method [192]. In this method, an antibody in a constant concentration is mixed with an antigen solution which is serially diluted. Then, the free antibody is calculated by applying indirect ELISA in antigen-coated plates. According to this method, when an scFv is incubated with an antigen, it can be defined as:

$$a=[scFv]=[scFv]_f+[scFv]_b \tag{2.6}$$

$$[BS]=[BS]_f+[BS]_b \tag{2.7}$$

whereas a refers to the total concentration, $[scFv]_f$ and $[scFv]_b$ denote the free and bound scFv concentrations, respectively. [BS] refers to binding site and it is summation of free ($[BS]_f$) and bound ($[BS]_b$) binding site concentrations. If the antigen denoted by x below, is monomeric, [BS] is equal to the antigen concentration. If the antigen is multimeric, its concentration is multiplied with number of sites (n):

$$[BS]=nx \tag{2.8}$$

Assuming one scFv has one binding site;

$$[BS]_b=[scFv]_b \tag{2.9}$$

Thus, dissociation constant can be written as,

$$K_d=\frac{[scFv]_f[BS]_f}{[BS]_b} \tag{2.10}$$

Since the free scFv concentration is measured with this method, $[scFv]_f$ is denoted by y, below. By combining equations (2.6), (2.7) and (2.9),

$$[BS]_f = nx - [scFv]_b = nx - a + y \tag{2.11}$$

$$[BS]_b = a - y \tag{2.12}$$

and combining equations (2.10), (2.11) and (2.12),

$$K_d = \frac{y(nx - a + y)}{a - y} \tag{2.13}$$

Thus, K_d value can be calculated from Equation 2.13 [197].

Beatty et al., [198] also described an indirect ELISA method in which antibody dilutions were mixed with different antigen concentrations. In this method, the total antibody concentration is plotted against absorbance, which gives the bound antibody. Dissociation constant is calculated from 50% of maximum absorbance (OD_{50}) values obtained from curves plotted for two coated antigen concentrations. Thus, equilibrium dissociation constant is found from the equation below:

$$K_d = \frac{n[scFv']_t - [scFv]_t}{n-1} \tag{2.14}$$

where $[scFv']_t$ and $[scFv]_t$ refer to total antibody concentrations at OD_{50}' and OD_{50} determined from ELISA applied with two coated antigen concentrations, while n denotes to the dilution factor of the antigen [198, 199].

It could be concluded that the Beatty method is based on OD_{50} ratio of two ELISA curves at different antigen concentrations, whereas Friguet method gives the direct relation between concentration and signal to calculate concentration of free antibody.

2.7.2. Surface Plasmon Resonance (SPR)

SPR is a label free technique which is used for determination of steady-state and kinetic binding affinities between interacting biomolecules [200]. Reaction rates (k_a and k_d) and equilibrium dissociation constant (K_d) of binding molecules can be calculated by following the immobilization of analyte and ligand on the sensor surface in real time [201].

For calculation of equilibrium constants by utilizing SPR, the dynamic equilibrium is given by,

$$A+B \rightleftharpoons A\text{-}B$$

where A refers to analyte which is binding molecule from solution and B denotes the ligand that is immobilized on the surface. Whereas the forward reaction rate is defined by the association rate constant (k_a), the reverse reaction rate is defined by the dissociation rate constant (k_d). The binding rate is expressed as,

$$\frac{d[AB]}{dt}=k_a[A][B]-k_d[AB] \tag{2.15}$$

where [B] refers to concentration of the free binding site and [AB] denotes the complex concentration. [AB_{max}], given below, refers to concentration of complex at saturation. [B] can be calculated as:

$$[B]=[AB_{max}]-[AB] \tag{2.16}$$

It can be considered that response (R) of binding scales linearly with [AB]. Thus, Equation 2.17 is obtained by combining equations (2.15) and (2.16).

$$\frac{dR}{dt}=k_a c_0(R_{max}-R)-k_d R \tag{2.17}$$

where c_0 denotes the analyte concentration and R_{max} is the signal obtained in saturation, where all ligand molecules interact with the analyte. In equilibrium, the net effect of association and dissociation becomes zero as given below:

$$\frac{dR}{dt}=k_a c_0\left(R_{max}-R_{eq}\right)-k_d R_{eq}=0 \tag{2.18}$$

where R_{eq} refers to equilibrium response obtained at c_0 analyte concentration. Hence, the equilibrium response is related to the affinity constant (K_a) and the dissociation constant (K_d). This relation can be expressed by the 1:1 Langmuir isotherm. Thus, K_a and K_d (inverse of K_a) can be calculated from equations (2.19) and (2.20), respectively [201].

$$R_{eq}=\frac{c_0 K_a R_{max}}{c_0 K_a+1} \tag{2.19}$$

$$R_{eq}=\frac{c_0 R_{max}}{c_0+K_d} \tag{2.20}$$

3. MATERIALS AND METHODS

3.1. Bacterial Strains, Plasmids and Chemicals

For molecular cloning experiments, *Escherichia coli* DH5α was used and *Escherichia coli* strains of SHuffle T7 Express [91] and BL21 (DE3) were used as expression hosts for scFv productions. The plasmids which were used and constructed in the scope of this study are given in Table 3.1.

Table 3.1. Plasmids constructed and used in the experiments.

Plasmid	**Description**	**Reference**
pET28a(+)	Cloning vector, IPTG-inducible, Kan^r	[202]
pMAZ360-scFv735	Expression vector containing scFv gene against polysialic acid (polySia), IPTG-inducible, Amp^r	[203]
pMAZ360-cIgG-Herceptin	Cloning vector containing IgG gene against HER2, IPTG-inducible, Amp^r	[28]
pET28a-scFv13R4-Flag-6xHis	Expression vector containing scFv gene against β-galactosidase, IPTG-inducible, Kan^r	[26]
pBAD18-Bgal-NStrepIItag	Cloning vector containing β-galactosidase with N-terminal StrepII tag, L-arabinose inducible, Amp^r	[26]
pET28a-anti-HER2-scFv-V_LV_H	Expression vector containing scFv gene against HER2 in V_LV_H orientation, IPTG-inducible, Kan^r	This study
pET28a-anti-HER2-scFv-V_HV_L	Expression vector containing scFv gene against HER2 in V_HV_L orientation, IPTG-inducible, Kan^r	This study
pET28a-anti-HER2-scFv-L2	Expression vector containing scFv gene against HER2 with L2 linker, IPTG-inducible, Kan^r	This study

pET28a-anti-HER2-scFv-L3	Expression vector containing scFv gene against HER2 with L3 linker, IPTG-inducible, Kan^r	This study
pET28a-anti-HER2-scFv-L4	Expression vector containing scFv gene against HER2 with L4 linker, IPTG-inducible, Kan^r	This study
pET28a-anti-HER2-scFv-L5	Expression vector containing scFv gene against HER2 with C-terminal L5 linker, IPTG-inducible, Kan^r	This study
pET28a-StrepIItag-Bgal-Histag	Expression vector containing β-galactosidase with N-terminal Strep II tag and C-terminal 6xHis tag, IPTG-inducible, Kan^r	This study
pET28a-scFv13R4-L2	Expression vector containing scFv gene against β-galactosidase with L2 linker, IPTG-inducible, Kan^r	This study
pET28a-scFv13R4-L3	Expression vector containing scFv gene against β-galactosidase with L3 linker, IPTG-inducible, Kan^r	This study
pET28a-scFv13R4-L4	Expression vector containing scFv gene against β-galactosidase with L4 linker, IPTG-inducible, Kan^r	This study

All chemicals and solvents were analytical grade except otherwise stated. Oligonucleotide primers and phusion high-fidelity DNA polymerase were used for PCR amplifications of the Herceptin® (trastuzumab) antibody and scFv domains. *Nco*I-HF, *Hind*III-HF and T4 DNA Ligase were used for directional cloning of genes encoding the anti-HER2 scFvs. Luria-Bertani (LB) and Hanahan's Broth (SOB medium) were used as growth media. Isopropyl β-D-1-thiogalactopyranoside (IPTG) was applied to induce the recombinant scFv expression. Bradford reagent, protein ladder and Coomassie stain were used for protein analysis. Sodium chloride, kanamycin monosulfate (Kan), ampicillin sodium crsytalline (Amp), spectinomycin dihydrochloride pentahydrate (Spec), bovine serum albumin (BSA), D-glucose monohydrate, tetramethylethylenediamine (TEMED), acrylamide/bisacrylamide 30% w/w solution, ammonium persulfate and sodium dodecyl sulfate (SDS) were used for preparation of analysis solutions. Rabbit anti-human IgG (Fc specific) conjugated to horseradish peroxidase (HRP), anti-6xHis-tag-HRP and Opti-4CN Substrate Kit was used to detect the expression of scFv-6xHis proteins. HER2/ERBB2 extracellular domain (human, recombinant) was used as antigen for anti-HER2 scFv constructs in ELISA assays. StrepTactin-HRP conjugate antibody was used as detection antibody in Western blot and ELISA experiments. Deionized water (18.2 MΩ cm^{-1}) was used in all experiments.

3.2. Plasmid Construction

Firstly, anti-HER2 scFv gene was designed based on the combination of the amino acid sequence of the variable domain (V_L) in the light chain and variable domain (V_H) in the heavy chain of the Herceptin constructed in a previous study [28]. These domains were connected together either by a standard linker containing 15 amino-acid $(G_4S)_3$ or linkers containing affinity peptides that interact with polystyrene surfaces mentioned in Table 2.1. Standard linker and new linkers constructed in this study are given in Table 3.2. The DNA sequences of the variable domains of the scFvs and linkers are given in Appendix 1. Furthermore, plasmid containing scFv13R4 [26] gene was redesigned to contain the new linkers (L2-L5).

Table 3.2. Amino acid sequences of linkers between V_L and V_H domains.

#	Linker Peptide	Amino Acid Sequence	Length of Linker (# of aa)
L1	GS linker	GGGGSGGGGSGGGGS	15
L2	PS19-V1	GGGGSRIIIRRIRRG	15
L3	PB-TUP-V1	GGGVHWDFRQWWQPS	15
L4	PS18-V1	GGGVRSWEEQARVTT	15
L5	Cterm-PS19	RIIIRRIRR	9

In addition to scFvs, β-galactosidase (antigen for scFv13R4) expression vector was designed by adding N-terminal StrepTag and C-terminal His-tag to use for detection in ELISA and purification analyses. Genetic engineering techniques were applied according to standard protocols [204] in all designs.

3.2.1. Primer Design

The primers used for construction of anti-HER2 scFv plasmids are given in Table 3.3. Restriction enzyme sequences in the primers are underlined in the table. Primers were designed for amplification of the variable domains in the light (V_L) and heavy (V_H) chains of the full-length antibody using the template vector pMAZ360-cIgG-Herceptin and addition of 30 base pair (bp) linker peptide sequences between the variable domains. Outer reverse primers also contained 6xHis tag sequence (18 bp) for purification and detection purposes and inner primers were composed of 15 bp common sequence for overlapping. In addition, the 5’ ends of restriction enzyme recognition sites contained extra nucleotides to enable digestion at the end of DNA fragments. Formation of primer dimer and self-complementation were controlled by the freeware OligoAnalyzer™ 3.1.

Table 3.3. Primers used for construction of anti-HER2 scFv plasmids

#	Primer Name	Sequence (5’-> 3’)
P1	*Nco*I-anti-HER2-scFv-VL-fwd	CCTATGCCATGGATATTCAAATGACCCAAAG
P2	Anti-HER2-scFv-VL-linker-rev	GCTGCCACCTCCGCCTGAACCGCCTCACCCGTGCGTTTAATCTCCAC
P3	Anti-HER2-scFv-VH-linker-fwd	GGCGGAGGTGGCAGCGGCGGTGGCGGATCGGAGGTTCAATTAGTGGAATC
P4	*Hind*III-anti-HER2-scFv-VH-rev	GCGATGAAGCTTTTAGTGATGATGATGATGATGAGAGCTGACCGTGACCAG
P5	*Nco*I-anti-HER2-scFv-VH-fwd	CCTATGCCATGGAGGTTCAATTAGTGGAATC
P6	Anti-HER2-scFv-VH-linker-rev	GCTGCCACCTCCGCCTGAACCGCCTCCACCAGAGCTGACCGTGACCAG

P7	Anti-HER2-scFv-VL-linker-fwd	GGCGGAGGTGGCAGCGGCGGTGGCG GATCGGATATTCAAATGACCCAAAGC
P8	*Hind*III-anti-HER2-scFv-VL-rev	ATGAAGCTTTTAATGGTGATGATGGTG ATGGCCGCCTCCTCCCGTGCGTTTAAT CTCCAC
P9	Anti-HER2-scFv-VH-PS19-fwd	CGTATCATCATCCGAAGGATCCGACGA GGCGAGGTTCAATTAGTGGAATC
P10	Anti-HER2-scFv-VL-PS19-rev	TCGGATGATGATACGTGAACCGCCTCC ACCCGTGCGTTTAATCTCCAC
P11	Anti-HER2-scFv-VH-PB-TUP-fwd	TGGGATTTCCGTCAGTGGTGGCAGCC GTCCGAGGTTCAATTAGTGGAATC
P12	Anti-HER2-scFv-VL-PB-TUP-rev	CTGACGGAAATCCCAATGCACGCCTCC ACCCGTGCGTTTAATCTCCAC
P13	Anti-HER2-scFv-VH-PS18-fwd	TCCTGGGAAGAACAGGCGCGTGTGAC CACCGAGGTTCAATTAGTGGAATC
P14	Anti-HER2-scFv-VL-PS18-rev	CTGTTCTTCCCAGGAACGCACGCCTCC ACCCGTGCGTTTAATCTCCAC
P15	*Hind*III-anti-HER2-scFv-CPS19-rev	CTTAAGCTTTTATCGTCGGATCCTTCG GATGATGATACGGTGATGATGATGATG ATGAGA

ScFv13R4 was used as another model scFv antibody. Primers were designed to amplify V_L and V_H domains of the template vector pET28a-scFv13R4-Flag-6xHis [26] and add 30 bp different linker peptide sequences between the variable domains. The primers used for construction of new scFv13R4 plasmids are given in Table 3.4. In addition, primers were created to amplify the DNA of β-galactosidase from pBAD18-Bgal-NStrepIItag plasmid and add 6xHis tag sequence (P16 and P17).

Table 3.4. Primers used for construction of scFv13R4 plasmids

#	Primer Name	Sequence (5’-> 3’)
P16	StrepTag-NcoI-Bgal-fwd	CCTATGCCATGGCAAGCTGGAG

P17	Bgal-His-*Hind*III-rev	ATGAAGCTTTTAATGGTGATGATGGTG ATGGCCGCCTCCTCCTTTTTGACACCA GACCAA
P18	NcoI-scFv13R4-VH-fwd	CCTATGCCATGGGCGCCGAGGTGCAG CT
P19	HindIII-scFv13R4-VL-rev	GCGATGAAGCTTTTAGTGATGATGATG ATGATGTCCCTTGTCGTCATCGTCC
P20	ScFv13R4-VL-PS18-fwd	TCCTGGGAAGAACAGGCGCGTGTGAC CACCCAGTCTGTGCTGACTCAGCCTGC CT
P21	ScFv13R4-VH-PS18-rev	CTGTTCTTCCCAGGAACGCACGCCTCC ACCTGAGGAGACGGTGACCAG
P22	ScFv13R4-VL-PS19-fwd	CGTATCATCATCCGAAGGATCCGACGA GGCCAGTCTGTGCTGACTCAGCCTGC CT
P23	ScFv13R4-VH-PS19-rev	TCGGATGATGATACGTGAACCGCCTCC ACCTGAGGAGACGGTG
P24	ScFv13R4-VL-PB-TUP-fwd	TGGGATTTCCGTCAGTGGTGGCAGCC GTCCCAGTCTGTGCTGACTCAGCCTGC CT
P25	ScFv13R4-VH-PB-TUP-rev	CTGACGGAAATCCCAATGCACGCCTCC ACCTGAGGAGACGGTGACCAG

3.2.2. Plasmid DNA Isolation from *E. coli*

A commercial mini-prep kit was applied to separate plasmid DNA from *E. coli* cells, according to manufacturer's instructions given in detail in Appendix 2. Briefly, a single colony from solid agar containing the selective antibiotic was inoculated into 6 ml liquid medium with the selective antibiotic and grown overnight at 37°C and 200 rpm. In the last step of the protocol, 40 µl of elution buffer (EB) was used to isolate DNA from the spin column and the eluted plasmid was stored at -20°C.

3.2.3. Polymerase Chain Reaction (PCR) of Variable Domains

ScFv genes were constructed by using a two-step overlapping PCR, which is also known as Splicing by Overlap Extension or SOE-PCR [205, 206]. In this PCR based protocol, V_L and V_H domains of the full antibody are firstly amplified by PCR with primers which have 15 bp overlapping sequences to create a linker region. Then, these fragments, which share a region of homology, are assembled with outer primers by another PCR. The 3′-end of the top strand of V_L fragment anneals onto the 3′-end of the bottom strand of V_H fragment, and the recombinant product forms. The SOE-PCR strategy used in this study for the assembly of variable domains is given in Figure 3.1.

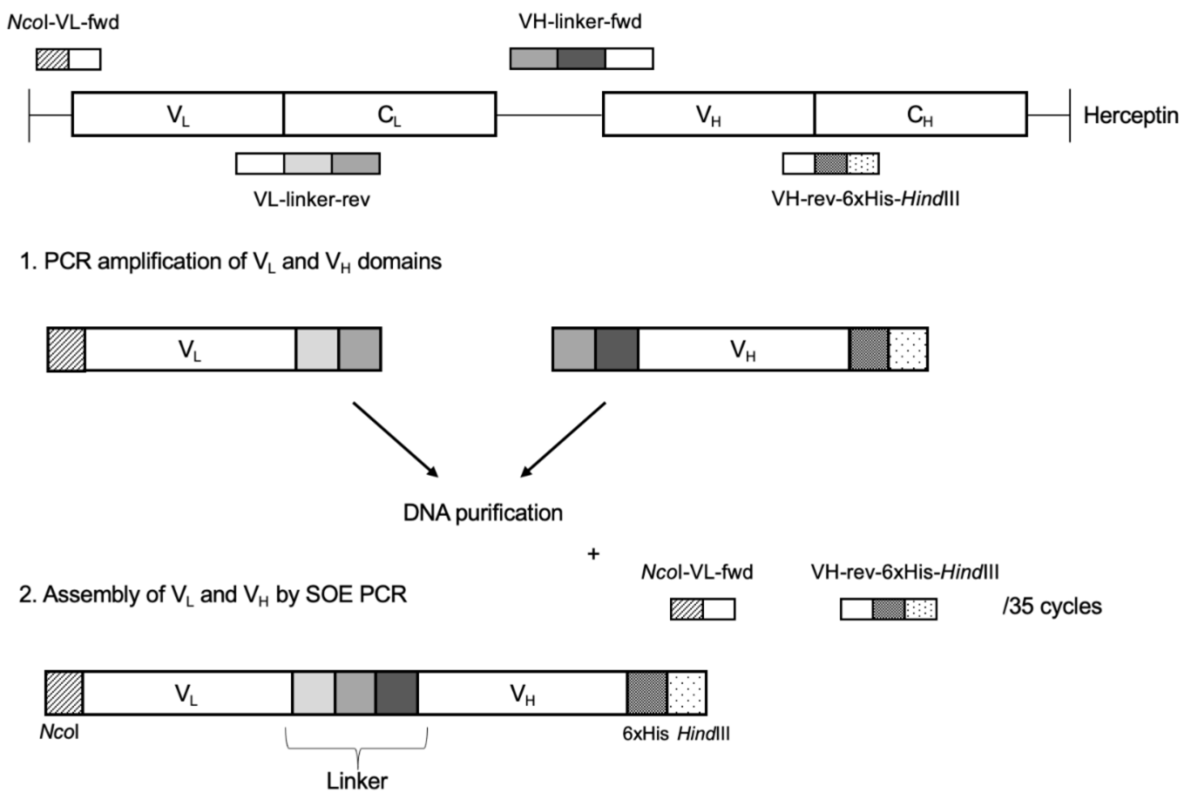

Figure 3.1. Schematic representation for assembly of scFv constructs based on the recombinant Herceptin whole antibody using SOE-PCR strategy

The amplification of V_L and V_H fragments were carried out by two separate PCRs. The reaction mixtures, prepared on ice, contained the following:

Mixture A (for V_L domain)
35 µl dH_2O
10 µl 5x Phusion Buffer
1 µl dNTP (10 mM stock)
1 µl DNA template (50 ng/µl)
1 µl P1 primer (outer)
1 µl P2 primer (inner)
1 µl Phusion Polymerase

Mixture B (for V_H domain)
35 µl dH_2O
10 µl 5x Phusion Buffer
1 µl dNTP (10 mM stock)
1 µl DNA template (50 ng/µl)
1 µl P3 primer (inner)
1 µl P4 primer (outer)
1 µl Phusion Polymerase

The PCR reaction parameters are given in Figure 3.2.

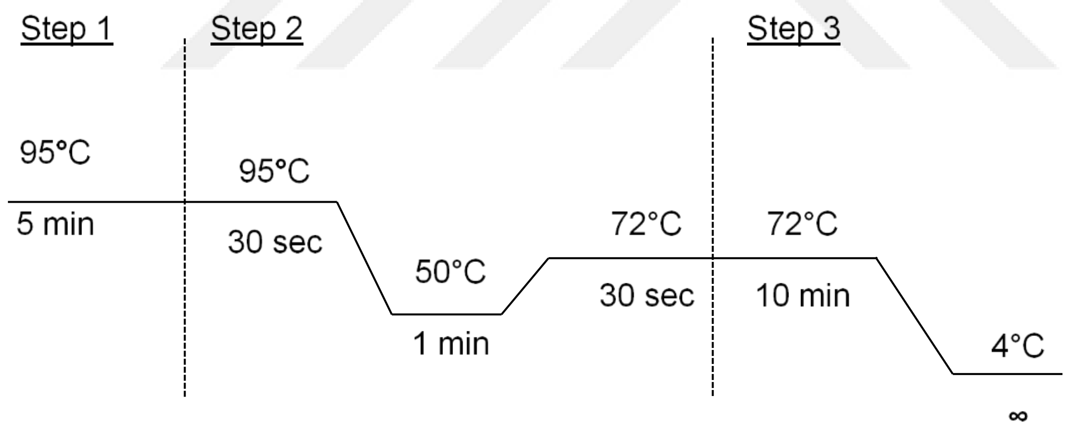

Figure 3.2. PCR reaction parameters

After the first set of PCRs, overlap PCR was set up to fuse the V_L and V_H fragments. For this, only outer primers were used and both gene fragments were taken in equivalent amounts (10 ng). The same PCR conditions given in Figure 3.2 were used. When the PCR was complete, a fraction of the product (~8 µl) was run on an agarose gel to verify whether the genes were fused. The PCR product was purified with a commercial PCR purification kit by following steps given in Appendix 2 for removal of primers, nucleotides, polymerases and salts. As a last step, 30 µl of dH_2O was used to elute purified DNA from spin columns.

3.2.4. Agarose Gel Electrophoresis

After PCR, agarose gel electrophoresis was applied to verify and purify the V_L and V_H fragments. Briefly, 0.8 g of agarose was added in 100 ml 1xTAE and was heated to dissolve the mix, until boiling point in a microwave oven. Then, it was cooled to about 50°C and 10 µl of gel stain was added. The gel was poured into a suitable gel tray and allowed to cool after inserting the appropriate comb. DNA samples mixed with loading buffer and also the DNA ladder (Appendix 3) were loaded into the wells. Electrophoresis was performed at 110 V for 20-30 min in the gel tank filled with 1xTAE buffer. The bands were visualized and photographed with gel documentation system.

3.2.5. DNA Extraction from Agarose Gels

The bands of amplified V_L and V_H fragments were separated from the gel with a scalpel and purified from agarose and salts using a commercial gel extraction kit by following the steps given in Appendix 2. As a last step, DNA was extracted in 30 µl of dH_2O and stored at -20°C until further use.

3.2.6. Digestion of DNA Using Restriction Endonucleases

The constructed scFv gene and pET28a(+) plasmid were digested with *Nco*I and *Hind*III restriction enzymes. Digestion reaction mixture was prepared in a tube with the following components:

DNA fragment : 0.5 to 2 µg
10x Reaction buffer : 2 µl
Restriction enzyme : up to 10 U/µg DNA
Alkaline Phosphatase, Calf Intestine (CIP) : 1 µl

Sterile dH_2O : to 20 µl

The digestion reaction was applied at 37°C for minimum 2 h. After restriction endonuclease digestion, scFv gene was purified with the PCR purification kit. At the end of the protocol, the purified DNA was eluted with 30 µl of dH_2O from the spin column. The digested vector was run on a gel, excised from the gel with a scalpel and purified from agarose and salts using a commercial gel extraction kit. To elute DNA from the spin column at the end of the protocol, 30 µl of dH_2O was used and the extracted DNA was stored at -20°C.

3.2.7. Ligation

The scFv gene was subcloned into pET28a(+) vector between *Nco*I and *Hind*III sites in 20 µl ligation reaction mixture containing:

10X ligation buffer	: 2 µl
Insert DNA (0.764 kb)	: 45 ng
Double digested vector DNA (5252 kb)	: 100 ng
T4 DNA ligase	: 1 µl
Sterile dH_2O	: to 20 µl

The amount of insert DNA was calculated based on the insert:vector ratio of 3:1 to add to the reaction. At the same time, reaction mixture without insert was prepared for control. The reaction was performed at 16°C for 16 h. The product was stored at -20°C.

3.2.8. Transformation of *E. coli*

Firstly, competent *E. coli* DH5α were prepared with $CaCl_2$ method given in Appendix 2, and stored as 50 µl aliquots at -80 °C. Ligation product (3 µl) was added to the tubes containing competent cells. The tube was incubated on ice for 30 min, then in 42°C water-bath for exactly 90 sec, and immediately placed on ice for 2 min. Then, 750 µl of SOB medium was added, and the tube was incubated at 37°C for exactly 45 min, at 200 rpm. The same procedure was applied for ligation control product and empty competent cells. The concentrated transformation mixture (~50 µl) was spread on prewarmed LB agar supplemented with 50 µg/ml kanamycin and incubated overnight, at 37°C.

3.2.9. DNA Sequencing

At least three colonies were selected from LB agar plates and each colony was cultured overnight in 5 ml LB medium containing 50 µg/ml kanamycin and shaken at 37°C, 200 rpm. Plasmid DNA was isolated as given in Section 3.2.2 and DNA was obtained in 40 µl of EB buffer. The extracted plasmid was stored at -20°C.

Plasmids were sequenced to confirm absence of mutations and to verify the correct expression frame using the standard pET sequencing primers. 0.5-1 µg of isolated plasmid DNA was mixed with sequencing primer of 1 µl and the total volume was adjusted to 18 µl by adding EB buffer. The provided data were analyzed using the freeware ApE v.2.0.51 [207] and SnapGene Viewer [208].

3.3. Recombinant Production of ScFv Constructs

Recombinant protein expression was carried out in laboratory scale air-filtered shake bioreactors.

3.3.1. Laboratory Scale Production of ScFvs

A single colony of *E. coli* strains BL21(DE3) or SHuffle T7 Express transformed with pET plasmids ligated with scFv genes were used to inoculate LB medium containing 50 µg/ml kanamycin and 25 µg/ml spectinomycin (for SHuffle T7 Express strain) in 250 ml flasks. Whereas SHuffle T7 Express were grown at 30°C, BL21 (DE3) cells were grown at 37°C. The next day, overnight grown cultures were added to flasks containing 50 ml or 1 L fresh LB media containing 50 µg/ml kanamycin. Volume of the cells for inoculation was determined by adjusting initial absorbance at 600 nm

(OD_{600}) as 0.06. The cells were incubated at either 37°C or 30°C depending on the type of strain. The media were induced with 0.1 mM IPTG at 30°C for 16 h, when OD_{600}=0.7. Cell pellets were obtained by harvesting cells via centrifugation at 4000xg for 20 min at 4°C, and the pellets were kept at -20°C.

3.3.2. Production of ScFv in Different Expression Conditions

To observe the effects of bioprocess parameters on the yield of soluble recombinant protein, the appropriate expression conditions including temperature of induction, duration of induction, concentration of the inducer, IPTG, and culture media type were investigated (Table 3.5). The compositions of all the culture media are given in detail in Appendix 4.

Table 3.5. Parameters for the production of anti-HER2 scFv.

Parameters	**Range or Media**
Induction temperature (°C)	16, 20, 25, 30
Duration of induction (h)	2, 4, 16, 20, 24
Concentration of IPTG (mM)	0.02, 0.1, 0.25, 0.5, 1
Culture Media	LB, TB, RMM [209], MR2 [210]

3.3.3. Preparation of Fractions

Cell pellets obtained from 4 ml LB medium were resuspended with 250 µl phosphate buffered saline (1x PBS) buffer. Cells were then ruptured via ultrasonic homogenizer (4 x 30 s on and 40 s off, on ice). To separate the soluble and insoluble fractions, it was centrifuged at 13000xg for 10 min and the supernatant, the soluble fraction, was taken into a new tube. Pellet was washed three times in 50 mM Tris-HCl, 1 mM EDTA at pH 8.0, to extract the insoluble fraction. Then, it was resuspended in 250 µl PBS and boiled for 10 min in the presence of 2% (w/v) SDS. Thus, this mixture was solubilized and centrifugation was applied at 13000xg for 10 min. At this time, the supernatant was recovered as the insoluble fraction.

3.3.4. Purification of ScFvs by Affinity

Cell pellets obtained from 100 ml or 1 L LB media were resuspended with equilibration buffer (20 mM sodium phosphate, 300 mM NaCl, 10 mM imidazole, pH 7.4) including a protease inhibitor cocktail. Then, cells were ruptured by either ultrasonic homogenizer or high pressure homogenizer at 16000–18000 psi. Centrifugation was performed at 12000xg for 15 min and soluble fractions were poured to the gravity-flow column loaded with resin and this mixture was incubated at 4°C for 1 h. Flow-through fractions were collected and the resin was washed with wash buffer (20 mM sodium phosphate, 300 mM NaCl, 50 mM imidazole, pH 7.4) until no absorbance was observed at the washing fractions at 280 nm. Lastly, scFvs that was adsorbed to resin were obtained with elution buffer (20 mM sodium phosphate, 300 mM sodium chloride, 250 mM imidazole, pH 7.4). Elution fractions were verified with SDS-PAGE, and then were pooled. ScFvs in elution buffer were desalted to remove imidazole and concentrated with 10K MWCO concentrator.

3.3.5. Preparation of Mammalian Cell Lysate

High-glucose DMEM supplemented with streptomycin (100 mg/ml), penicillin (100 U/ml), and 10% Hyclone FetalClone I serum was used for growth of HER2-positive SKOV3 cells. After growth was achieved, the medium was separated from cells by spinning down. Cells were washed three times with 10 ml 1xPBS. Then, cell pellets were resuspended in lysis buffer (150 mM NaCl, 50 mM Tris-Cl, 1% Triton X-100, pH 8.0). 1 ml lysis buffer was used for 10^7 cells. Cells in the lysis buffer were incubated on ice for 30 min, then centrifuged at 13500xg for 10 min, 4°C. The supernatant was stored at -20°C as the antigen for immunoassays.

3.4. Characterization

3.4.1. Cell Concentration

UV-Vis spectrophotometer was used to determine the cell concentration via the absorbance at 600 nm. For this purpose, sample was taken from liquid medium and diluted with 1xPBS by 1:1 - 1:5 ratio depending on the cell growth. OD_{600} was read between 0.1 – 0.8 to observe more accurate results.

3.4.2. Total Protein Concentration

Bradford analysis [211] was performed to determine the total protein concentration by a spectrophotometric method. Briefly, 200 µl of Bradford reagent was mixed with 10 µl sample in a microplate. After incubation for 10 min at room temperature (RT), the absorbance was measured by a microplate reader at 595 nm. BSA was used as a standard to prepare a calibration curve and determine the protein concentration in the range of 0-1.0 mg/ml.

3.4.3. SDS-Polyacrylamide Gel Electrophoresis (SDS-PAGE)

To separate proteins based on their molecular weight, SDS-PAGE analysis is applied. In this method, the use of SDS and reducing agent causes the linear structure with negative charges by destroying the tertiary structure of protein and masking the intrinsic charge of the protein. When SDS-treated proteins are loaded onto gel matrix in an electric field, proteins with negative charges move toward the anode at different speeds causing protein separation by a molecular sieving effect. In this study, SDS-PAGE method described by Laemmli [212] was used. For this purpose, protein samples in cell lysates or purified recombinant proteins (maximum 10 µg) were mixed with the 4x loading buffer combined with 2-mercaptoethanol (reducing agent) and proteins were denaturated by heating at 95°C for 5 min. Prestained dual color protein MW marker (3 µl) and samples up tp 50 µl were separated on a 12% SDS-polyacrylamide gel simultaneously at 100V of constant voltage.

The SDS-PAGE gels that were not going to be used in western blotting were stained using Coomassie stain and photographed. For Coomassie staining, the gel was stained 1 h at RT with gentle shaking after three washes for 5 min with water. Then, the gel was destained by washing with water for at least 2 h until the background was clear and the separated proteins were visualized by the gel documentation system. Percentage of target protein in the total protein was used to determine the purity of protein by densitometry analysis [213].

3.4.4. Western Blot Analysis

To detect scFvs in soluble and insoluble fractions, Western blotting was performed. This method is comprised of three steps: (1) separation of proteins by SDS-PAGE (2) transfer from the polyacrylamide gel to a membrane, and (3) incubation with primary antibodies specific for the target proteins and secondary antibodies for visualization [214]. For this purpose, samples were prepared by mixing with the sample buffer and loaded on 12% SDS-polyacrylamide gel. Then, separated proteins were transferred onto polyvinylidene fluoride (PVDF) membrane for blotting. The blot was blocked with 5% (w/v) milk in TBS (tris-buffered saline) containing 0.1% Tween-20 (TBST) for 1 h, after washing with TBS. Anti-6xHis-tag-HRP antibody, 1:7000 diluted, was applied for 1 h to probe the membrane, after three washes with TBST. After incubation with the antibody, washing with TBST and TBS was done. Lastly, the membrane was incubated with Western substrate to observe the bands. Relative quantification analysis was done to determine the ratio between soluble and insoluble expression. Hence, the band of insoluble fractions was taken as reference and the band intensities of soluble scFvs were divided by the reference.

3.4.5. Size Exclusion Chromatography (SEC)

Separation of multimeric protein structures from monomers, or desalting and buffer exchange applications to separate small molecules can be performed with size exclusion chromatography (SEC), also described as gel filtration. This separation occurs according to the permeation properties of the molecules through a bed of porous beads with distinct pore sizes. When the molecules go through the column by the buffer flow, smaller molecules diffuse into the pores that causes a longer retention time compared to larger molecules [215]. In this method, gel filtration buffer is passed through the system by the pump and sample is injected through inject valve by a syringe. A detection system placed after the column is applied for analysis of separation. A 96-well tray is used to collect proteins. A schematic representation of the SEC system used in the experiments is given in Figure 3.3.

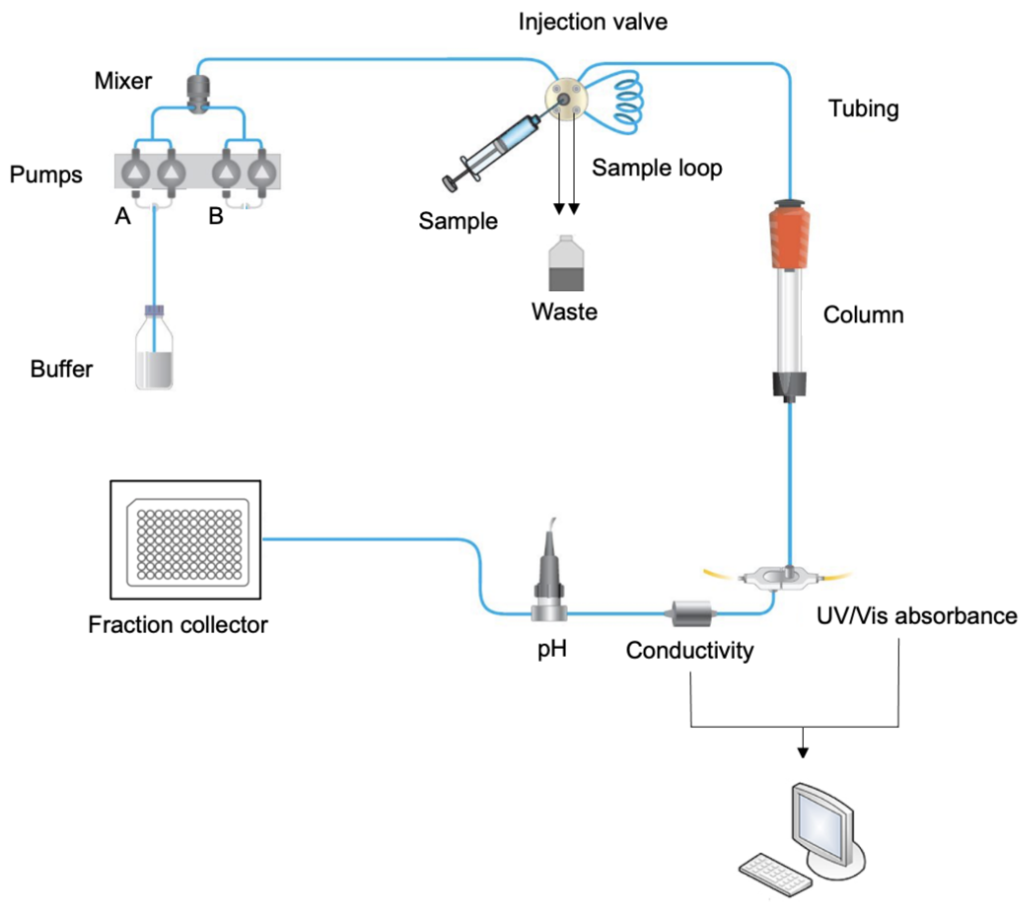

Figure 3.3. Representation of the SEC system. Figure modified from [216] and [217]

SEC analysis was performed for anti-HER2 scFvs in different domain orientations. An FPLC (Fast Protein Liquid Chromatography) system and Superdex-75 gel filtration column was used for separation of dimeric and monomeric structures. As a first step, equilibration of the column with 50 ml HBS-EP buffer (0.01 M HEPES, 0.15 M NaCl, 3 mM EDTA, 0.005% Tween, pH 7.4) at a flow rate of 0.5 ml/min was applied

[218]. Purified scFv (1 ml) was injected into the sample loop and the sample passes through the column at 0.5 ml/min with the buffer. A 96-well collection tray was used for sample collection. Absorbance values of fractions at 280 nm were recorded by the software. Hence, these values were graphed to observe multimeric/monomeric structures.

3.4.6. Enzyme-linked Immunosorbent Assay (ELISA)

Experiments are performed using hydrophobic and hydrophilic polystyrene plates. Based on the ELISA type, antibody/antigen coating, an analyte, a primary and/or secondary detection antibody and substrate are required for the experiment. In this study, direct, indirect and sandwich ELISA were applied.

3.4.6.1. Direct ELISA

ELISA plate was coated with serial diluted anti-HER2 scFvs, for 3 h at RT. Then, the plate was washed three times with wash buffer (0.05% Tween-20, 0.3% BSA in PBS). The coated wells were blocked with 200 µl/well of 5% (w/v) milk in wash buffer for 2 h at RT. After washing, 100 µl of 1:10,000 diluted anti-6xHis-tag-HRP antibody was added to each well for detection of scFvs. Last washing step was applied and 100 µl of TMB substrate was added to plate for development of color. Absorbance was read at 450 nm after reaction temination with 2 M H_2SO_4.

3.4.6.2. Indirect ELISA

ELISA plate was coated with commercial recombinant human HER2 of 0.2 µg/ml or mammalian cell lysate of 5-50 µg/ml in PBS, at 4°C overnight. Next day, the plate was washed three times with wash buffer. Blocking was performed by incubating the plate with blocking buffer at RT for 3 h. Subsequently, the wells were washed with the wash buffer three times. Then, 100 µl of purified scFvs with serial dilutions were added to plate and incubated for 1 h at RT. Concentrations of scFvs added to wells were calculated by multiplying purity of protein with total protein concentration determined with Bradford assay. After three times washing, bound scFvs were determined by addition of 100 µl of 1:10,000 diluted anti-6xHis-tag-HRP antibody in wash buffer. After incubating 1 h and applying same washing steps, 100 µl of TMB substrate was added to plate for development of color. The reaction was terminated with 2 M H_2SO_4. Using a microplate reader, the absorbance was measured at 370 nm before quenching, or 450 nm after treatment with H_2SO_4.

3.4.6.3. Sandwich ELISA

Sandwich ELISA was performed to test binding of scFvs to surfaces and affinity to the antigen. Briefly, different types of ELISA plates were coated 3 h with purified anti-HER2 scFv or scFv13-R4 constructs. After washing step, plate was blocked with blocking buffer for 2 h at RT. After another washing step, plate was incubated with serial dilutions of purified β-gal or HER2 antigen in the wells (100 µl/well) for 1 h at room temprature. After washing, 100 µl of 1:5000 diluted StrepTactin-HRP or 1:5000 diluted rabbit anti-human IgG (Fc specific)-HRP antibody was added to each well for 1 h incubation. After the last wash, 100 µl of TMB substrate was added to plate for development of color. Absorbance was read at 450 nm after reaction temination with 2 M H_2SO_4.

3.4.7. Statistical Analysis

To compare the differences between soluble/insoluble ratios of scFvs, statistical analysis was performed. For this purpose, One-way ANOVA with Tukey's multiple test was applied via GraphPad Prism software. Based on the analysis, the probability (*P*) value less than 0.05 was accepted as significantly different.

3.5. Determination of Binding Affinity

3.5.1. Surface Plasmon Resonance (SPR) Method for K_d Calculation

SPR method was applied for equilibrium binding-affinity measurements by following similar steps of published studies [218, 219]. Firstly, optimum concentration of HER2 to immobilize on the sensor surface and the optimum pH of the buffer was determined as 8 µg/ml in 10 mM sodium acetate and pH 5.0, respectively. Covalent immobilization of HER2 antigen on CM5 chip sensor surface was achieved by amine coupling with a level of 800 response units (RU). ScFvs were in diluted in running buffer (HBS-EP buffer) in the range of 0.625 – 80 nM. Then, each sample was injected over the chip with the same buffer at a flow rate of 20 µl/min (3 min injection time, 10 min stabilization time, 15 min dissociation). The surface of the chip was regenerated by 20 µl/min of 10 mM glycine, pH 1.5 (2.5 min injection time, 5 min stabilization time) after each injection. The equilibrium response units of each concentration were fitted to 1:1 Langmuir binding isotherm to calculate the dissociation constant (K_d) value of scFvs. GraphPad Prism software was used for nonlinear regression analysis to calculate K_d based on the Equation 2.20.

3.5.2. ELISA Method for K_d Calculation

K_d values of anti-HER2 scFvs were determined by ELISA using two different approaches determined by Friguet [192] and Beatty [198].

In the Friguet [192] method, firstly, two identical plates were coated with 0.2, 0.1, 0.05 and 0.01 µg/ml commercial HER2 to determine the antigen coating amount. Two plates were handled at same time and unbound scFv from first plate was recovered and used in the second plate. ELISA procedure given in Section 3.4.6.2 was applied. Signals obtained from the two plates were compared and the coating amount of antigen that gave the signal difference around 10% was chosen. Then, the ELISA plate was coated with the predetermined amount of HER2. During blocking part, serial dilutions of HER2 in a final volume of 150 µl and 0.01 µg/ml scFv (0.37 nM) in 150 µl were prepared. ScFv, 150 µl, was added to each antigen dilution, mixed and incubated for 1h at RT. Then, this mix was used for the ELISA plate and the same procedure with Section 3.4.6.2 was applied. K_d was calculated using Equation 2.13.

For the Beatty [198] method, ELISA plates were coated with 0.2, 0.1, 0.05 µg/ml commercial HER2 and the same procedure with Section 3.4.6.2 was performed. K_d was calculated using Equation 2.14.

3.6. *In silico* Methods

3.6.1. Tertiary Structure Prediction

The 3D models of scFv structures were constructed using homology modeling as implemented in SWISS Model [181] by following the algorithm given in Figure 2.5. Anti-HER2 scFvs with V_LV_H order were modeled based on the crystal structure of a single chain disulfide-stabilized construct (sc-dsFv), diabody (resolution 2.4 A°, PDB entry:3auv.1.A); while, anti-HER2 scFv-V_HV_L order was modeled based on the crystal structure of diabody (resolution 1.7 A°, PDB entry:5gs3.1). 3D structure of HER2 (PDB entry:1N8Z) was used for docking studies. PyMOL software was used for visualization of 3D structures.

3.6.2. Molecular Docking of HER2 and Anti-HER2 scfvs

Molecular docking of anti-HER2 scFvs with HER2 antigen was carried out using ClusPro 2.0, which is a web-based program [184]. Docking was performed in antibody mode; the scFvs were submitted as the receptor, and HER2 as the ligand. Default parameters were chosen for analysis. The predicted models were selected based on the energy scores given by ClusPro.

3.6.3. Molecular Dynamics Simulation

MD simulations of anti-HER2 scFvs and scFv-HER2 complexes were performed using GROMACS version 2018 [29]. Firslty, the proteins were embedded in a cubic box to create boundary conditions. Then, the system was solvated with water using spc216 water model, and AMBER99SB-ILDN force field was used. Subsequently, neutralization was applied by the addition of Cl^- or Na^+ ions. Energy minimization was performed with two steps before the main run of simulation. The whole system was energy minimized for 50000 iterations until 1000 kj/mol/nm force was observed. Equilibration was performed in two phases by maintaining temperature at 300 K and pressure at 1 atm. The resulting system was subjected to MD simulation for 20 ns. All the resulting trajectories were analyzed and graphed utilizing from g_energy, g_gyrate, g_rmsf, g_rms and do_dssp tools of GROMACS.

MM-PBSA approach supplemented with the g_mmpbsa script program [190] was used to calculate binding free energy of the selected molecules to investigate the relative binding affinity, and equations given in Section 2.6.4 were used.

4. RESULTS AND DISCUSSION

In this study, the production of model scFvs with soluble, active and correctly folded properties in *Escherichia coli* strain was proposed and the effects of linker region on scFvs for diagnostic applications were investigated. In the first part of the study, scFv version of Herceptin^{TM} [28] was constructed in two different orientations, and appropriate strain and growth conditions for expression of soluble scFvs were determined. Then, the expressed recombinant scFvs in different orientations were compared in terms of solubility, monomer/dimer formation, binding activity and affinity. Soluble production was shown using SDS-PAGE and Western blot analyses; while *in vitro* immunological characterization of scFvs was performed with ELISA and SPR. In the second part of the study, scFvs containing linkers with different amino acid composition were constructed and evaluated by both computational and experimental analyses. ELISA was used to compare the binding activity and affinity of purified recombinant scFvs. In addition, homology modelling and molecular dynamics simulation were applied to observe the differences of scFvs related to their functionality.

4.1. Design and Construction of Plasmids for Anti-HER2 scFv Expression

The antigen-binding site of antibodies forms at the interface of their two variable domains (V_L and V_H), where V_L and V_H domains are naturally not directly linked as in the case of artificially connected scFvs. Different approaches predicting the correct V_H and V_L orientation have been developed in antibody humanization and antibody modeling studies to preserve original antibody domain orientation [220, 221]. An scFv construct can be formed by fusing a linker between the V_L and V_H genes of the antibody in either the V_H-linker-V_L or the V_L-linker-V_H orientation. Previous studies showed that domain orientation, the length and amino acid content of the linker peptide could affect antigen-binding activity, expression efficiency and stability of scFvs [5, 222]. Based on these results, two scFv constructs containing two different orientations of variable domains (V_H-linker-V_L and V_L-linker-V_H) were designed in this study (Figure 4.1), due to lack of information about the native domain orientation of the antibody targeting HER2.

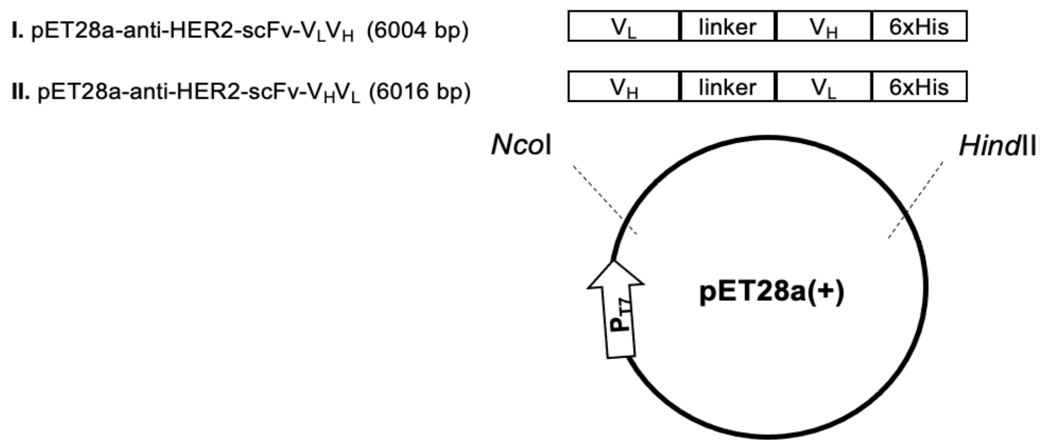

Figure 4.1. Diagram of the pET28a vector encoding anti-HER2 scFvs in V_LV_H and V_HV_L orientations [223]

V_H and V_L genes were obtained from the heavy and light chain domains of pMAZ360-cIgG-Herceptin plasmid [28]. Primers were designed to amplify V_H and V_L domains of the antibody, which are 330 bp and 360 bp, respectively, and combine these fragments via the most common $(Gly_4Ser)_3$ linker peptide. In addition, primers designed for the C-terminus contained the polyhistidine tag (6xHis) for immuno-detection and purification purposes and a stop codon.

P1 and P2 primers (Table 3.3) were used to amplify the V_L fragment while P3 and P4 primers were used for the V_H fragment (Section 3.2.1) in constructing the anti-HER2-scFv-V_LV_H gene. The V_L gene cassette was 362 bp and V_H gene cassette was 417 bp, as shown in Figure 4.2.

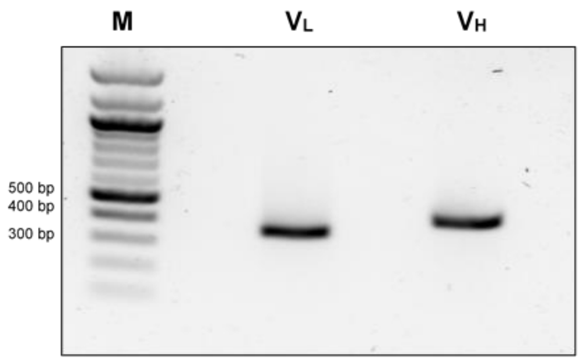

Figure 4.2. Agarose gel electrophoresis of V_L and V_H genes amplified by PCR to construct anti-HER2-scFv-V_LV_H gene; M: 100 bp DNA Ladder

P5 and P6 primers were used to amplify the V_H fragment while P7 and P8 primers were used for the V_L fragment (Section 3.2.1) to construct anti-HER2-scFv-V_HV_L gene. The V_H gene cassette was 395 bp and the V_L gene cassette was 396 bp (Figure 4.3).

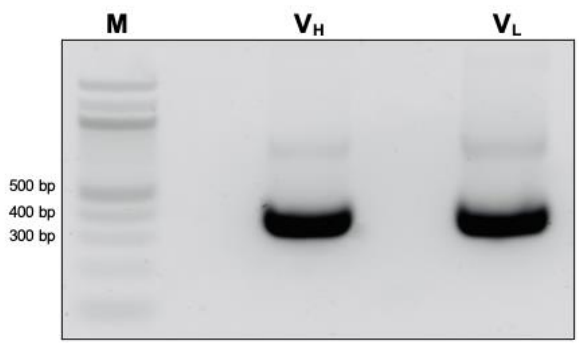

Figure 4.3. Agarose gel electrophoresis of V_H and V_L genes amplified by PCR to construct anti-HER2-scFv-V_HV_L gene; M:100 bp DNA Ladder

After verifying the bands of V_L and V_H domains, equal amounts of the linker, V_L and V_H domains joined by SOE-PCR generated the anti-HER2 scFv gene in both orientations, yielding two 764-bp products (Figure 4.4).

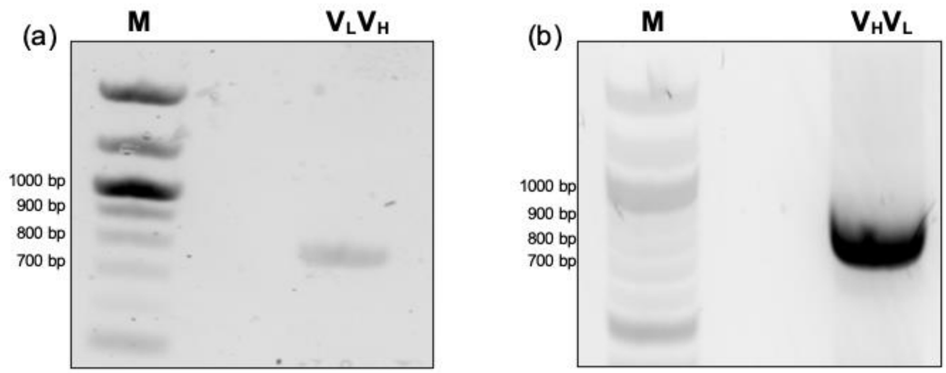

Figure 4.4. Agarose gel electrophoresis of overlap extension PCR products of (a) anti-HER2-scFv-V_LV_H and (b) anti-HER2-scFv-V_HV_L; M: 100 bp DNA Ladder

The pET28 plasmid (5369 bp) was digested with *Nco*I-HF and *Hind*III-HF to create the backbone and visualized in agarose gel electrophoresis after digestion (Figure 4.5, Lane 2). Undigested plasmids run faster on agarose gel and thus, are not useful in determining the actual plasmid size (Figure 4.5, Lane 4).

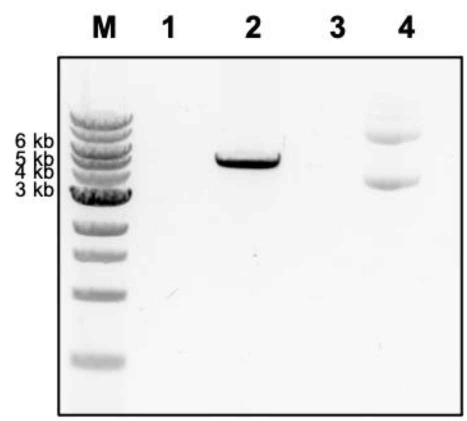

Figure 4.5. Agarose gel electrophoresis of pET28a plasmid. Lane 2: digested with *Nco*I-HF and *Hind*III-HF, (5252 bp), Lane 4: undigested, M: 1 kb DNA Ladder

The ligation reaction was performed to clone the double digested PCR products into double digested vector (pET28a) DNA. Finally, expression plasmids pET28a-anti-

HER2-scFv-V_HV_L and pET28a-anti-HER2-scFv-V_LV_H were generated and the constructs were verified via DNA sequence analysis.

4.2. Selection of Bacterial Expression System

In this study, cytoplasmic expression of scFvs was proposed due to the larger production space of the cytoplasm compared to the periplasmic region. However, expression of scFvs, which have two intramolecular disulfide bonds, could be difficult in the cytoplasm since reducing environment of this compartment prevents the disulfide bond formation that is crucial for structural stability and correct folding [224]. Hence, two different bacterial strains, *E.coli* SHuffle T7 Express and BL21(DE3), were chosen as candidates for the expression of scFvs. While BL21(DE3) that is the most widely used bacterial expression host is deficient in proteases OmpT and Lon, which degrade many proteins, SHuffle T7 Express has been genetically engineered to provide the oxidizing environment for disulfide bond formation [91, 93, 225].

Firstly, soluble production of scFvs in both strains was investigated by small-scale expression. Anti-HER2 scFv-V_LV_H and scFv735 [203] were selected as model antibody fragments to compare and understand the versatility of effects of the selected expression hosts on solubility for any scFv. Both strains were induced by 1 mM IPTG at 30°C for 16 h. The predicted sizes of scFvs were ~27 kDa, which were verified by Western blot (Figure 4.6) with the anti-6x-His-tag-HRP antibody. While soluble cell lysate protein concentration of BL21(DE3) strain expressing anti-HER2 scFv was 2.8 mg/ml and that of scFv735 was 6.9 mg/ml, these values were 1.5 mg/ml and 4.8 mg/ml for SHuffle strain, respectively. These results indicated that the soluble cell lysates of *E. coli* BL21(DE3) had higher total protein concentration than SHuffle strain. This could be possibly due to co-expression of the DsbC in the cytoplasm of the SHuffle strain that restricts the targeted recombinant protein production [104]. Moreover, protease deficient genotype of BL21(DE3) could be the reason for higher levels of total protein in this strain [226]. When equal amounts of total proteins were compared in terms of solubility, both recombinant scFvs exhibited greater soluble accumulation in the soluble fractions when expressed in SHuffle cells compared to expression in BL21(DE3), as expected.

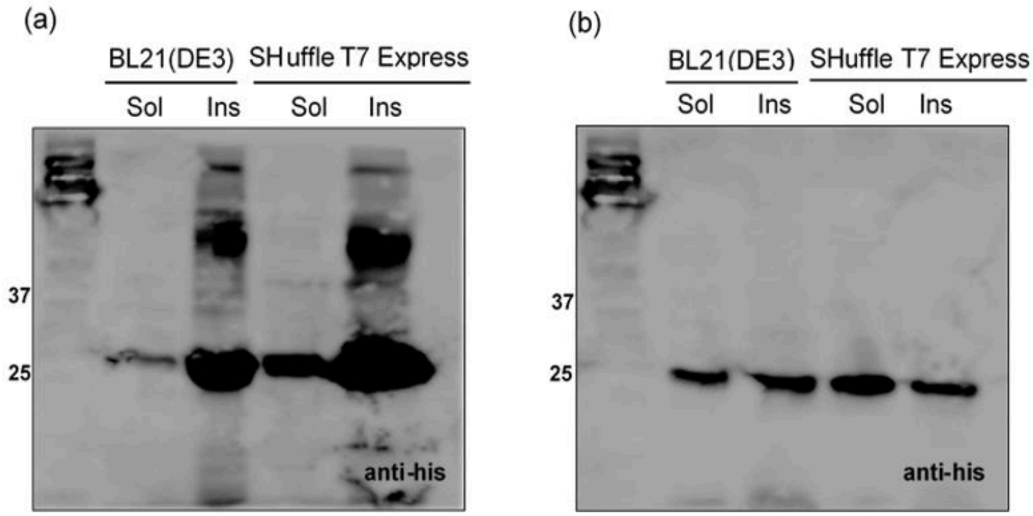

Figure 4.6. Western blot analysis of insoluble and soluble fractions from SHuffle T7 Express or BL21(DE3) strains expressing (a) anti-HER2-scFv or (b) scFv735, normalized based on total protein

In addition to solubility, anti-HER2 scFvs expressed in SHuffle T7 Express and BL21(DE) were also compared according to their binding activities by ELISA. HER2 positive SKOV3 cell lysate was used as an antigen and soluble fractions of cell lysates were used as binders for an in-house ELISA test. Firstly, plates were coated with 5-50 µg/ml mammalian cell lysate to optimize the coating antigen amount. Binding of the cell lysate decreased with increasing antigen concentration as shown in Figure 4.7. Hence, the optimum concentration for cell lysate was determined as 5 µg/ml. Then, scFv-V_LV_H obtained from both strains were affinity purified. Using the purified proteins in ELISA tests, antibody fragments obtained from SHuffle T7 Express cells showed up to four-fold higher binding signal compared to that expressed in BL21(DE3) as shown in Figure 4.8. In addition, PBS and BSA were used as negative controls, with absence of binding activity towards HER2.

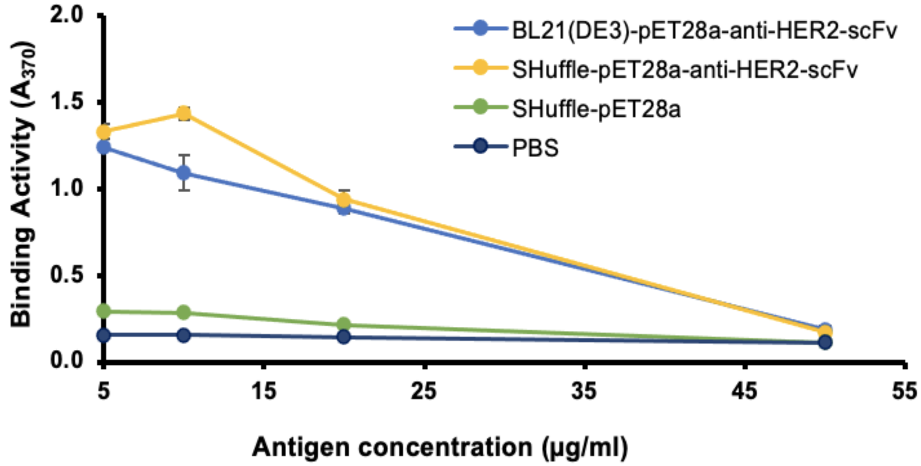

Figure 4.7. Antigen-binding of cell lysates containing anti-HER2 scFv to determine the optimum antigen concentration. Plates were coated with 5-50 μg/ml mammalian cell lysate and 50 μg total protein was applied to plate. The empty pET28a and PBS served as negative controls.

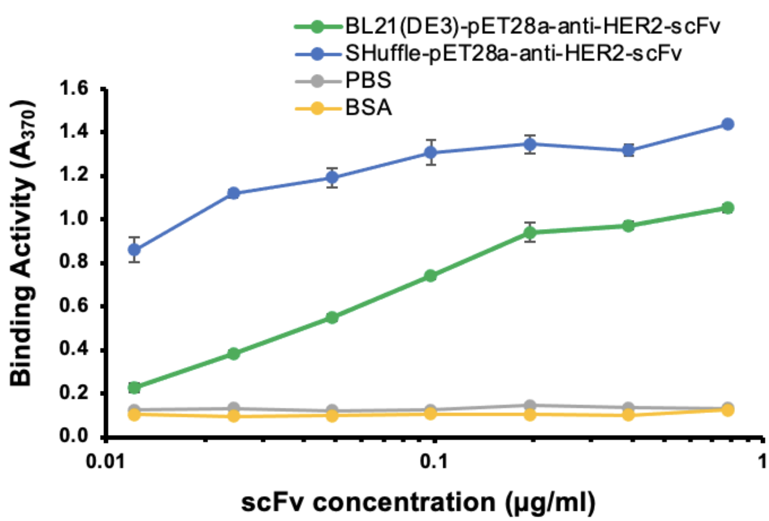

Figure 4.8. Binding activity of purified anti-HER2 scFv-V_LV_H expressed in *E. coli* SHuffle T7 Express and BL21(DE3) against HER2 antigen obtained from mammalian cell lysate. Experiment was performed in triplicate and error bars display standard deviation (SD) of the mean [223].

The difference in binding activity could be explained as formation of the disulfide bonds which stabilized the recombinant scFv, thus affected the antigen-binding activity. This result was also consistent with a recent study [17]. Additionally, Safarpour and coworkers compared TNF-α expression in *E. coli* SHuffle and BL21(DE3) cells and observed 1.5 times higher disulfide bridge band in SHuffle than that of BL21(DE3) via Fourier transform infrared spectroscopy (FTIR) analysis [227]. Overall, the subsequent expressions of anti-HER2 scFv were decided to be performed with SHuffle T7 Express strain owing to higher solubility production and binding-activity. Moreover, HER2 binding-activity of anti-HER2 scFv obtained from SHuffle was compared with a full-length antibody (trastuzumab) obtained from a mammalian cell line [228]. As seen in Figure 4.9, full-length antibody had a higher binding-activity owing to its two antigen binding sites, whereas scFv having one binding site also showed a similar binding trend with trastuzumab.

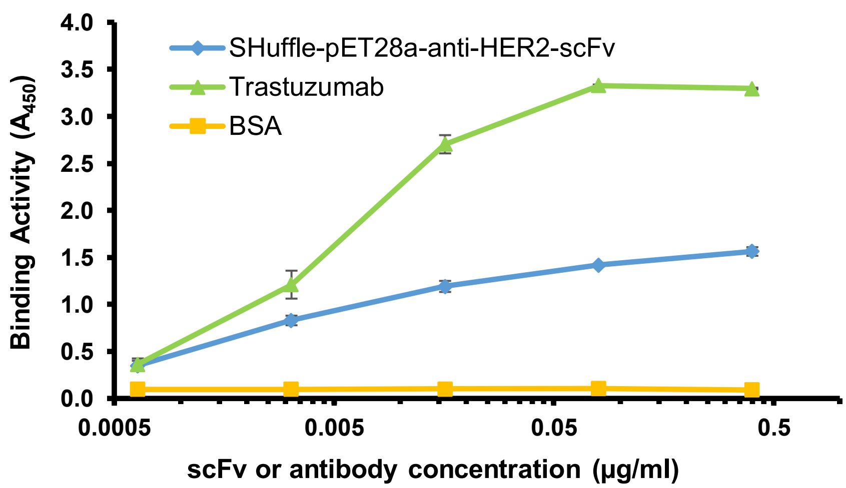

Figure 4.9. Binding-activity of purified anti-HER2 scFv-V_LV_H construct expressed in *E. coli* SHuffle T7 Express cells and trastuzumab expressed in a mammalian cell. Experiment was performed in triplicate and error bars display SD of the mean.

4.3. Expression of Anti-HER2 scFvs in Different Orientations

As seen in Figure 4.6.a, insoluble accumulation of scFv-$V_L V_H$ expressed in SHuffle T7 Express strain was fairly higher than the soluble fraction, while this situation was the opposite for scFv735 (Figure 4.6.b). Therefore, the effects of bioprocess parameters such as induction temperature, duration of induction and inducer concentration were investigated for anti-HER2 scFv expressed in SHuffle cells to increase the soluble fraction yield.

4.3.1. Effects of Different Induction Conditions on Expression

It was reported that lower cultivation temperatures often cause improved amounts of correctly folded soluble protein as well as increased intracellular stability of the protein [229]. Therefore, post-induction temperature (T_{ind}) was decreased from 30°C to 16°C to observe the effect of temperature. Western blot analysis was performed to compare insoluble and soluble fractions (Figure 4.10.b). It was observed that the soluble/insoluble ratio increased approximately three-fold when T_{ind} was lowered to 16°C from 30°C (Figure 4.10.a). In addition, an absorbance value of OD_{600}=3.5 was obtained at the end of cultivation for T_{ind}=30°C, while it was 1.9 for 16°C, thus showing decrease in bacterial growth at lower temperatures, as expected. Hence, it can be concluded that whereas expression at 30°C results in greater biomass, better soluble expression was attained at 16°C, since lower temperatures reduces the tendency to aggregate and misfold, as well as the proteolytic degradation.

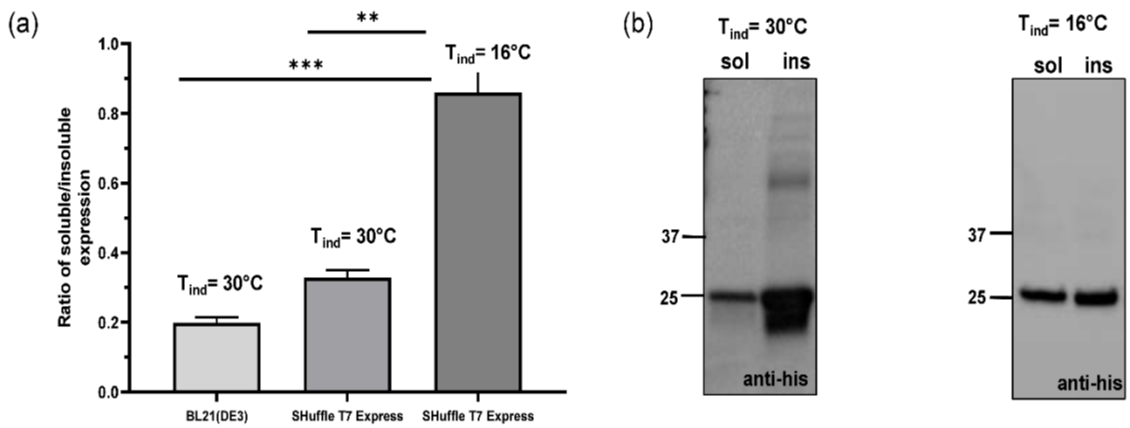

Figure 4.10. (a) Soluble/insoluble ratio for anti-HER2 scFv-V_LV_H expressed in BL21 (DE3) and SHuffle T7 Express, at different T_{ind} (16°C or 30°C). (b) Western blots of insoluble (ins) and soluble (sol) fractions from *E. coli* SHuffle T7 Express cells expressing anti-HER2 scFv-V_LV_H induced at either 30°C (left panel) or 16°C (right panel) for 16 h. Samples were normalized based on total volume. All data are the average of two independent experiments; error bars are the standard deviation of the mean. ** and *** represent the significant differences at *P*-value<0.01 and *P*-value<0.001, respectively [223].

After observing the increase in soluble fraction yield at lower temperatures, anti-HER2 scFv expressions in both V_H-linker-V_L and V_L-linker-V_H order were compared at four induction temperatures of 16, 20, 25 and 30°C. Growth of SHuffle cells containing anti-HER2 scFv-V_HV_L and anti-HER2 scFv-V_LV_H were observed by measuring the absorbance values of OD_{600} between 0-24 hours after induction. Protein expression was induced when OD_{600} values of SHuffle cells reached approximately 0.6. As shown in Figure 4.11.a and Figure 4.11.b, strains reached their log phase 4 h after inoculation. When equal volumes of total proteins were loaded on SDS-PAGE gels, band of overexpression at ~27 kDa was observed in all induction temperatures for both orientations (Figure 4.11.c and Figure 4.11.d).

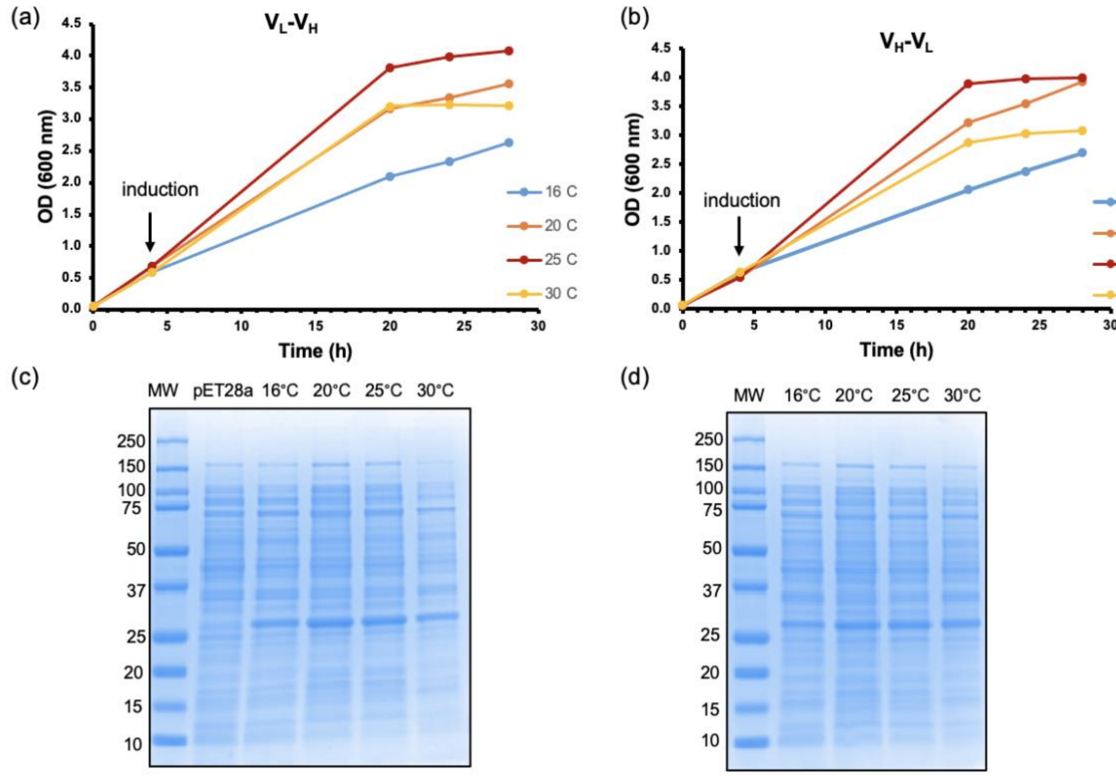

Figure 4.11. Growth curve of SHuffle T7 Express containing (a) pET28a-anti-HER2-scFv-V_LV_H and (b) pET28a-anti-HER2-scFv-V_HV_L. SDS-PAGE analysis of total cell protein containing (c) anti-HER2 scFv-V_LV_H and (d) anti-HER2 scFv-V_HV_L expressed in *E. coli* SHuffle at 16, 20, 25 and 30°C, 16 h after induction

It was reported that IPTG in higher concentrations could cause toxic effects on cells which resulted in reduction in cell growth rate and increase in the amounts of proteins in the form of aggregations [230]. Therefore, the effect of IPTG on expression of anti-HER2 scFvs were examined by varying concentrations between 0.02 – 1 mM. As seen Figure 4.12, band of overexpression at ~27 kDa was observed in all induction concentrations for both orientations, and IPTG concentration showed no significant effect on scFv expression and cell growth.

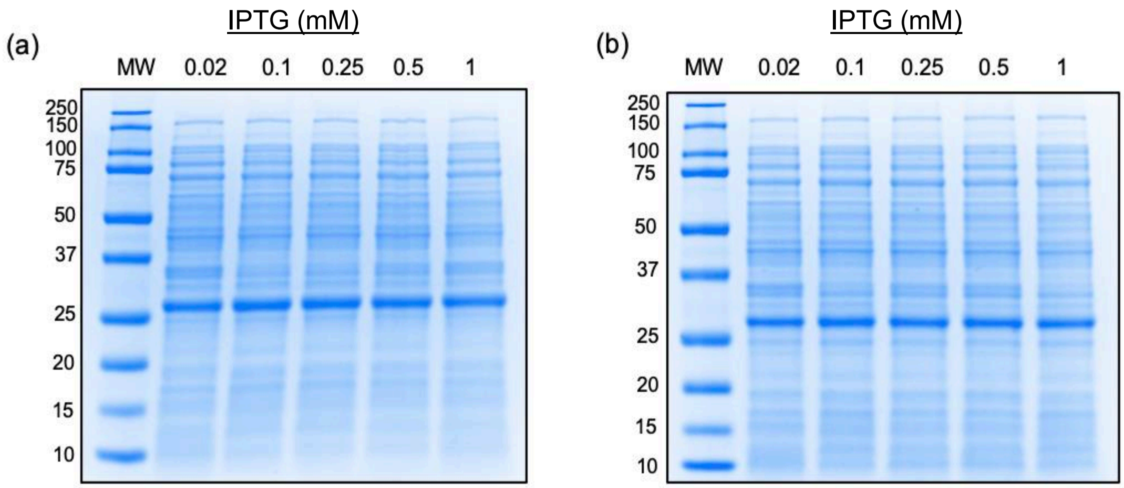

Figure 4.12. SDS-PAGE analysis of total cell protein containing (a) anti-HER2 scFv-V_LV_H and (b) anti-HER2 scFv-V_HV_L induced at various IPTG concentrations (0.02, 0.1, 0.25, 0.5 and 1 mM) at 16°C for 16 h

In addition, the cell pellet of SHuffle cells containing pET28a-anti-HER2-scFv-V_LV_H were collected at 2, 4, 16, 20 and 24 h after induction. As seen Figure 4.13, band of overexpression at ~27 kDa increased with time. However, total protein concentration decreased after 20 h of induction.

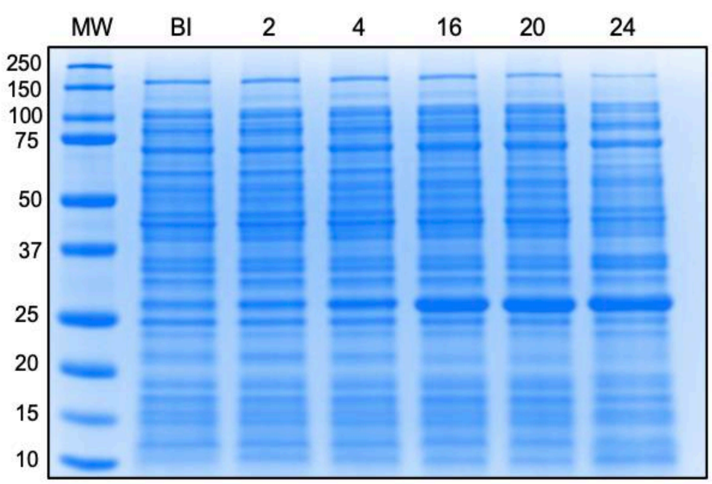

Figure 4.13. SDS-PAGE analysis of proteins from whole cell lysate containing anti-HER2 scFv-V_LV_H at different post-induction times (2, 4, 16, 20 and 24 h); induction with 0.1 mM IPTG at 16°C. BI: Before induction

Overall, production conditions were optimized as 0.1 mM IPTG induction at 16°C for 16 h after induction. Indeed, expression of anti-HER2 scFvs at 20°C and 25°C were high in terms of both cell growth and total protein concentration. Nevertheless, 16°C was chosen as the induction temperature, mainly for contunuity of experiments. Since, lower induction temperature decreased aggregation and favored correct folding as reported in previous studies, and an acceptable amount of recombinant protein expression was obtained, being a satisfactory condition for further experiments. While a recent study indicated 30°C as the optimal induction temperature for SHuffle strain expressing anti-HER2-scFv [17], another report showed that an active anti-*Listeria monocytogenes* scFv could be obtained in the cytoplasm of SHuffle strain, at T_{ind}=16°C [231].

4.3.2. Effects of Different Media on Expression

According to the literature, recombinant protein production in a chemically defined minimal medium is important for large-scale industrial productions. However, there has been no study about efficient soluble protein expression in engineered cells such as the SHuffle strain at bioreactor scale by using chemically defined minimal media, because cells need a rich growth medium including yeast extract or soytone [15]. Nevertheless, in a recent study, Δgor/ΔtrxB *E. coli* Rosetta-gami B(DE3)pLysS strain was cultivated in a defined medium and it was the first report for an *E. coli* having oxidizing cytoplasm to reach high cell densities in a minimal medium [232].

Hence, two complex media, LB and TB, and two minimal media, RMM [209] and MR2 [210] were investigated. Batch fermantations were performed in the shake flasks to compare the four different media. Anti-HER2 scFv-V_LV_H was expressed in 50 ml culture media, induced by 0.1 mM IPTG at 16°C. In Table 4.1, final OD_{600} values of SHuffle cells and total protein concentrations are given. Depending on the media, final OD_{600} reached ~9 in MR2 which was superior to the other media in terms of cell density. Total protein concentrations of cells expressed in different media were in the similar range.

Table 4.1. Growth characteristics of SHuffle cells in different media.

Medium	OD_{600} at harvest	Total protein (g/L)
LB	3.5	3.1
RMM	3.4	4.5
MR2	8.9	4.7
TB	6.3	5.0

Expression of anti-HER2 scFv-V_LV_H was analyzed by SDS–PAGE (Figure 4.14). Overexpression bands of scFv appeared around 27 kDa in four different culture media. Hence, our results showed soluble expression of scFvs in SHuffle cells also in minimal media without complex additives. In summary, TB medium can also be used as alternative complex media; and for chemically defined media, especially MR2, can be an alternative with regard to better cell growth and expression for further high cell-density fermentation experiments.

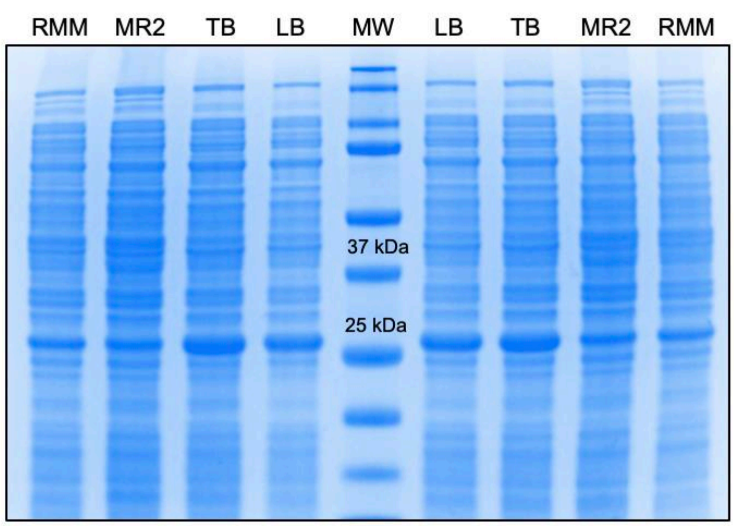

Figure 4.14. SDS-PAGE analysis of total cell protein containing anti-HER2 scFv-V_LV_H expressed in different culture media (LB, TB, MR2 and RMM). (Left side shows equal volume loading, right side shows equal amount of total protein loading)

4.4. Comparison of Anti-HER2 scFvs

Previous studies on expression of scFv versions against HER2 constructed the scFvs in the orientation V_H–linker–V_L [17, 78]. Since scFvs can be engineered in both orientations and optimal domain order is specific for each individual scFv, comparison of two different orientations of scFv was performed for evaluation of the effect of domain orientation on expression level, biological activity and prevalence of monomeric/dimeric forms.

4.4.1. Expression Yield of Anti-HER2 scFvs

Anti-HER2 scFvs with V_L-V_H and V_H-V_L order were expressed in 1 L culture media, induced by 0.1 mM IPTG at 16°C post-induction temperature. Before purification, total protein in empty plasmid and plasmids with anti-HER2-scFv-V_HV_L and anti-HER2-scFv-V_LV_H were observed by SDS-PAGE gel (Figure 4.15.a). Then, purification was applied with 1 ml Ni-NTA resin. The amounts of anti-HER2-scFv-V_HV_L and anti-HER2-scFv-V_LV_H after purification were determined as 6.2 mg and 9.3 mg, respectively. Moreover, the purities of both constructs were above 99%, as seen in Figure 4.15.b.

In a recent study, 5 mg/L of scFv version of pertuzumab in the V_HV_L order was produced from the soluble fraction, whereas scFv obtained from the insoluble fraction was 24 mg/L, though an extra *in vitro* refolding process was applied to make it biologically active [233]. In another study, 8 mg/L anti-HER2-scFv with 92% purity was produced in a widely used eukaryotic expression host *Pichia pastoris* [234]. Thus, it can be concluded that the purity and yields determined for anti-HER2 scFv-V_LV_H and scFv-V_HV_L constructs in this study are compatible with the previous studies. It is worth noting that both anti-HER2-scFv-V_HV_L and anti-HER2-scFv-V_LV_H showed soluble expression in this study. For example, Ayyar and coworkers reported that only the scFv with V_L-V_H orientation was produced in soluble form when two different domain orientations of the scFv developed for an autoimmune disease were compared [235].

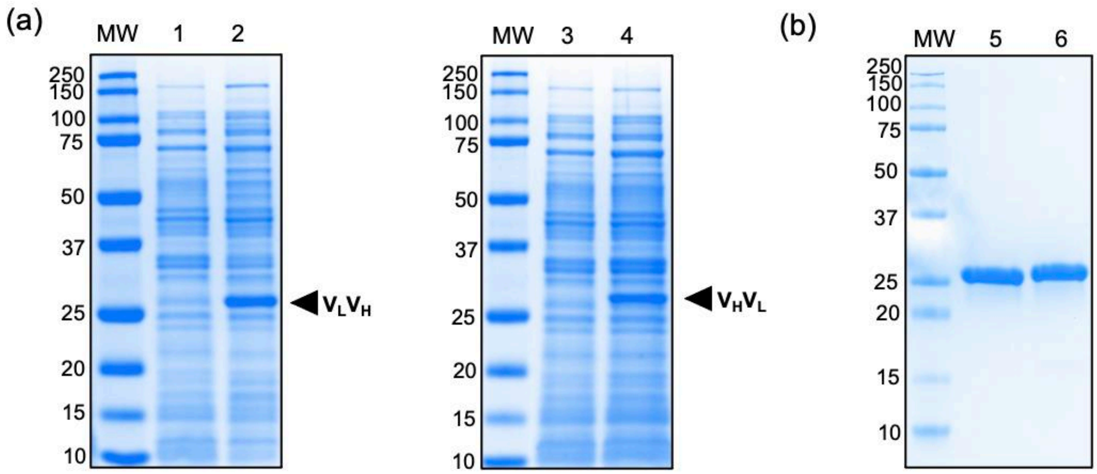

Figure 4.15. SDS-PAGE analysis of anti-HER2-scFvs expressed in *E. coli* SHuffle T7 cells at 16°C, 16 h. (a) Total protein from pET28a (lane 1 and lane 3), pET28a-anti-HER2 scFv-V_LV_H (lane 2), and pET28a-anti-HER2 scFv-V_HV_L (lane 4). (b) Purified anti-HER2 scFv-V_LV_H (lane 5) and anti-HER2 scFv-V_HV_L (lane 6) [223]

4.4.2. Monomer/Dimer Formation of Anti-HER2 scFvs

The formation of monomer/dimer or aggregates is specific for each antibody fragment, which can be designed with linkers containing different length and amino acid concentration [236]. Therefore, SEC was applied to examine the formation of monomeric/dimeric structures of the purified anti-HER2 scFvs. Two elution peaks referring to monomeric and dimeric forms of scFvs were observed in graphs plotted with absorbance values of elution fractions as seen in Figure 4.16. Both domain orders of scFv showed monomeric and dimeric forms. While scFv-V_LV_H had mostly dimeric and also a major monomeric portion, scFv-V_HV_L was mainly in the monomeric structure.

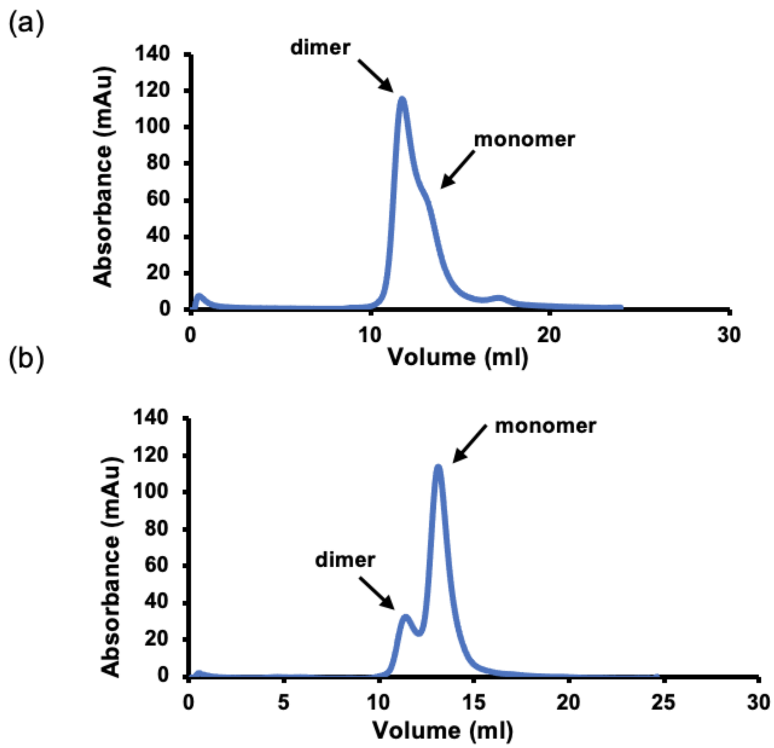

Figure 4.16. SEC analysis of (a) anti-HER2 scFv-V_LV_H and (b) anti-HER2 scFv-V_HV_L using a Superdex 75 10/300 GL gel filtration column

Monomeric and dimeric fractions that showed a peak in Figure 4.16 were analyzed by loading them onto SDS-PAGE gels and staining by Coomassie blue. Since the reducing conditions of loading dye with mercaptoethanol breaks the dimers while boiling the samples, all the fractions indicated a single band at molecular size of anti-HER2 scFv, 27 kDa (Figure 4.17). Additionally, purified anti-HER2 scFv-V_LV_H and anti-HER2 scFv-V_HV_L were loaded on the SDS-PAGE under reducing (presence of mercaptoethanol) and non-reducing (absence of mercaptoethanol) conditions as shown in Figure 4.18. As shown in the figure, the presence of two bands corresponding to monomeric and dimeric forms were detected, which are approximately 27 kDa and 54 kDa, respectively. Presence of the band showing the dimeric structure for anti-HER2 scFv-V_LV_H was consistent with the SEC analysis. Based on these results, it can be deduced that dimeric form of scFvs could be formed by disulfide bridges between free cysteine moieties of scFvs when protein was expressed in the oxidizing environment. Since domain order of scFv changes the prevalence of monomeric and dimeric forms, the order of the V_L and V_H domains can be a significant parameter while constructing the scFv based on the purpose of application.

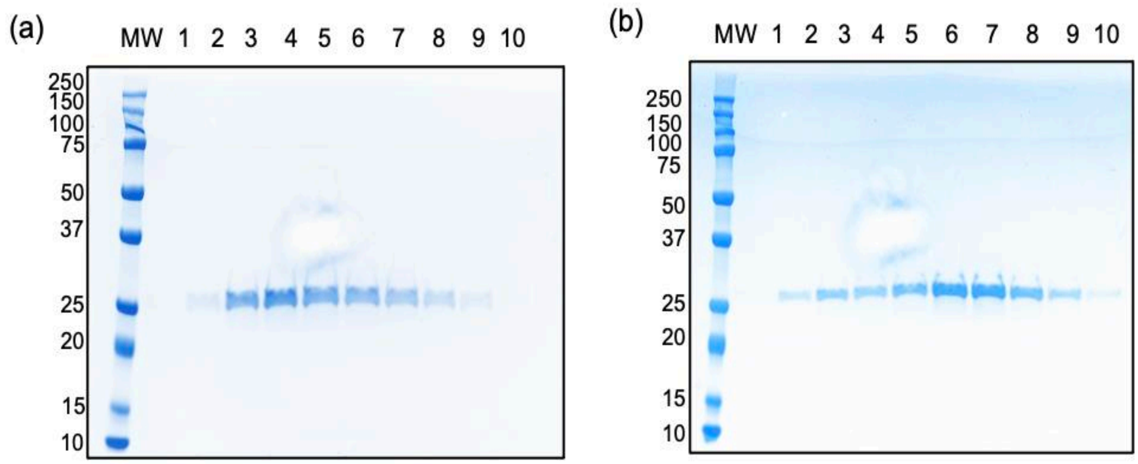

Figure 4.17. SDS-PAGE analysis for SEC fractions of (a) anti-HER2 scFv-V_LV_H and (b) anti-HER2 scFv-V_HV_L.

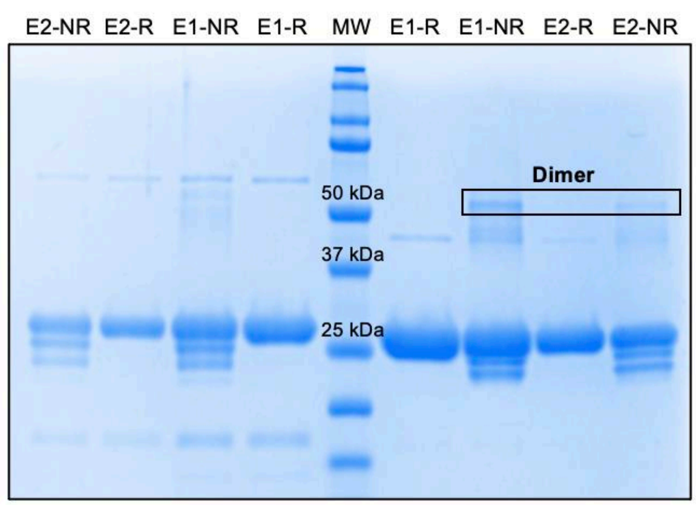

Figure 4.18. SDS-PAGE analysis of purified anti-HER2 scFv-V_LV_H (right side) and anti-HER2 scFv-V_HV_L (left side) under reducing and non-reducing conditions. R: reducing; NR: Non-reducing

4.4.3. Antigen-Binding Activities of Anti-HER2 scFvs

It was reported that variable domain orientation also affects antigen-binding properties of the scFv in addition to expression. It could be explained by the effect of order of variable domains on the regulation of antigen-binding site geometry [59, 237]. In this study, ELISA and SPR analyses were utilized to investigate the binding properties of anti-HER2 scFvs. ELISA was applied by interaction of commercial HER2 as immobilized antigen with anti-HER2 scFvs diluted serially. It was observed that anti-HER2 scFv-V_HV_L showed higher binding activity than anti-HER2-scFv-V_LV_H between 0.001-0.04 µg/ml scFv concentration (Figure 4.19). It could be also concluded that dimer formation of anti-HER2-scFv-V_LV_H discussed in previous title does not block the HER2 binding site. In addition, Histidine-tagged scFv13-R4 targeting β-galactosidase was applied to ELISA plates, expecting no binding activity against HER2.

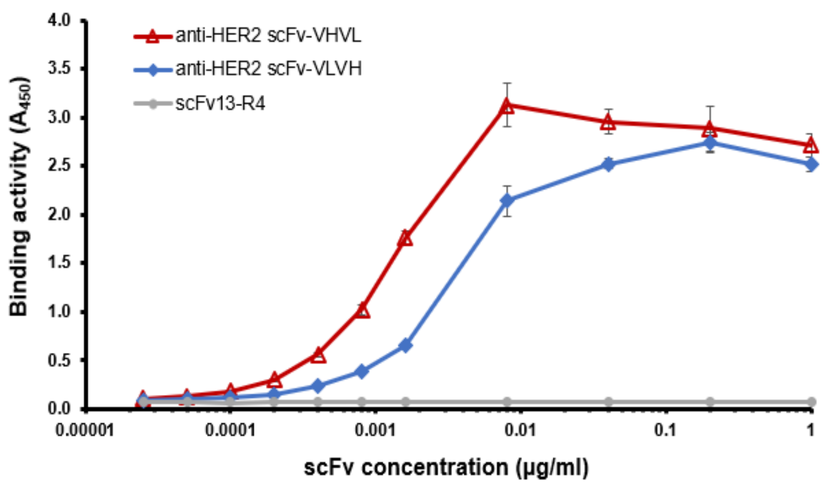

Figure 4.19. Antigen-binding activities of purified anti-HER2 scFv-V_LV_H and anti-HER2 scFv-V_HV_L against commercial HER2. Experiment was performed in triplicate and error bars display SD of the mean [223].

4.4.4. Binding Affinity of Anti-HER2 scFvs

Surface plasmon resonance (SPR) analysis was applied to determine equilibrium binding affinity of scFvs towards HER2. For this purpose, purified anti-HER2 scFvs diluted serially (0.625-80 nM) was interacted with SPR sensor chip coated with commercial HER2. Binding responses obtained by SPR sensorgram (Figure 4.20) were used to plot against concentration of scFvs and to fit a 1:1 Langmuir binding isotherm for determination of the equilibrium dissociation constant, K_d.

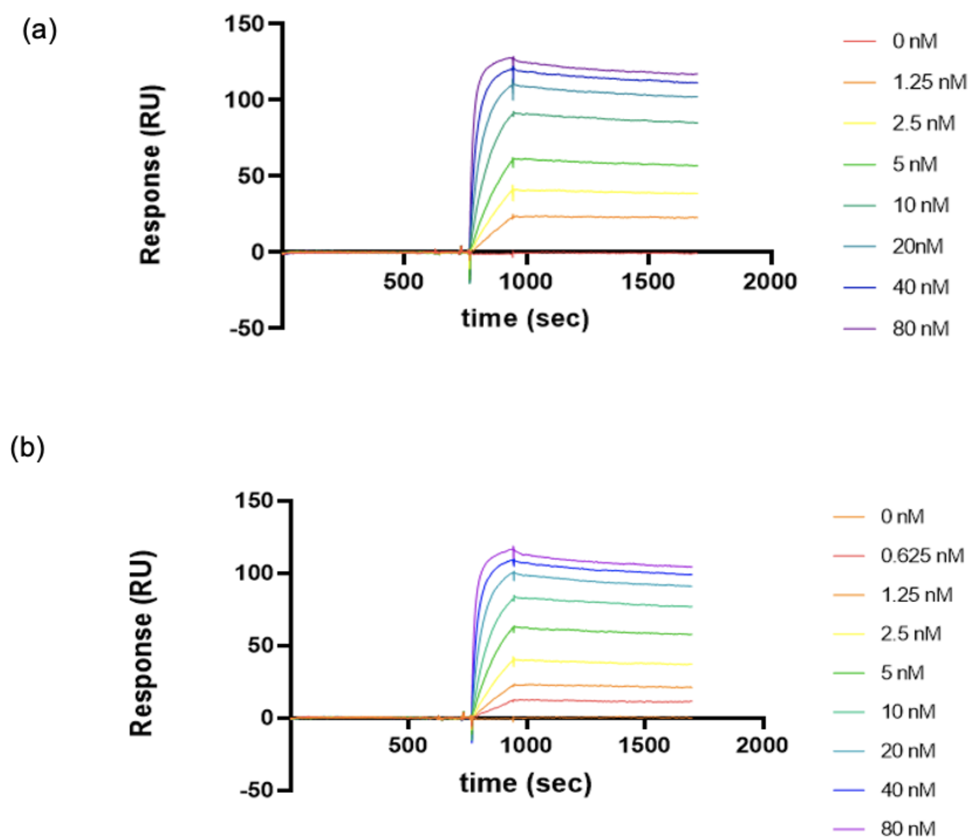

Figure 4.20. SPR sensorgrams of purified (a) anti-HER2 scFv-V_LV_H (b) anti-HER2 scFv-V_HV_L

From Figure 4.20, the response values at the steady state or equilibrium phase were chosen for each concentration of scFv constructs as given in tables in Appendix 5 for anti-HER2 scFv-V_LV_H and anti-HER2 scFv-V_HV_L. Response values in Table A5.1 and Table A5.2 plotted in Figure 4.21 shows saturation at binding through 80 nM.

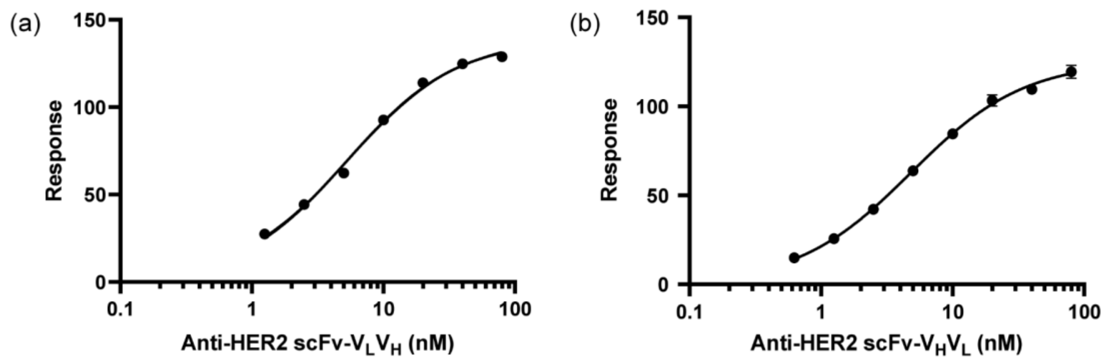

Figure 4.21. Binding affinity analysis of purified (a) anti-HER2 scFv V_LV_H and (b) anti-HER2 scFv-V_HV_L [223]

K_d values for anti-HER2-scFv-V_LV_H and anti-HER2-scFv-V_HV_L were calculated based on the Equation 2.20 given in Section 2.7.2 by using Hill Slope nonlinear regression analysis. Consequently, K_d values of anti-HER2-scFv-V_LV_H and anti-HER2-scFv-V_HV_L were calculated as 5.30 and 4.82 nM, respectively (Table 4.2). K_d values of scFvs indicated that anti-HER2-scFv-V_LV_H and anti-HER2-scFv-V_HV_L had similar affinity towards HER2.

Table 4.2. K_d values for binding of purified anti-HER2 scFv to HER2 by SPR

Sample	K_d (nM)	Std Error	R-squared
Anti-HER2-scFv-V_LV_H	5.30	1.05	0.9959
Anti-HER2-scFv-V_HV_L	4.82	1.00	0.9970

K_d values obtained for the anti-HER2 scFvs via SPR were in nM ranges, which shows a high binding affinity. In a recent study, K_d value of pertuzumab scFv against HER2 expressed in the periplasm of *E. coli* BL21 (DE3) was determined as 21 nM via flow cytometry technique [78]. It should be also noted that it would not be correct to compare the K_d values obtained from different methods due to their individual phenomena. In another study, K_d value of scFv version of trastuzumab expressed in the cytoplasm of *E. coli* using CyDisCo system was determined as 97 nM via SPR method [238]. When K_d value in the referred study was compared the values (5.30 and 4.82 nM) obtained in this study via SPR, it could be concluded that anti-HER2 scFvs with higher affinity was produced in this study. Although there was a recent study on expression of anti-HER2 scFv in V_HV_L orientation in SHuffle T7 Express [17], no information was given about affinity of the scFv to HER2 antigen in the study.

As a result, anti-HER2 scFv-V_LV_H was expressed in higher amounts while anti-HER2 scFv-V_HV_L showed a slightly higher binding activity. The scFvs show tendency to form dimers, trimers and larger oligomers that limit their applications. Due to the weak interactions between variable domains, scFvs stay in equilibrium between an opened state in which domains are disassembled and a closed state in which domains are assembled. If scFvs stay mainly in the open state, this situation triggers the inter-chain domain interactions, thus oligomer structures are formed. It was reported that dimerization could enhance binding-activity owing to avidity effect [239]. Therefore, it would be expected that V_LV_H orientation composed of mostly dimer forms could show a higher antigen-binding capacity. However, differences in binding site geometry can also disfavor binding. Other studies reported that scFvs are generally constructed in the V_HV_L orientation due to distance between linker peptide and CDR-H3, which is important for antigen-binding [235, 237]. However, in our case, anti-HER2 scFvs were expressed soluble and showed high binding affinity, independent of the orientation of the variable domains [223]. Kim and coworkers also reported that scFv against C-met in the V_HV_L orientation had productivity five times higher than scFv in the V_LV_H format, while both of them showed almost the same antigen-binding activities [59].

Based on the obtained results in this study, anti-HER2 scFv in V_LV_H scFv format was selected for further experiments considering its soluble and functional expression yield.

4.5. Design and Expression of Anti-HER2 scFvs with Different Linkers

In the literature, scFvs have been designed in different ways in terms of domain orientation, linker length and composition, which are crucial for stability, soluble and functional expression. After having investigated domain orientation, linkers containing different amino acid compositions were evaluated in this part of the thesis study. Linker amino acid compositions were decided considering the material binding peptides which were designed for oriented immobilization of proteins on to biosensor surfaces. Polystyrene surface, which is commonly used in diagnostic and immunoassay applications was selected as the model surface. Thus, linker compositions containing PS binding peptides were designed. These peptides are generally composed of 9-12 residues as given in Table 2.1. Hence, amino acids such as glycine (G), serine (S) were added to create linkers in 15 aa length. Since both amino acid composition and length of linkers influence scFv properties, only the effect of different amino acids were investigated by keeping the length at 15 aa.

Amino acid compositions of new linkers are given Table 3.1. Firstly, cloning of new constructs were performed. Gene containing $(G_4S)_3$ linker was used as the template for the new constructs. Primers in Table 3.2 were used for amplification of V_L and V_H domains of anti-HER2 scFv. Amplified V_L and V_H domains contained sequences of PS19-V1 (Lane 1 and 2), PBTUP-V1 (Lane 3 and 4) and PS18-V1 (Lane 5 and 6) linkers. As shown in Figure 4.22, the V_L genes were 362 bp, whereas V_H genes were 417 bp.

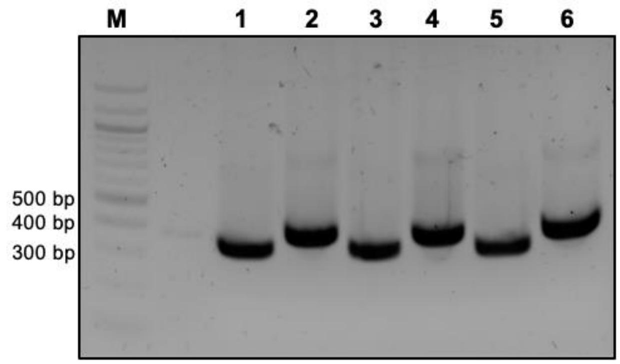

Figure 4.22. Agarose gel electrophoresis of V_L and V_H genes amplified by PCR to construct anti-HER2-scFv gene (Lane 1,3,5: VL products; Lane 2,4,6: VH products of genes containing PS19V1, PBTUP-V1 and PS18-V1, respectively). M: 100 bp DNA Ladder

Two separate PCR products comprised overlapping linker regions given in Figure 4.22 were joined by SOE-PCR to generate a full-length gene of 764 bp (Figure 4.23). Lane 1, 2 and 3 were the scFvs containing PS19-V1, PBTUP-V1 and PS18-V1 linkers, respectively. In addition, Lane 4 is the PCR product of scFV with standart linker $(G_4S)_3$ contanining C-terminal PS19 with the size of 791 bp.

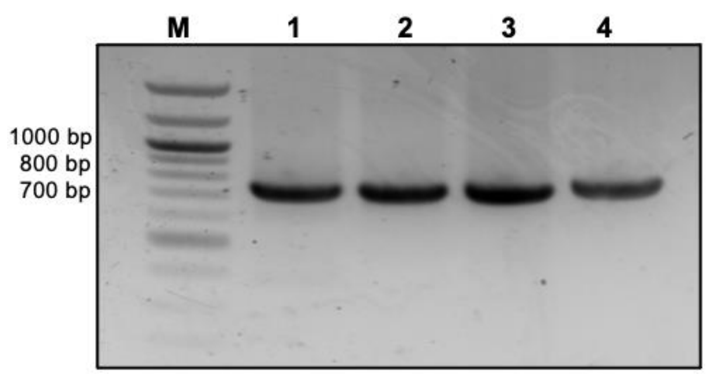

Figure 4.23. Agarose gel electrophoresis of overlap extension PCR products. M:100 bp DNA Ladder

The ligation reaction was carried out for cloning the double digested PCR products into double digested vector DNA (pET28a). Finally, various recombinant plasmid constructs between *Nco*I and *Hind*III restriction sites were verified with sequencing analysis. ScFvs containing $(G_4S)_3$, PS19-V1, PBTUP-V1 and PS18-V1 linkers and C-terminal PS19 were named as anti-HER2 scFv-L1, anti-HER scFv-L2, anti-HER2 scFv-L3, anti-HER2 scFv-L4 and anti-HER2 scFv-L5, respectively, for further experiments.

Firstly, the expression of new constructs was performed to evaluate the linkers on whether they influenced the solubility. Anti-HER2-scFvs were expressed by inducing with 0.1 mM IPTG at 16°C for 16 h. After sonication, the concentrations of soluble fractions of cell lysates obtained from anti-HER2 scFv-L1, anti-HER scFv-L2, anti-HER2 scFv-L3, anti-HER2 scFv-L4 were 2.2, 1.8, 1.7 and 1.5 mg/ml, respectively. Same amounts of cell lysates were loaded on to SDS-PAGE gel and Western blot was performed for analysis of expression with anti-6xHis-tag-HRP antibody. As seen in Figure 4.24, new anti-HER2 scFvs were expressed in soluble form with a predicted size of ~27 kDa. The different linkers did not enhance nor inhibit the solubility.

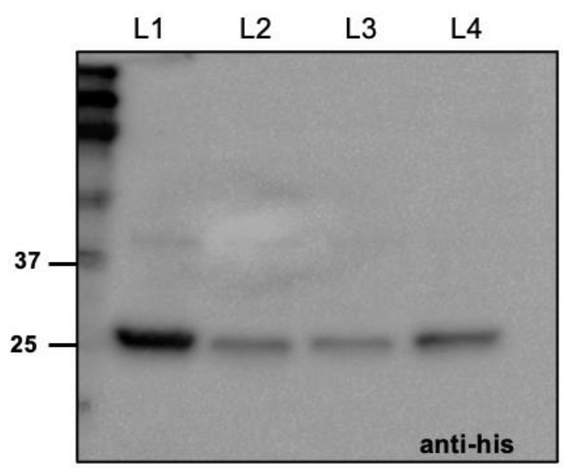

Figure 4.24. Western blot analysis of anti-HER2 scFvs with different linker regions, normalized based on total protein

Anti-HER2 scFvs were then purified, desalted and concentrated for further analyses. The purities of all constructs were above 95% as seen in Figure 4.25.

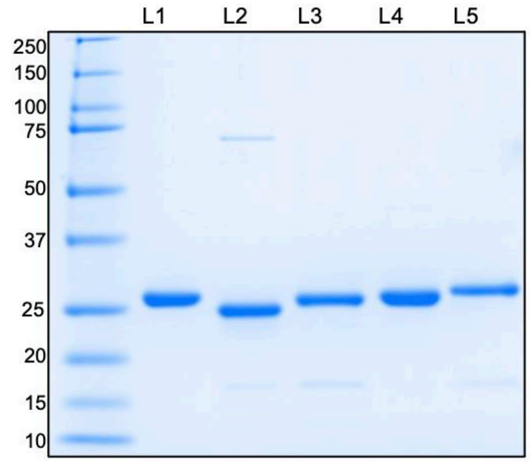

Figure 4.25. SDS-PAGE analysis of purified anti-HER2 scFv constructs expressed in *E. coli* SHuffle T7 Express at 16°C, 16 h

4.6. Characterization of Anti-HER2 scFvs with Different Linkers

In this part of the study, effects of linker composition on the antigen-binding activity, binding affinity and efficiency of immobilization to a polystyrene surface were investigated. Binding activity and binding affinity values were determined by indirect ELISA, whereas immobilization efficiency was examined by sandwich ELISA.

4.6.1. Antigen-Binding Activity of Anti-HER2 scFvs with Different Linkers

ELISA was applied by interacting serial dilutions of purified scFvs with different linkers and commercial HER2 as immobilized antigen. ELISA analysis showed that newly designed scFvs had the similar binding activity with scFv containing the standard linker (L1), as shown in Figure 4.26. Hence, changing the linker region did not affect the binding activity of anti-HER2 scFv towards HER2. In addition, binding activity of scFv construction with C-terminal PS19 could not be shown by ELISA due to the internal His-tag, which was also a problem in Western blot analysis.

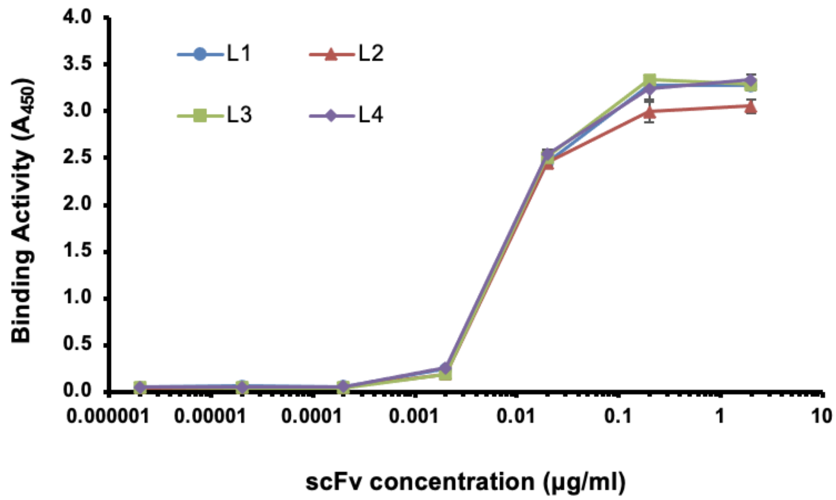

Figure 4.26. Antigen-binding activity of purified anti-HER2 scFvs against commercial HER2. Experiment was performed in triplicate and error bars display SD of the mean.

4.6.2. Binding Affinity of Anti-HER2 scFvs with Different Linkers

Equilibrium dissociation constant, K_d values of anti-HER2 scFvs were determined by ELISA using two different approaches determined by Friguet [192] and Beatty [198]. Firstly, dissociation constant of anti-HER2 scFv-V_LV_H, which was also determined by SPR, was calculated by Friguet's method. For this purpose, two identical plates were coated with 0.2, 0.1, 0.05 and 0.01 µg/ml commercial HER2 to determine the antigen coating amount. Two plates were handled at same time and unbound scFv from first plate was recovered and applied in the second plate. To compare the signals obtained in two ELISA plates, the proportion of bound scFv was calculated from the slope of graphs given in Figure 4.27 as 15.7, 14, 12.2 and 18.6% for 0.2, 0.1, 0.05 and 0.01 µg/ml coating concentrations, respectively. Coating amount was chosen as 0.05 µg/ml since it was the lowest difference between the two signals (Figure 4.27).

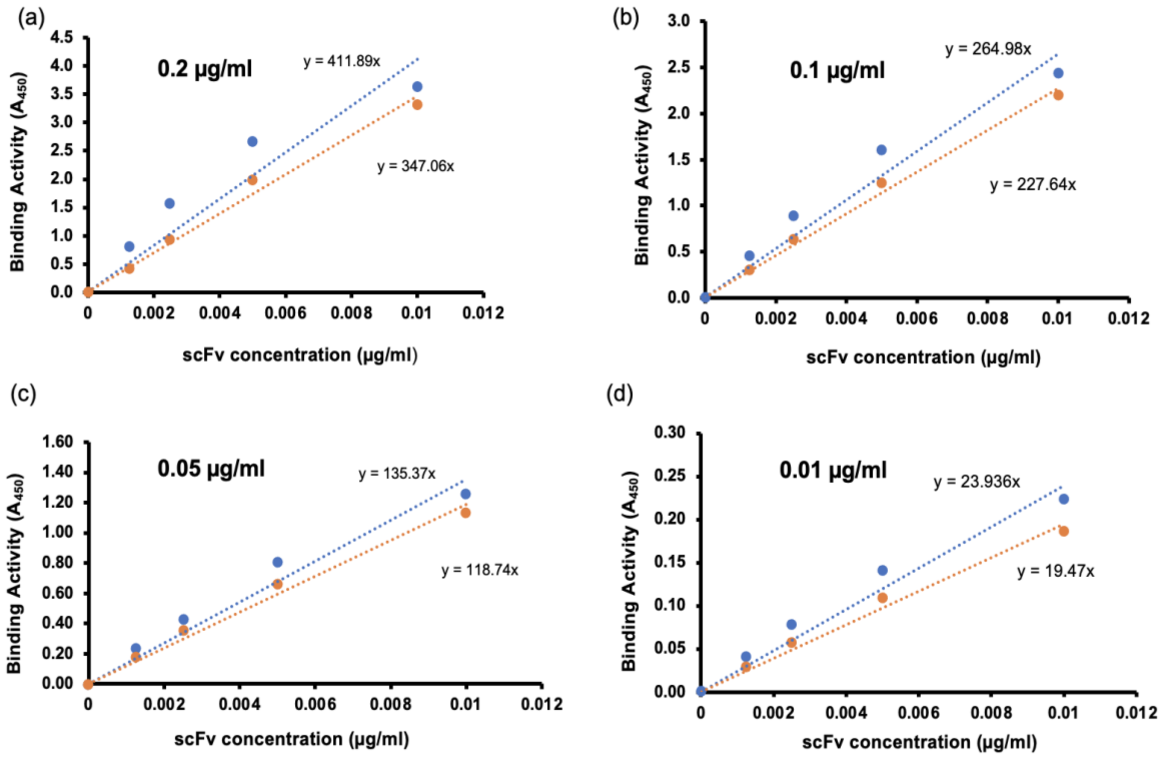

Figure 4.27. Slope of ELISA applied by (a) 0.2 µg/ml, (b) 0.1 µg/ml, (c) 0.05 µg/ml and (d) 0.01 µg/ml coating concentration of HER2

After determination of coating, another ELISA was set up to measure free scFv as a function of the antigen concentration. Then, based on the absorbance values obtained from ELISA, antigen concentrations and free scFv concentrations, $[scFv]_f$ were calculated as given in Table A6.1 in Appendix 6. Data from the table were plotted and fitted to Equation 2.13 to calculate K_d by using the CurveExpert software. K_d was calculated as 0.49±0.06 nM by using the ELISA method (Figure 4.28).

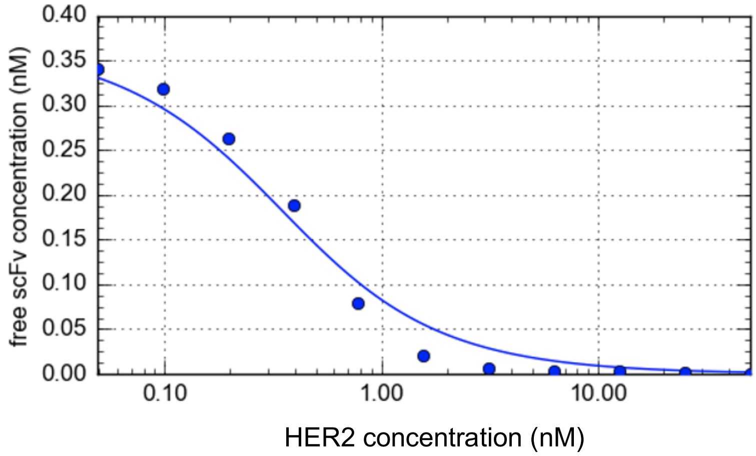

	Value	Std Err	Range (95% confidence)
Kd	0.493882	0.063520	0.354076 to 0.633689

Figure 4.28. Data from Table A6.1 which was fitted to Equation 2.13 for determination of K_d of anti-HER2 scFv-V_LV_H

While K_d value determined from SPR was around 5 nM, K_d value determined from ELISA was 0.49 nM, which was ca. 10-fold lower than that determined by SPR. This indicated that higher binding affinities were observed by ELISA. There have been studies on comparison of the K_d values determined by SPR and ELISA. Two reports [240, 241], that are independent from each other, compared the K_d values and they both reported approximately 10-fold difference between the two methods, which shows that our results was on par with those studies in literature. The possible reasons of this difference was reported as (i) more immobilization of antigen on the plate and (ii) longer incubation time of antigen-antibody complex during ELISA. These properties could contribute to rebinding effects, which caused an increase on binding affinities calculated by ELISA [242].

Secondly, Beatty's method was applied for the K_d calculation of anti-HER2 scFv-V_LV_H. For this purpose, the procedure of indirect ELISA was performed with 0.2, 0.1 and 0.05 µg/ml coating concentrations of HER2 as shown in Figure 4.29. Equation 2.14 was used for calculation of the dissociation constant. Anti-HER2 scFv-V_LV_H

concentration at half the maximum absorbance was determined by an online fitting program (raw data given in Appendix 7).

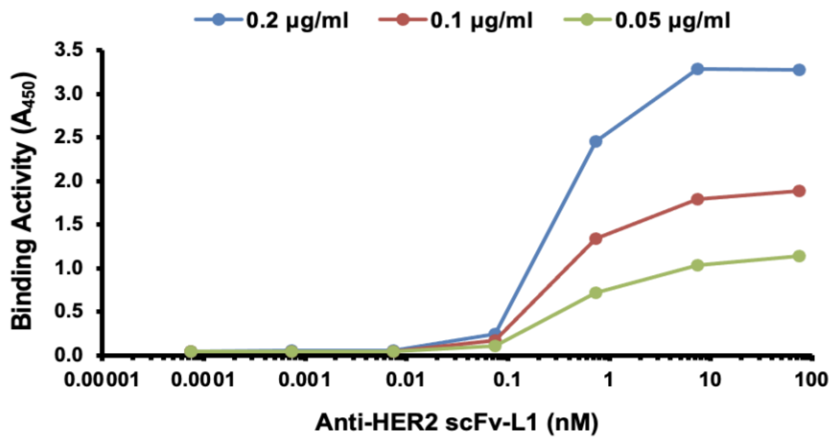

Figure 4.29. Measurement of anti-HER2 scFv-V_LV_H affinity by ELISA using antigen concentrations of 0.2 µg/ml, 0.1 µg/ml and 0.05 µg/ml

Based on the three concentrations of HER2, three dissciation constants (two for n=2, one for n=4) were calculated. The calculated K_d values for anti-HER2 scFv-V_LV_H, was 0.39 nM using antigen concentrations of 0.2 µg/ml and 0.1 µg/ml, 0.53 nM using antigen concentrations of 0.1 µg/ml and 0.05 µg/ml, and 0.49 nM using antigen concentrations of 0.2 µg/ml and 0.05 µg/ml. Thus, mean K_d value was calculated as 0.47±0.07 nM, which is compatible with K_d value obtained from Friguet's method. Overall, two methods were consistent with each other, and Beatty's method was chosen for further calculations since it was more practical and time-saving. In the next step, affinity measurements of scFvs containing different linkers were performed to evaluate the effect of linker composition on affinity (Figure 4.30).

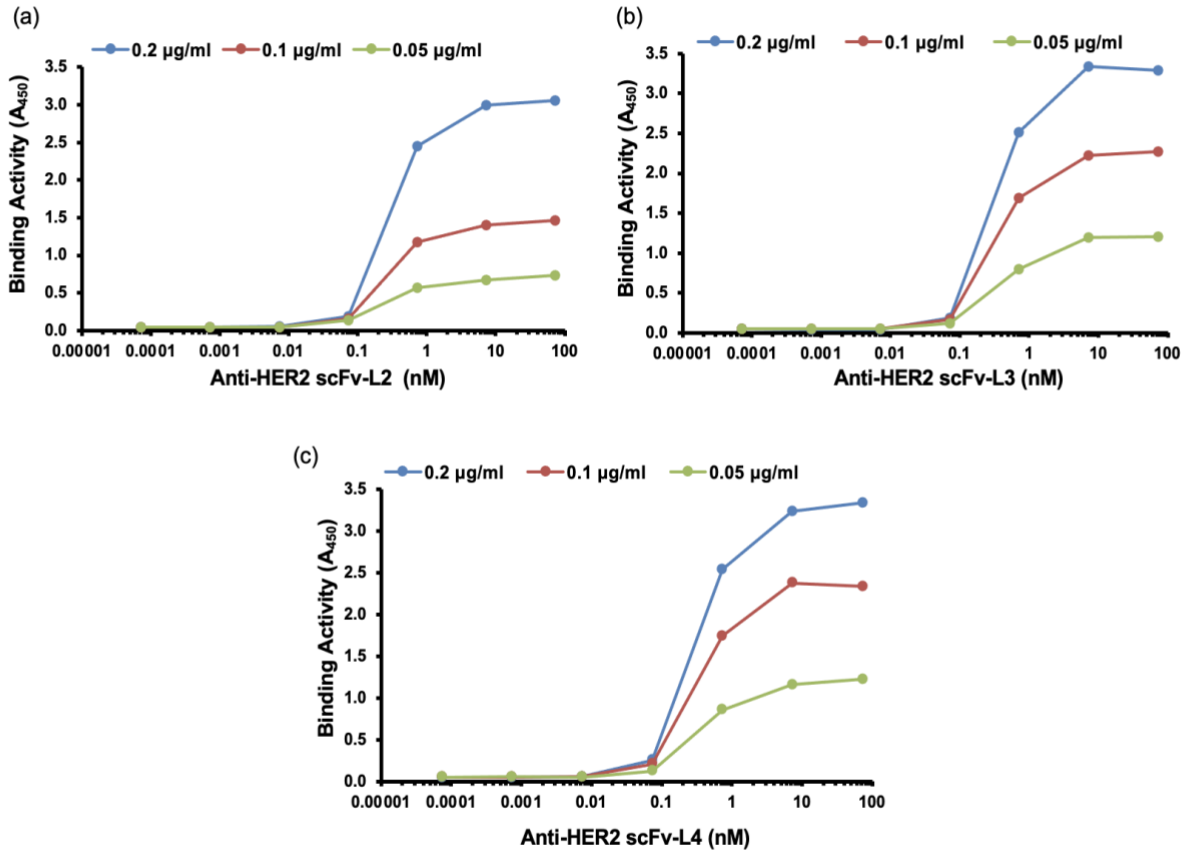

Figure 4.30. Affinity measurement of (a) anti-HER scFv-L2, (b) anti-HER scFv-L3 and (c) anti-HER scFv-L4 by ELISA using antigen concentrations of 0.2 µg/ml, 0.1 µg/ml and 0.05 µg/ml

The K_d values calculated from Figure 4.30 are given in Table 4.3. Consequently, it could be concluded that changing linker composition did not significantly affect antigen-binding activity (Figure 4.26) nor affinity. In addition, the scFv containing PS19 peptide (RIIIRRIRR) within the linker region (scFv-L2) showed an increase in affinity towards HER2, as given in Table 4.3.

Table 4.3. K_d values for binding of purified anti-HER2 scFv constructs to HER2 determined by ELISA

Sample	K_d (1)	K_d (2)	K_d (3)	K_d (average)
Anti-HER2 scFv-L1	0.39	0.53	0.49	0.47±0.07
Anti-HER2 scFv-L2	0.24	0.22	0.23	0.23±0.01
Anti-HER2 scFv-L3	0.37	0.53	0.47	0.46±0.07
Anti-HER2 scFv-L4	0.4	0.4	0.4	0.4±0.001

4.6.3. Immobilization of Anti-HER2 scFvs to Polystyrene Surface

One of the aims of this thesis study was to investigate whether the tags developed for a certain surface affect the immobilization of scFvs when inserted to the linker region. Polystyrene is one of the most common solid supports used in immunoassays and have potential protein-based biochip applications [20]. Kumada and coworkers screened affinity peptides named as PS-tags that showed an increased interaction with PS surfaces. They demonstrated successful site-directed immobilization of proteins, which were fused with PS-tags by genetic or chemical methods [153]. Among screened PS-tags, some peptides showed higher immobilization efficiency than others based on their amino acid compositions. It was reported that PS-tags containing basic amino acids such as arginine and lysine increased the binding affinity of proteins towards hydrophilic PS plates, which had a negative surface charge [20]. Based on the these results, three different PS-tags in terms of aliphatic and basic amino acid compositions were selected to add to the scFv linker region in this study. Among them, PS19-6 (RIIIRRIRR) tag showed strong binding affinity towards a hydrophilic PS surface in a study reported by Kumada and coworkers [155].

In studies that evaluated the PS-tags, two kinds of PS plates were used. One of them was hydrophobic PS plate that was non-treated and used in standard assays. The other was a hydrophilic plate that was treated for high binding and used in immunoassays and protein-protein interaction analyses [155]. Previous studies that used PS-tags at C-terminal of proteins generally immobilized the proteins on the PS plates in a buffer containing Tween 20 or BSA [20]. In this study, immobilization of anti-HER2 scFvs on the two types of PS plates depending on the absence or presence of Tween 20 was performed, as a first step. The immobilization of the anti-HER2 scFvs was quantified through direct ELISA by detection of 6x-His at the C-terminal.

Firstly, in direct ELISA, anti-HER2 scFv was attached on the hydrophilic PS plate in PBS containing 0.1% Tween 20 (PBST). As shown in Figure 4.31, anti-HER2 scFvs with different linkers showed no difference at the low concentrations of scFvs and most of the signals overlapped one another, which made it difficult to distinguish individual points. However, after 0.5 µg/ml scFv concentration, L1 and L2 linkers showed improved immobilization relative to the L3 and L4 linkers. In addition, L2 showed slightly higher binding than the standard linker.

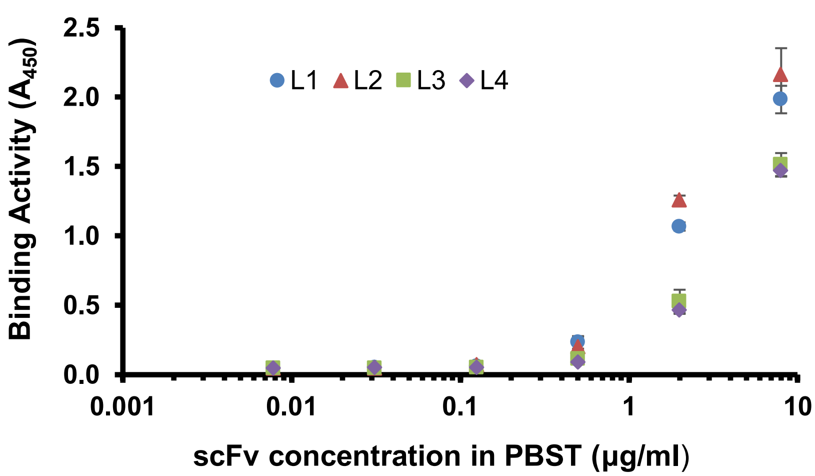

Figure 4.31. Detection of anti-HER2 scFvs immobilized on hydrophilic PS plate in PBST in the adsorption state. Experiment was performed in duplicates and error bars display SD of the mean.

Then, anti-HER2 scFvs were attached on the hydrophilic PS plate in the 1xPBS buffer as shown in Figure 4.32. In this case, signal intensities of scFvs with L3 and L4 increased and scFvs showed a similar binding trend. Thus, absence of Tween 20 had positive effects for anti-HER2 scFv-L3 and anti-HER2 scFv-L4 constructs and increased the immobilization efficiency at low concentrations overall.

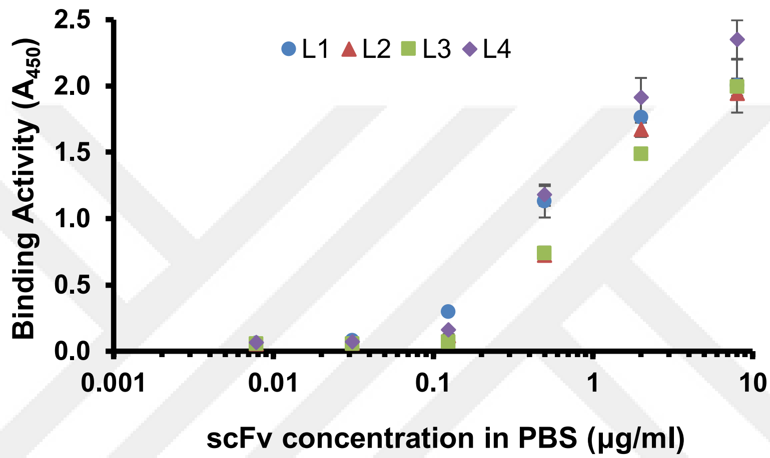

Figure 4.32. Detection of anti-HER2 scFvs in PBS immobilized on hydrophilic PS plate. Experiment was performed in duplicates and error bars display SD of the mean.

In previous studies, it was reported that barely detectable signals were obtained from the protein attached onto hydrophobic PS surfaces in PBST [155]. This could be explained by inhibition of the physical adsorption of proteins due to Tween 20 addition since binding sites were quickly occupied by the surfactant. Based on these results, anti-HER2 scFvs in PBST were immobilized onto the hydrophobic plate and no signal was detected as expected, compatible with the previous studies.

It was reported that when proteins immobilized on the hydrophobic PS surface in the absence of Tween 20, they were randomly oriented and conformational changes occurred regardless of the PS-tags. Anti-HER2 scFvs were also immobilized on the hydrophobic plate in PBS as shown in Figure 4.33. In this case, similar signals were detected from scFvs containing different linkers. In addition, the signal of scFv containing PS19-6 (RIIIRRIRR) in the linker region decreased as expected, since this peptide composed of mostly basic amino acids was reported as effective for hydrophilic surfaces in the presence of a surfactant. Furthermore, high differences between duplicates were observed as seen in error bars. This could have occurred due to the random orientation of scFvs.

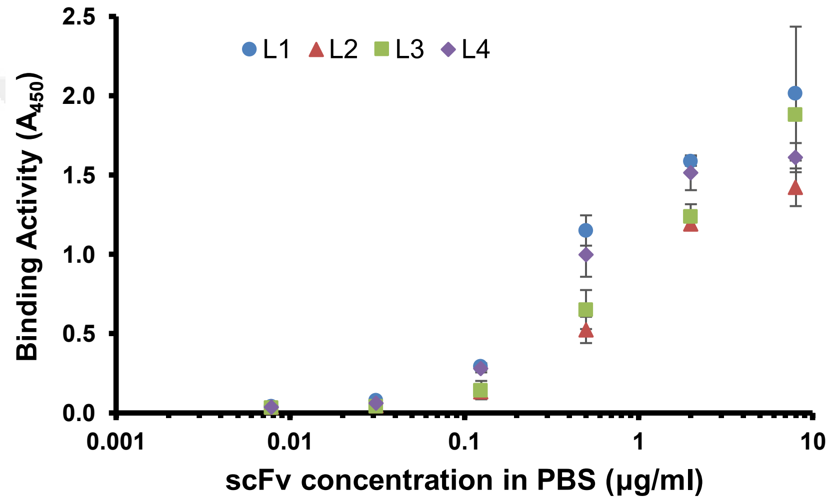

Figure 4.33. Detection of anti-HER2 scFvs in PBS immobilized on hydrophobic PS plate. Experiment was performed in duplicates and error bars display SD of the mean.

Binding activities of anti-HER2 scFvs were also evaluated by applying sandwich ELISA with scFvs showing higher immobilization on the hydrophilic and hydrophobic surfaces. In the sandwich ELISA, anti-HER2 scFv-L5, which contains C-terminal PS19-6 peptide sequence, was also used to detect HER2. As seen in Figure 4.34, anti-HER2 scFv with the standard linker had still the highest HER2 binding activity when scFvs were coated in PBS. Anti-HER2 scFv-L5 with C-terminal PS-tag showed lower binding activity in the absence of PBST, which was compatible with a previous study [155]. As seen in Figure 4.35, HER2 binding activities of anti-HER2 scFv-L1 and anti-HER scFv-L2 were similar at the tested concentrations. In addition, C-terminal PS-tag showed significant difference in antigen-binding activity in the presence of Tween 20. One explanation for this result could be that lower flexibility of internal PS-tag could cause the decrease in the affinity compared with the C-terminal PS-tag.

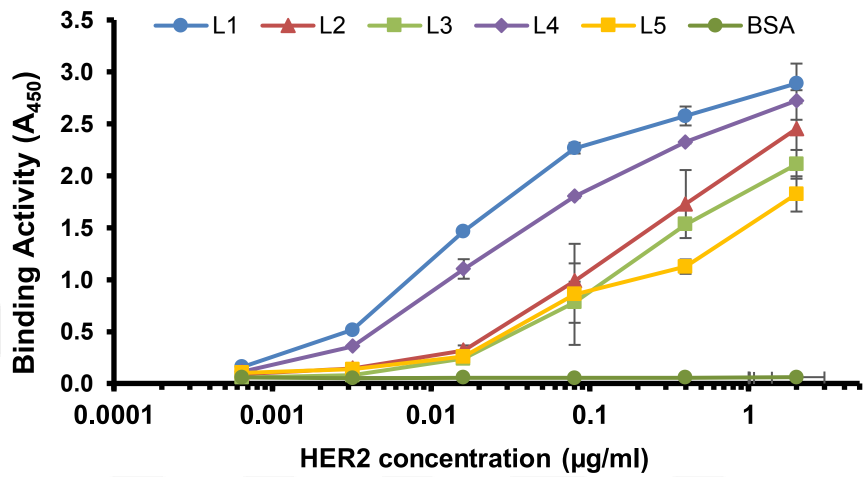

Figure 4.34 Sandwich ELISA for detection of HER2 using hydrophilic PS plates coated with anti-HER2 scFvs in PBS. Experiment was performed in duplicates and error bars display SD of the mean.

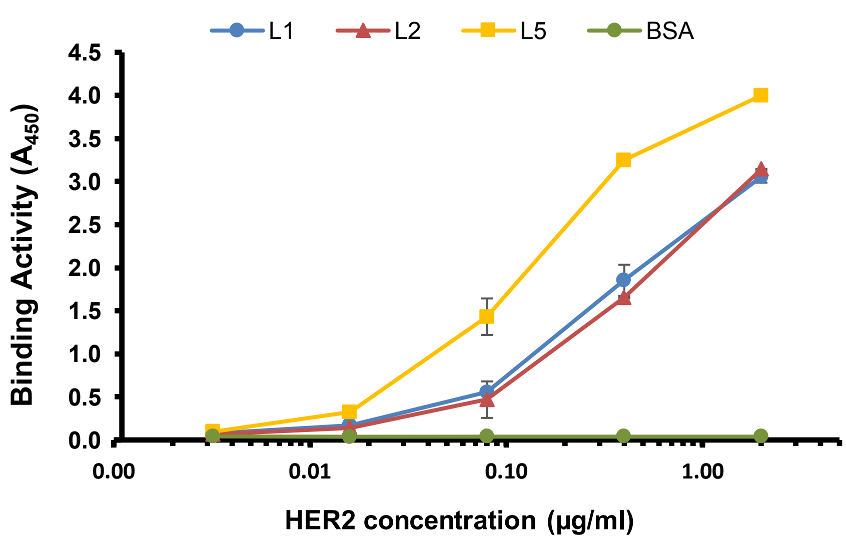

Figure 4.35. Sandwich ELISA for detection of HER2 using hydrophilic PS plates coated with anti-HER2 scFvs in PBST. Experiment was performed in duplicates and error bars display SD of the mean.

Overall, all anti-HER2 scFv constructs were successfully produced as soluble and functional. Although all scFvs had a high dissociation constant and showed similar binding activity, anti-HER2 scFvs with L3 (GGGVHWDFRQWWQPS) and L4 (GGGVRSWEEQARVTT) linker peptides showed lower binding to ELISA plates than other scFvs. Therefore, anti-HER2 scFvs with L3 and L4 linkers could be eliminated towards applications for diagnostic tools having PS surfaces. Yet, the highest oriented binding towards PS and the highest detection of HER2 antigen was observed in C-terminal PS-tag, anti-HER2 scFv with internal PS-tag could be also an alternative owing to its high affinity and higher absorbance values in the sandwich ELISA.

4.7. Design and Expression of ScFv13R4 with Different Linkers

In this part of the thesis, linkers containing PS-tags were added to the linker region of scFv13R4 against β-galactosidase to determine whether effects of the linker composition are versatile or specific for each individual scFv.

Firstly, cloning of new constructs was performed. ScFv13R4 gene containing $(G_4S)_3$ linker was used as the template for the new constructs [26]. Primers given in Table 3.4 were used for amplification of V_H and V_L domains of scFv13R4. Two separate PCR products containing overlapping linker regions were joined by SOE-PCR to generate a full-length gene of 827 bp (Figure 4.36). Lane 1, 2 and 3 were the scFvs containing PS19-V1, PBTUP-V1 and PS18-V1 linkers, respectively.

The ligation reaction was performed to clone the double digested PCR products into double digested vector DNA (pET28a). Finally, various recombinant plasmid constructs between *Nco*I and *Hind*III restriction sites were verified with DNA sequencing.

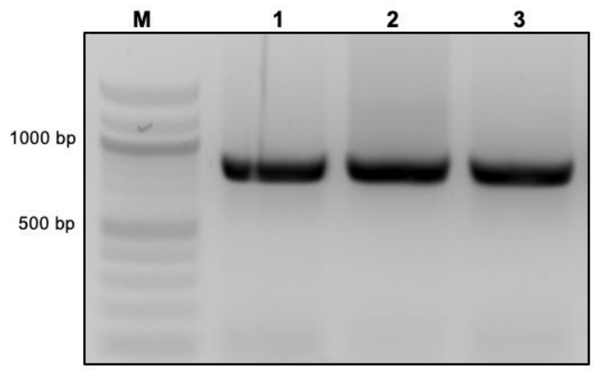

Figure 4.36. Agarose gel electrophoresis of overlap extension PCR products. M:100 bp DNA Ladder

Before evaluating the new constructs, ELISA was performed by coating 1 µg commercial β-gal and using serial dilutions of scFv13R4 to test specificity of scFv to β-gal. ScFv13R4 showed binding to antigen as seen in Figure 4.37.

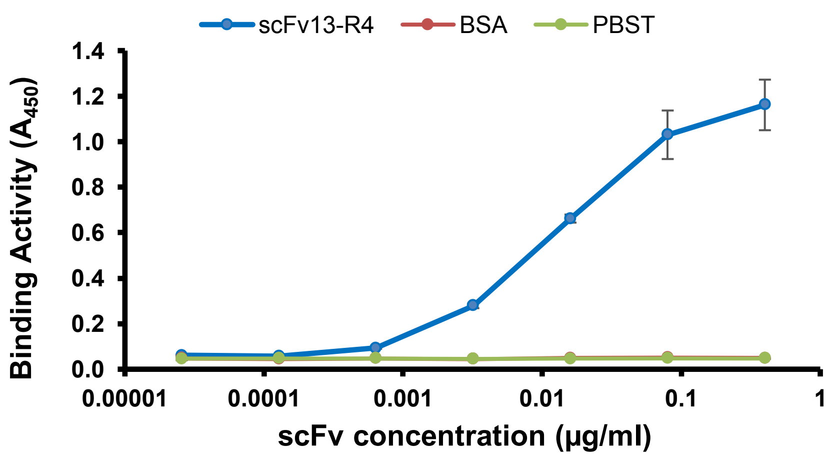

Figure 4.37. Binding activity of purified scFv13-R4 against commercial β-gal

To use in ELISA experiments, pET28a-NStrep-βgal-6xHis construct was designed by using pBAD18-Bgal-NStrepIItag as a template [26] and cloning experiments were performed. After verification with sequencing analysis, expression was tested by Western blotting. Membranes were probed with anti-6xHis-tag-HRP, anti-βgal antibody and StrepTactin antibody, and the predicted size of the protein, ~118 kDa, was confirmed (Figure 4.38).

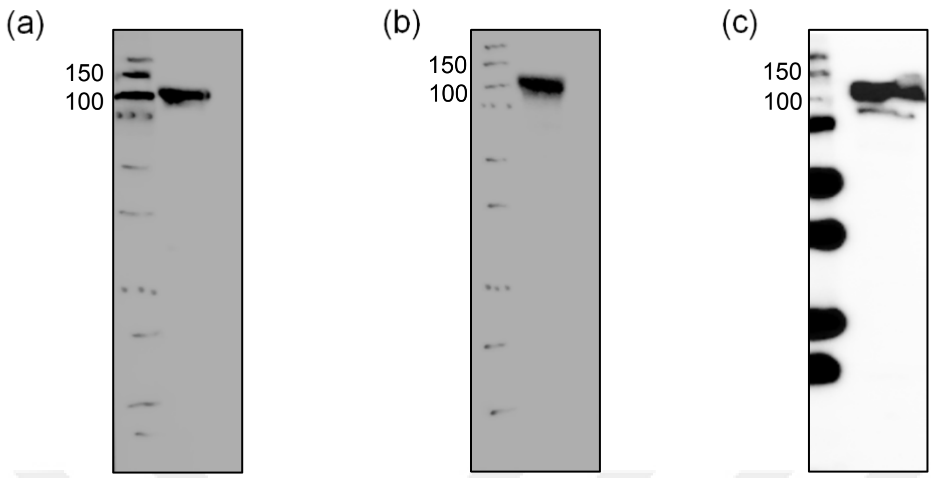

Figure 4.38. Western blot analysis of soluble fraction obtained from SHuffle T7 Express cells expressing β-galactosidase probed with (a) anti-6xHis-tag-HRP antibody (b) anti-βgal antibody and (c) StrepTactin antibody

β-galactosidase was purified from 400 ml culture to use for ELISA as an antigen (Figure 4.39). Desalting column was used to exchange the buffer to PBS and concentrate. Bradford assay was used to determine the protein concentration and ~2 mg protein was obtained.

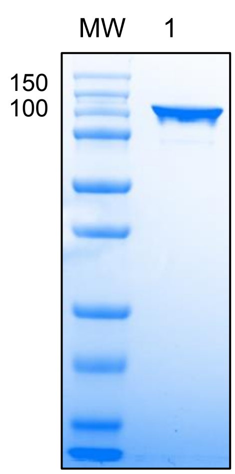

Figure 4.39. SDS-PAGE analysis of the purified β-galactosidase

ScFv13R4 constructs were expressed in *E. coli* BL21(DE3) since it was mutated to be produced folded and functional in the cytoplasm in a previous study [27]. Cells were grown by inducing with 0.1 mM IPTG at 25°C post-induction temperature. Same amounts of cell lysates were loaded on to SDS-PAGE gel and Western blot was applied to detect expression with anti-6xHis-tag-HRP antibody. As seen Figure 4.40, new scFv13R4 constructs were expressed in soluble form with a predicted size of ~29 kDa.

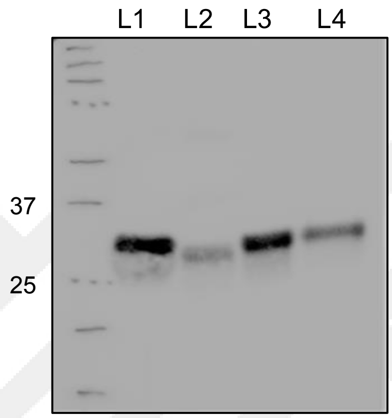

Figure 4.40. Western blot analysis of scFv13R4 with different linker regions, normalized based on total protein

ScFv13R4 antibodies were then purified, desalted and concentrated.The purities of all constructs were above 95% as seen Figure 4.41.

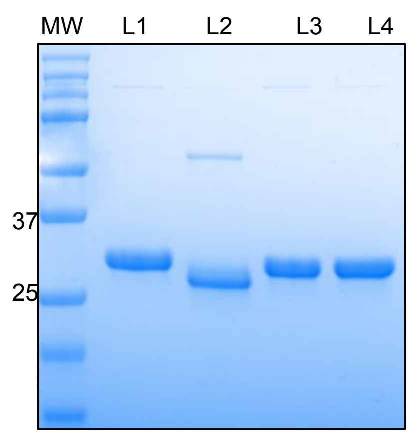

Figure 4.41. SDS-PAGE analysis of purified scFv13R4 constructs

4.8. Characterization of ScFv13R4 with Different Linkers

ELISA was applied by interacting serial dilutions of purified scFvs with different linkers and purified β-galactosidase as immobilized antigen. ELISA analysis showed that newly designed scFvs had the similar binding activity with scFv containing standard linker (L1) as shown in Figure 4.42. Hence, changing of linker region did not affect the binding activity. These results were also consistent with binding activities in Figure 4.26.

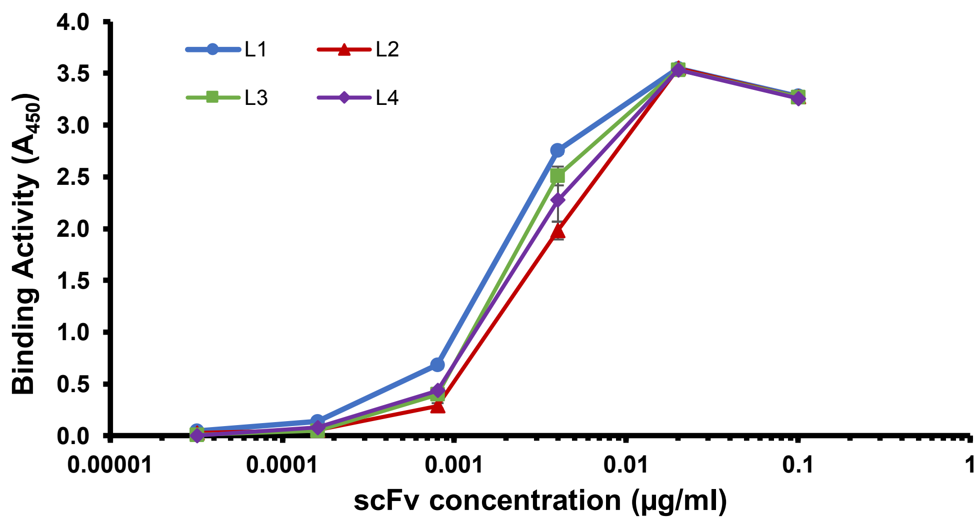

Figure 4.42. Antigen-binding activity of purified scFv13R4 against β-galactosidase. Experiment was performed in triplicate and error bars display SD of the mean.

Then sandwich ELISA was performed by coating purified scFv13R4 constructs to test binding to β-galactosidase in hydrophilic PS plates. As shown in Figure 4.43, scFvs showed binding activities compatible with Figure 4.34. It was confirmed by different studies that scFvs with C-terminal PS-tags showed high binding activities in sandwich ELISA [157, 158]. However, there is no information about soluble and active expression of scFvs with internal PS-tags. Based on the results of this study, a PS-tag in the linker region of an scFv does not increase their solubility or decrease antigen-binding activity. However, they could affect flexibility and cause conformational changes, thus affect immobilization on the PS surface. Therefore this situation can also cause a decrease in binding to the antigen in sandwich ELISA.

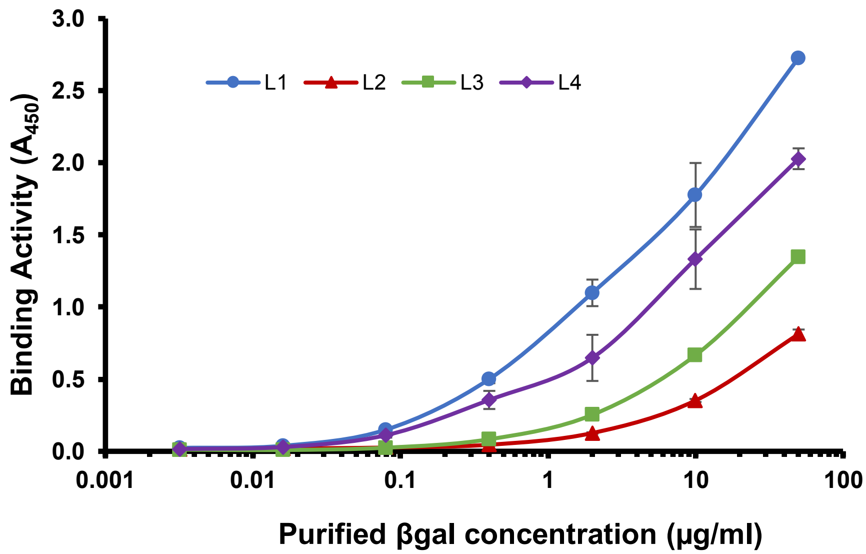

Figure 4.43. Sandwich ELISA for detection of β-galactosidase using hydrophilic PS plates coated with scFv13R4 constructs in PBS. Experiment was performed in duplicates and error bars display SD of the mean.

4.9. *In silico* Analysis of ScFvs

Based on our experimental results and literature knowledge, it could be concluded that amino acid composition is a significant design parameter of linker selection for construction of antibody fragments. However, only experimental results could not be sufficient for evaluation and optimization of linker composition. Therefore, molecular dynamic simulations were also applied in this study to understand the effects of linkers on the structure, stability, folding and binding energies of antibody fragments and antibody fragment-antigen complexes for further design of antibodies. For this purpose, SWISS MODEL [181] was used for homology modelling and MD simulations were performed using GROMACS [29].

4.9.1. Tertiary Structure Prediction

Three dimensional structures of anti-HER2 scFvs with different linkers and V_HV_L orientation with standard linker were constructed by homology modelling method as shown in Figure 4.44. As seen in the three dimensional models, different linker peptides caused different flexibilities and structures in the linker region of scFvs.

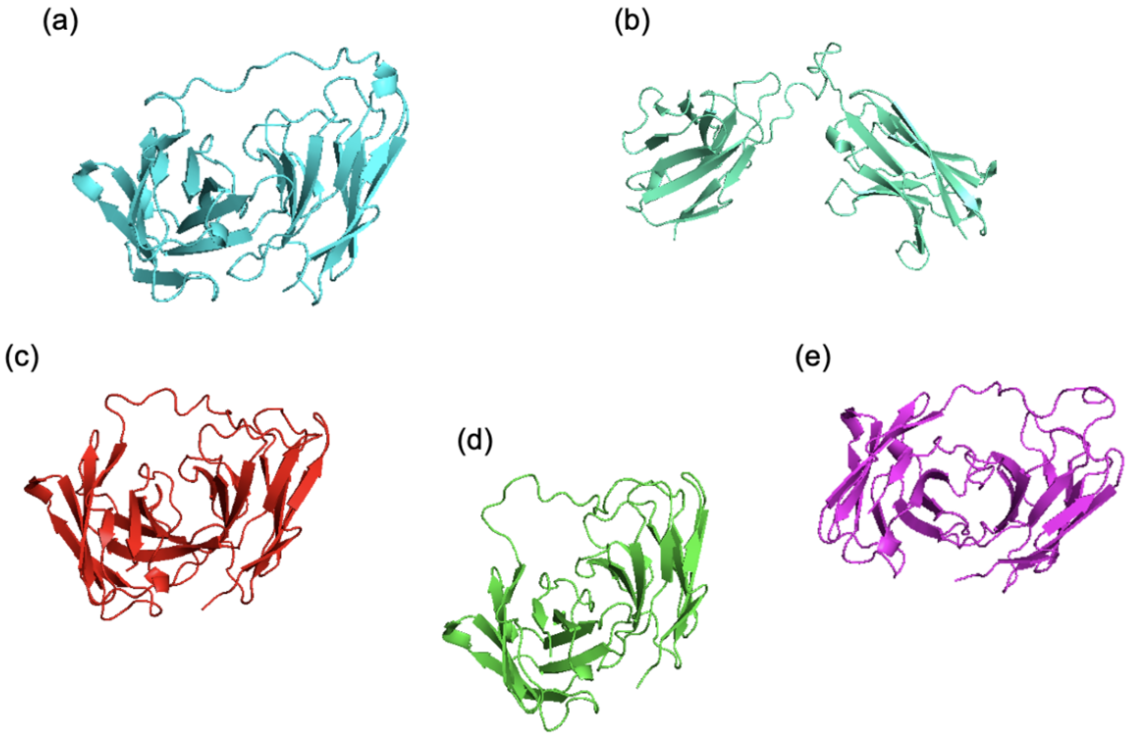

Figure 4.44. Three dimensional models of (a) anti-HER2 scFv V_LV_H, (b) anti-HER2 scFv V_HV_L , (c) anti-HER2 scFv-L2, (d) anti-HER2 scFv-L3 and (e) anti-HER2 scFv-L4

For evaluation of predicted models, ERRAT and Verify-3D tools in the SAVES server were used. Based on the scores obtained from these programs, all structures were acceptable (Table 4.4). In addition, scores given in the table were compatible with a recent study that reported the molecular modelling of scFvs constructed in four different linker sequences [243].

Table 4.4. Model validation scores obtained from online tools

Tool	anti-HER2 scFv V_LV_H	anti-HER2 scFv V_HV_L	anti-HER2 scFv-L2	anti-HER2 scFv-L3	anti-HER2 scFv-L4
ERRAT	94.1	95.9	84.2	93.5	95.6
Verify 3D	97.1	98.8	95.5	87.6	87.6

4.9.2. Molecular Docking of HER2 and Anti-HER2 scFvs

Molecular docking was applied with ClusPro [184] web server by uploading structures of anti-HER2 scFvs obtained from homology modelling and structure of HER2 from database. The best model with the lowest energy was selected among the 29 models given by the server. In Figure 4.45, the structures of anti-HER2-scFvs-HER2 complexes are given.

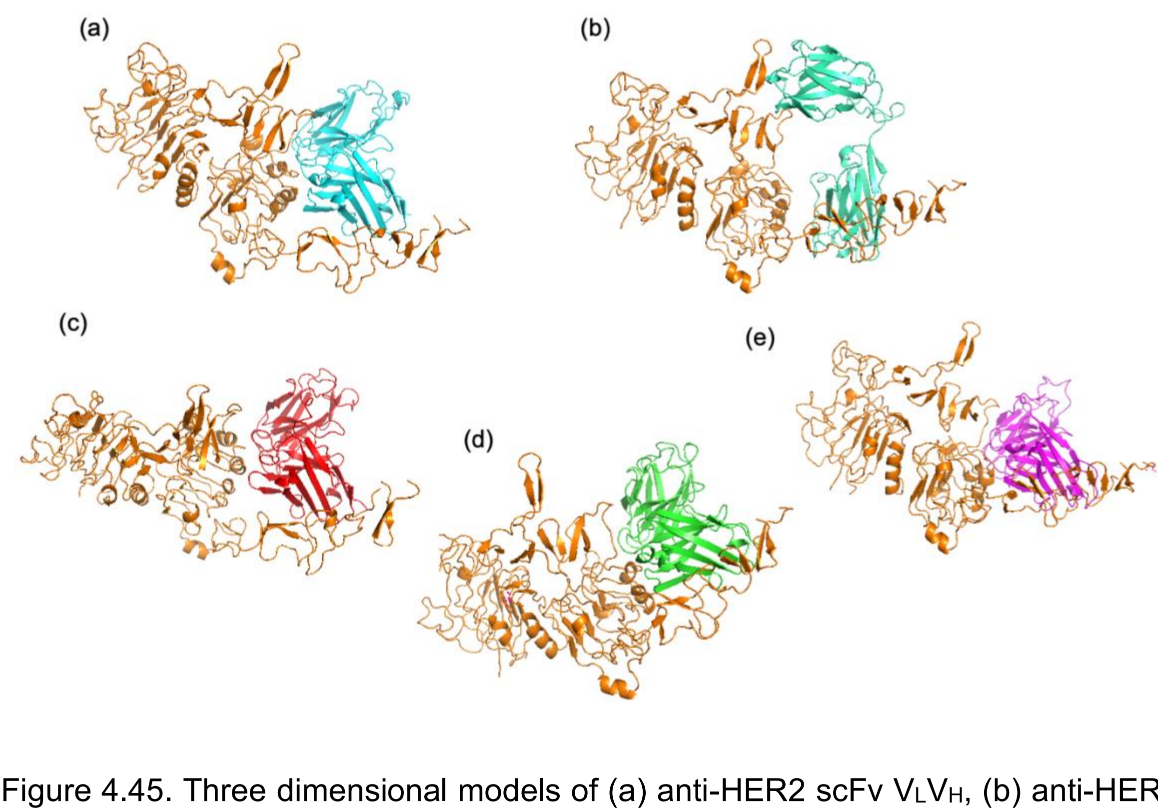

Figure 4.45. Three dimensional models of (a) anti-HER2 scFv V_LV_H, (b) anti-HER2 scFv V_HV_L , (c) anti-HER2 scFv-L2, (d) anti-HER2 scFv-L3 and (e) anti-HER2 scFv-L4 docked with HER2 antigen.

In addition, binding sites of the scFvs on HER2 antigen given in Figure 4.45 was consistent with a previous study showing the binding complex of Fab domain of trastuzumab with HER2 extracellular domain [244].

4.9.3. Molecular Dynamics (MD) Simulation Results

Molecular dynamics simulations were carried out during 20 ns by GROMACS. Firstly, anti-HER2 scFvs with different domain orientations were analyzed by root mean square deviation (RMSD) and radius of gyration (Rg). RMSD is one of the most important factors used for understanding stability of protein and closeness to the experimental structure. In a RMSD plot, fluctuations between 0.1-0.3 nm are suitable for small proteins, whereas larger changes show a possibility of misbehaving of the protein. The backbone RMSDs of anti-HER2 scFv V_LV_H and anti-HER2 scFv V_HV_L docked with HER2 are given in Figure 4.46. As shown in the figure, V_LV_H orientation remained stable around 0.3 nm while V_HV_L orientation stabilized around 0.5 nm. In addition, V_HV_L orientation showed more fluctuation in the first 10 ns, however changes remained in the range of 0.1-0.3 nm, which can be accepted.

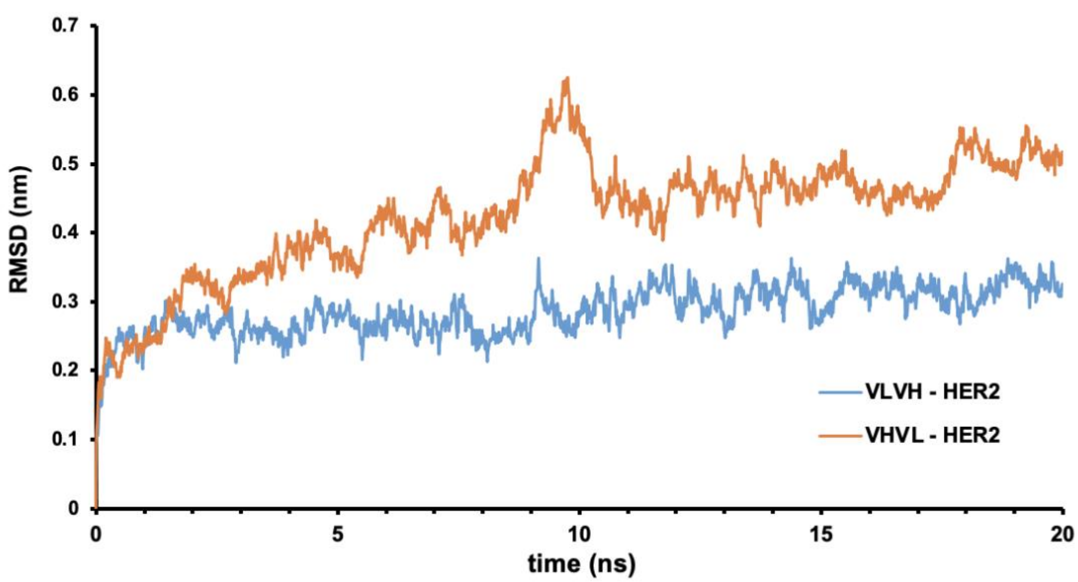

Figure 4.46. Root mean square deviation (RMSD) evaluation of anti-HER2 scFv V_LV_H and anti-HER2 scFv V_HV_L docked with HER2

To evaluate the compactness of the complexes, Rg was also compared (Figure 4.47). As shown in the figure, the average radius of gyration of the two complexes oscillated between 3.3 nm and 3.5 nm. While anti-HER2 scFv V_LV_H-HER2 showed a stabile behaviour, the decreasing trend of the anti-HER2 scFv V_HV_L-HER2 also indicated that the complex became stable.

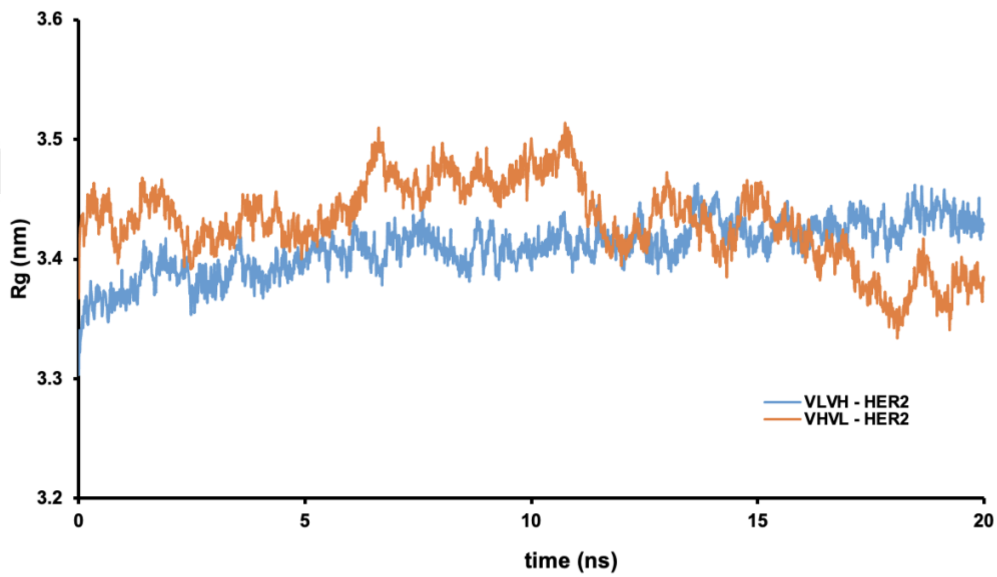

Figure 4.47. Radius of gyration evaluation of anti-HER2 scFv V_LV_H and anti-HER2 scFv V_HV_L complex with HER2

Root mean square fluctuations (RMSF) of anti-HER2 scFvs were graphed in relation to residue number to indicate the fluctuation of all residues. As seen in Figure 4.48, anti-HER2 scFv V_HV_L had more flexibility with fluctuation up to 0.5 nm compared with anti-HER2 scFv V_LV_H that fluctuated up to 0.25 nm. It is also worth noting that residue numbers that fluctuated were different in the two constructs and the linker region have shifted in V_HV_L since V_H domain of the anti-HER2 scFv had more residues than that of V_L domain. Overall, the effects of the domain orientation on formation of monomer/dimer and binding activities of anti-HER2 scFvs to HER2 were investigated experimentally as discussed in previous sections. Hence, it is obvious that structural differences between the two domain orientations affected the binding site geometry and stability of proteins. Additionally, higher binding activity of anti-HER2 scFv V_HV_L could be explained by the higher flexibility in the linker region.

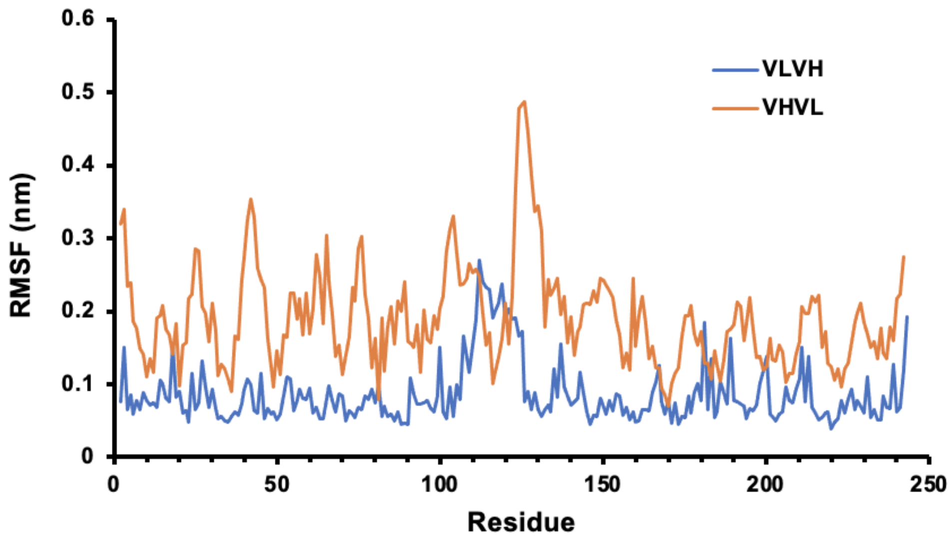

Figure 4.48. Root mean square fluctuation (RMSF) evaluation of anti-HER2 scFv V_LV_H and anti-HER2 scFv V_HV_L

In the next step, anti-HER2 scFvs with different linkers were analyzed by RMSD, radius of gyration and RMSF. The backbone RMSDs of anti-HER2 scFv constructs and anti-HER2 scFv complexes with HER2 are given in Figure 4.49. As shown in the figure, all structures reached the stability (Figure 4.49a). Anti-HER2 scFv with L2 linker showed fluctuation when docked with HER2 (Figure 4.49b). Furthermore, changes in RMSD values remained in the range of 0.1-0.3 nm, which is acceptable.

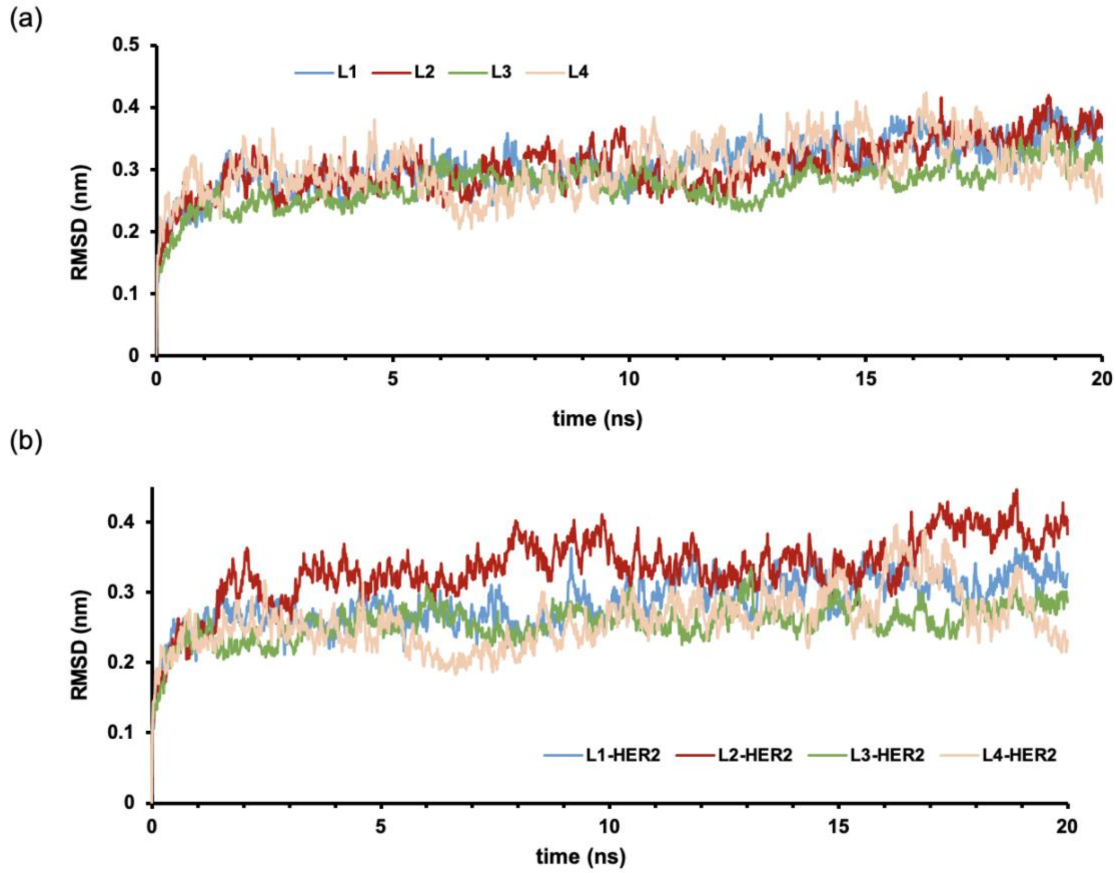

Figure 4.49. Root mean square deviation (RMSD) evaluation of (a) anti-HER2 scFv constructs and (b) anti-HER2 scFv constructs complex with HER2

Figure 4.50 shows the radius of gyration comparison of anti-HER2 scFv-HER2 complexes. R_g values changed between 3.55 and 3.3 nm and anti-HER2 scFv with L4 linker had more fluctuation than others.

RMSF analysis giving information about flexibility of linker region was applied for anti-HER2 scFv with different linker peptides. As seen in Figure 4.51, anti-HER2 scFvs having the standard linker and L2 linker showed the highest fluctuation in the linker region that indicates flexibility of the linkers.

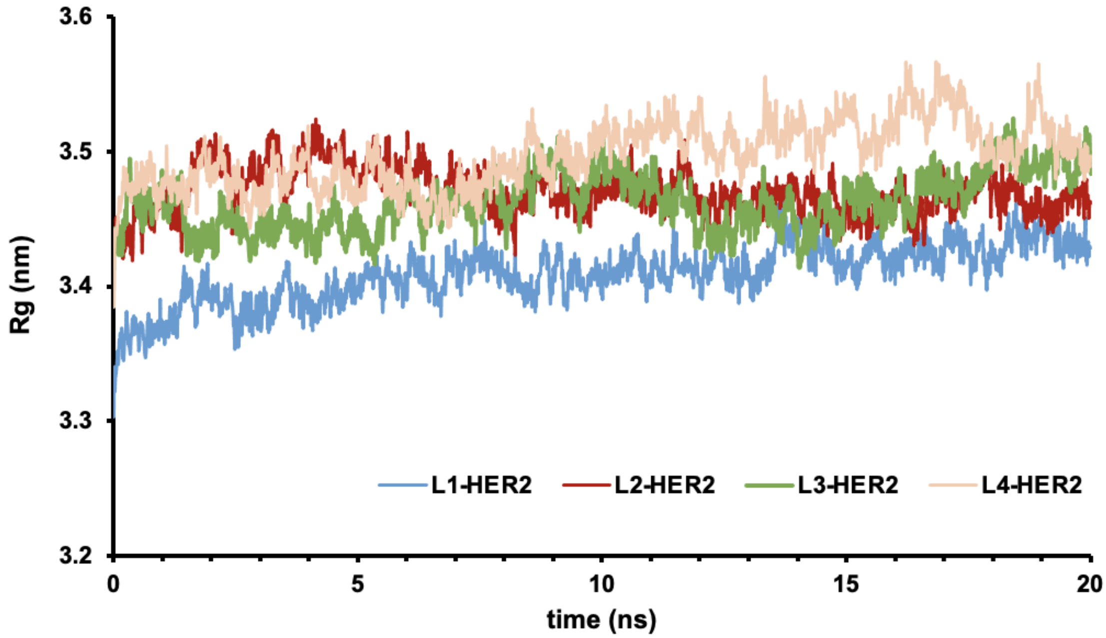

Figure 4.50. Radius of gyration of anti-HER2 scFv constructs docked with HER2

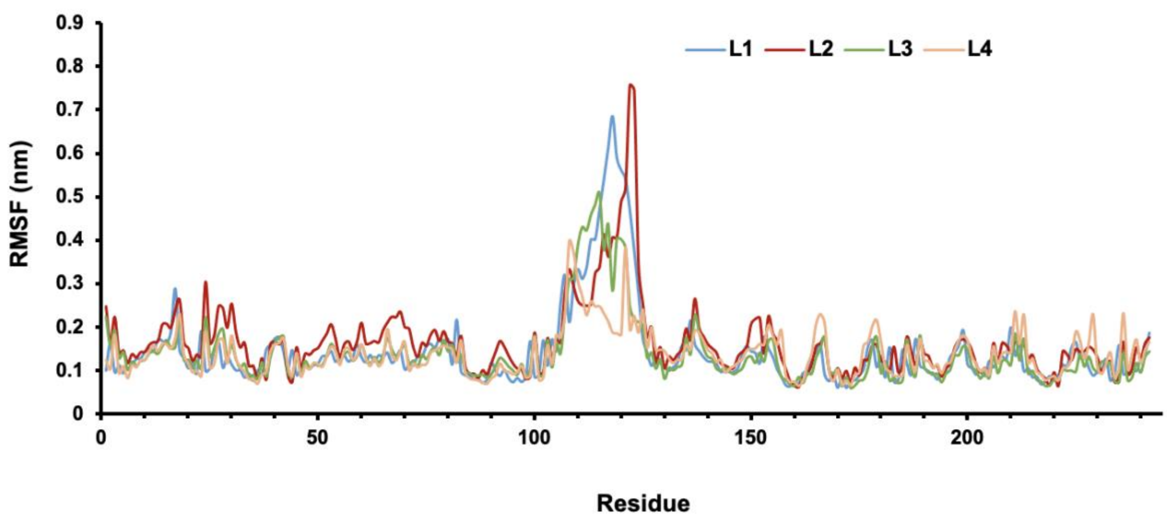

Figure 4.51. Root mean square fluctuation (RMSF) evaluation of anti-HER2 scFv constructs

The conformations of all the anti-HER2 scFv-HER2 complexes were sampled from the equilibrated MD simulation trajectories and the binding free energies were calculated via the g_mmpbsa tool (Table 4.5). The final binding energy is a cumulative sum of van der Waals, polar solvation, electrostatic, and apolar energy. While three energy types except polar solvation energy positively contributed to total binding energy, contribution of polar solvation energy which is positive value is unfavorable. In addition, since this tool does not calculate entropy term given in Equation 2.2, it gives relative binding energies. Thus, it is unable to provide absolute binding free energy used for the calculation of affinity (Equation 2.5). In a previous study, Platani and coworkers analyzed each term individually, and they reported that there was a correlation between ΔG_{Apolar} and experimental K_d [245], that means the hydrophobic effect is substantially responsible for affinity. It was the opposite in our case, where the anti-HER2 scFv-L2 had the lowest K_d value (Table 4.3), and the highest ΔG_{Apolar} and $\Delta E_{binding}$ among the various versions constructed.

Table 4.5. Binding free energies (kJ/mol) computed by the MM-GBSA method

Sample	**ΔE_{VdW}**	**$\Delta E_{Eloctrostatic}$**	**ΔG_{Polor}**	**ΔG_{Apolar}**	**$\Delta E_{binding}$**
Anti-HER2 scFv-V_HV_L	-853	-1327	1790	-127	-517
Anti-HER2 scFv-L1	-775	-1220	1501	-110	-604
Anti-HER2 scFv-L2	-548	-1235	1802	-91	-71
Anti-HER2 scFv-L3	-692	-1465	2127	-112	-142
Anti-HER2 scFv-L4	-816	-1134	2004	-128	-74

Collectively, it could be concluded that analysis of MD simulations resulted in compatibility with experimental results in terms of stability, folding and flexibility of linkers. All anti-HER2 scFv constructs in this study were successfully produced as soluble, correctly folded and functional. RMSD and radius of gyrations graphs also showed stability and compactness which means folding of proteins for all constructions of anti-HER2 scFv. When experimental results and analysis of MD simulations were investigated in term of binding to the PS surfaces, anti-HER2 scFv with L3 and L4 linkers showed lower binding to ELISA plates experimentally. As seen in the Figure 4.51, linker regions of anti-HER2 scFvs with L3 and L4 showed lower flexibility relative to anti-HER2 scFvs with standard linker and L2 linker. Therefore, lower binding of these scFvs could be explained by the lower flexibility of linker region. In addition, all constructed anti-HER2 scFv showed similar binding activity against HER2 experimentally, consistent results could not be obtained with relative binding energies of simulations.

5. CONCLUSION

In this study, model scFvs having different constructs were successfully produced with soluble, active and correctly folded properties in *Escherichia coli*. In the first part, anti-HER2 scFv antibodies were constructed in different orientations and these recombinant scFvs were assessed in terms of solubility, binding activity, monomer/dimer formation and binding affinity. In the second part of the study, model scFvs were developed by adding linkers with different amino acid composition towards immobilization on to polystyrene surfaces and characteristics of new scFvs were investigated via both computational and experimental analyses. The results obtained from the expression and characterization of scFv constructs are given below:

- Anti-HER2 scFv genes yielding 764-bp products were constructed by connecting V_L and V_H domains of the full-length antibody with a standard linker via SOE-PCR method. Expression vectors of pET28a-anti-HER2-scFv-V_LV_H and pET28a-anti-HER2-scFv-V_HV_L were generated by the ligation reaction of pET28a plasmid and the anti-HER2 scFv genes.

- Anti-HER2 scFv and scFv735 were evaluated with regard to soluble expression at 30°C in the cytoplasm of *E. coli* strains SHuffle T7 Express and BL21(DE3), the former of which is engineered to provide the oxidizing environment for disulfide bond formation in the cytoplasm. Western blot analysis resulted in detection of anti-HER2 scFv and scFv735 bands at the predicted sizes of ~27 kDa with anti-6xHis-tag-HRP antibody. While the soluble cell lysates of *E. coli* BL21(DE3) had higher total protein concentration than that of SHuffle strain, both scFvs had higher accumulation in the soluble fractions obtained from SHuffle strain.

- When binding activity evaluation of purified anti-HER2 scFvs expressed in BL21(DE3) and SHuffle strains were performed via ELISA, anti-HER2 scFv derived from SHuffle cells showed up to four-fold higher binding signal against HER2 antigen in the mammalian cell lysate.

- SHuffle T7 Express strain was used as the expression host for subsequent experiments owing to higher solubility and binding activity of the scFvs.

- Production parameters such as induction temperature, induction period and inducer concentration for expression of scFvs in SHuffle cells were optimized. Because of the higher accumulation of scFv in the insoluble fraction obtained from expression at 30°C, post-induction temperature (T_{ind}) was decreased from 30°C to 16°C. Hence, the soluble/insoluble ratio increased nearly three-fold by lowering the induction temperature. Additionally, when growth and production of SHuffle cells containing anti-HER2 scFv-V_LV_H and anti-HER2 scFv-V_HV_L were evaluated together, 20°C and 25°C were high in terms of both cell biomass and total protein concentration. It was shown that IPTG concentration did not significantly affect the anti-HER2 scFv expression. Higher amount of soluble anti-HER2 scFvs were observed between 16-20 h after induction when compared to 2 and 4 h post-induction time. Overall, these results could give an insight in the evaluation of these parameters simultaneously for further statistical design of experiments with less number of tests.

- SHuffle cells containing anti-HER2 scFvs could be alternatively grown in chemically defined minimal medium or in TB complex medium to obtain high cell densities and high yields of soluble protein.

- Considering the overall parameters, growth of SHuffle cells was performed at 16°C for 16 h with 0.1 mM IPTG induction, which gave a satisfactory expression for continuity of experiments.

- Anti-HER2 scFvs with V_L-V_H and V_H-V_L order were assessed with regard to soluble expression and properties of scFvs. Consequently, production of anti-HER2-scFv-V_LV_H and anti-HER2-scFv-V_HV_L from 1 L cell culture was 9.3 mg and 6.2 mg, respectively. Monomer/dimer formation was investigated by SEC analysis and SDS-PAGE. As a result, scFv-V_HV_L showed predominantly monomeric form whereas scFv-V_LV_H was mostly dimeric but also had a significant portion in monomeric form. Both scFvs generally showed high binding activity and selectivity against HER2, whereas scFv-V_HV_L had a higher binding activity, between 0.001-0.04 µg/ml scFv concentration than scFv-V_LV_H. Equilibrium dissociation constants (K_d) were calculated by SPR and K_d values of anti-HER2-scFv-V_LV_H and anti-HER2-scFv-V_HV_L were determined as 5.30 and 4.82 nM, respectively. Collectively, it can be concluded that each scFv was expressed in soluble and active form regardless of the variable domain orientation. Based on the higher expression yield of anti-HER2-scFv-V_LV_H, following experiments were confined to V_LV_H orientation.

- In the second part of this study, three anti-HER2 scFvs with different linkers containing polystyrene (PS) binding peptides were constructed. In addition, PS-tag was added in C-terminal of anti-HER2 scFv with the standard linker. New anti-HER2 scFvs were successfully produced in soluble form with a predicted size of ~27 kDa. An affect on solubility was not observed with the new linkers.

- Changing of linker composition did not affect the binding activity and selectivity of anti-HER2 scFvs against HER2 antigen. Binding affinities of new constructs were determined by ELISA and K_d values were calculated in the same range (about 0.4 nM) except anti-HER2 scFv-L2 construct showing higher affinity (0.23±0.01 nM). In addition, K_d value of anti-HER2 scFv-V_LV_H was calculated about 10-fold lower by ELISA when compared with SPR. This indicated that a higher binding affinity was observed by ELISA, which was consistent with studies comparing calculated affinity by both ELISA and SPR.

- When immobilization of new anti-HER2 scFv constructs on the PS surfaces were investigated, it was observed that immobilization activities of scFvs with different linkers changed in relation to PS plates, and absence or presence of Tween 20.

- HER2 binding activities of immobilized anti-HER2 scFvs were investigated by sandwich ELISA. Anti-HER2 scFv with standard linker and anti-HER2 scFv containing L2 linker showed similar binding activity. However, other anti-HER2 scFv constructs showed less binding activity due to lower immobilization yield on the PS surface. In addition, anti-HER2 scFv containing C-terminal PS-tag showed the highest binding activity among all scFv constructs.

- Designed linkers were also added between V_L and V_H regions of scFv13R4, which was the other model antibody fragment to determine if the effects of linkers are versatile or specific for each individual scFv. ScFv13R4 constructs were expressed in *E. coli* BL21(DE3) by inducing with 0.1 mM IPTG at 25°C post-induction temperature. Similar to the anti-HER2 scFvs, scFv13R4 constructs were expressed in soluble form with no enhancement and all constructs showed similar β-galactosidase binding activity.

- Anti-HER2 scFvs were also evaluated by molecular dynamics (MD) simulation analyses. Firstly, three dimensional structures of scFvs with different linkers and orientation were predicted with homology modelling. Then, anti-HER2 scFv-HER2 docking was performed. RMSD values of constructs reached stability at the end of 20 ns simulation. MD simulation was applied to investigate the effect of linker composition on the stability, folding, flexibility and binding energies of scFvs.

In conclusion, anti-HER2 scFvs constructed in this study hold great potential as biorecognition elements in immunoassays or diagnostic tools for detection of HER2 antigen owing to their highly soluble expression and biologically active forms. Based on the experimental results and MD simulations, anti-HER2 scFv with L2 linker can be an appropriate substitution for standard linkers in scFvs in immunoassay applications. Additionally, the *in silico* analysis strategy used in this study can also be used for the selection and optimization of linkers or other peptide tags with regard to stability, flexibility and functionality of proteins, prior to any application.

REFERENCES

[1] D.M. Ecker, S.D. Jones, H.L. Levine, The therapeutic monoclonal antibody market, mAbs, 7 **(2015)** 9-14.

[2] O. Yang, M. Qadan, M. Ierapetritou, Economic Analysis of Batch and Continuous Biopharmaceutical Antibody Production: a Review, Journal of Pharmaceutical Innovation, 15 **(2020)** 182-200.

[3] R. Bakhtiar, Therapeutic Recombinant Monoclonal Antibodies, Journal of Chemical Education, 89 **(2012)** 1537-1542.

[4] R. Bird, K. Hardman, J. Jacobson, S. Johnson, B. Kaufman, S. Lee, T. Lee, S. Pope, G. Riordan, M. Whitlow, Single-chain antigen-binding proteins, Science, 242 **(1988)** 423-426.

[5] X. Chen, J.L. Zaro, W.C. Shen, Fusion protein linkers: property, design and functionality, Advanced drug delivery reviews, 65 **(2013)** 1357-1369.

[6] X. Gu, X. Jia, J. Feng, B. Shen, Y. Huang, S. Geng, Y. Sun, Y. Wang, Y. Li, M. Long, Molecular Modeling and Affinity Determination of scFv Antibody: Proper Linker Peptide Enhances Its Activity, Annals of Biomedical Engineering, 38 **(2010)** 537-549.

[7] B.V. Ayyar, S. Arora, S.S. Ravi, Optimizing antibody expression: The nuts and bolts, Methods, 116 **(2017)** 51-62.

[8] P. Holliger, P.J. Hudson, Engineered antibody fragments and the rise of single domains, Nat Biotechnol, 23 **(2005)** 1126-1136.

[9] R. Wang, S. Xiang, Y. Feng, S. Srinivas, Y. Zhang, M. Lin, S. Wang, Engineering production of functional scFv antibody in E. coli by co-expressing the molecule chaperone Skp, Front Cell Infect Microbiol, 3 **(2013)** 72.

[10] A. Frenzel, M. Hust, T. Schirrmann, Expression of recombinant antibodies, Front Immunol, 4 **(2013)** 217.

[11] V. Joosten, C. Lokman, C.A. van den Hondel, P.J. Punt, The production of antibody fragments and antibody fusion proteins by yeasts and filamentous fungi, Microbial Cell Factories, 2 **(2003)** 1-1.

[12] K.I. Na, S.J. Kim, D.S. Choi, W.K. Min, S.G. Kim, J.H. Seo, Extracellular production of functional single-chain variable fragment against aflatoxin B(1) using Escherichia coli, Lett Appl Microbiol, 68 **(2019)** 241-247.

[13] A. Karyolaimos, H. Ampah-Korsah, T. Hillenaar, A. Mestre Borras, K.M. Dolata, S. Sievers, K. Riedel, R. Daniels, J.W. de Gier, Enhancing Recombinant Protein Yields in the E. coli Periplasm by Combining Signal Peptide and Production Rate Screening, Front Microbiol, 10 **(2019)** 1511.

[14] K.S. Rostinawati T1*, Yusuf M2, Gaffar S2 and Subroto, T2, Construction and Expression of Synthetic-gene encoding anti-HER2 scFv Fused with pelB in Escherichia coli BL21 (DE3), Journal of Pharmaceutical Sciences and Research, Vol. 9(11) **(2017)**.

[15] A. Gąciarz, N.K. Khatri, M.L. Velez-Suberbie, M.J. Saaranen, Y. Uchida, E. Keshavarz-Moore, L.W. Ruddock, Efficient soluble expression of disulfide bonded proteins in the cytoplasm of Escherichia coli in fed-batch fermentations on chemically defined minimal media, Microbial Cell Factories, 16 **(2017)** 108.

[16] C. Liu, Y. Kobashigawa, S. Yamauchi, Y. Toyota, M. Teramoto, Y. Ikeguchi, N. Fukuda, T. Sato, Y. Sato, H. Kimura, H. Morioka, Preparation of single-chain Fv antibodies in the cytoplasm of Escherichia coli by simplified and systematic chaperone optimization, J Biochem, 166 **(2019)** 455-462.

[17] M. Ahmadzadeh, F. Farshdari, L. Nematollahi, M. Behdani, E. Mohit, Anti-HER2 scFv Expression in Escherichia coli SHuffle®T7 Express Cells: Effects on Solubility and Biological Activity, Molecular Biotechnology, 62 **(2020)** 18-30.

[18] V. Crivianu-Gaita, M. Thompson, Aptamers, antibody scFv, and antibody Fab' fragments: An overview and comparison of three of the most versatile biosensor biorecognition elements, Biosens Bioelectron, 85 **(2016)** 32-45.

[19] X. Zeng, Z. Shen, R. Mernaugh, Recombinant antibodies and their use in biosensors, Anal Bioanal Chem, 402 **(2012)** 3027-3038.

[20] Y. Kumada, D. Kuroki, H. Yasui, T. Ohse, M. Kishimoto, Characterization of polystyrene-binding peptides (PS-tags) for site-specific immobilization of proteins, Journal of Bioscience and Bioengineering, 109 **(2010)** 583-587.

[21] T. Ikeda, Y. Hata, K.-i. Ninomiya, Y. Ikura, K. Takeguchi, S. Aoyagi, R. Hirota, A. Kuroda, Oriented immobilization of antibodies on a silicon wafer using Si-tagged protein A, Analytical Biochemistry, 385 **(2009)** 132-137.

[22] E. Juan-Franco, A. Caruz, J.R. Pedrajas, L.M. Lechuga, Site-directed antibody immobilization using a protein A–gold binding domain fusion protein for enhanced SPR immunosensing, Analyst, 138 **(2013)** 2023-2031.

[23] P. Navabi, M.R. Ganjalikhany, S. Jafari, M. Dehbashi, M. Ganjalikhani-Hakemi, Designing and generating a single-chain fragment variable (scFv) antibody against IL2Rα (CD25): An in silico and in vitro study, Iran J Basic Med Sci, 24 **(2021)** 360-368.

[24] J. Cheng, Q. Dul, Zhang, Y. Ren, B. Zhang, X. Feng, Study on the relationship between the structure and functions of anti-human cervical cancer single-chain antibody and the lengths of linkers, Eur J Gynaecol Oncol, 37 **(2016)** 171-177.

[25] F.I. Khan, D.-Q. Wei, K.-R. Gu, M.I. Hassan, S. Tabrez, Current updates on computer aided protein modeling and designing, International Journal of Biological Macromolecules, 85 **(2016)** 48-62.

[26] A.D. Portnoff, E.A. Stephens, J.D. Varner, M.P. DeLisa, Ubiquibodies, synthetic E3 ubiquitin ligases endowed with unnatural substrate specificity for targeted protein silencing, J Biol Chem, 289 **(2014)** 7844-7855.

[27] P. Martineau, P. Jones, G. Winter, Expression of an antibody fragment at high levels in the bacterial cytoplasm, J Mol Biol, 280 **(1998)** 117-127.

[28] M.-P. Robinson, N. Ke, J. Lobstein, C. Peterson, A. Szkodny, T.J. Mansell, C. Tuckey, P.D. Riggs, P.A. Colussi, C.J. Noren, C.H. Taron, M.P. DeLisa, M. Berkmen, Efficient expression of full-length antibodies in the cytoplasm of engineered bacteria, Nature Communications, 6 **(2015)** 8072.

[29] S. Pronk, S. Pall, R. Schulz, P. Larsson, P. Bjelkmar, R. Apostolov, M.R. Shirts, J.C. Smith, P.M. Kasson, D. van der Spoel, B. Hess, E. Lindahl, GROMACS 4.5: a high-throughput and highly parallel open source molecular simulation toolkit, Bioinformatics (Oxford, England), 29 **(2013)** 845-854.

[30] J.B. Adlersberg, The immunoglobulin hinge (Interdomain) region, Ricerca in clinica e in laboratorio, 6 **(1976)** 191.

[31] T.H. Kang, B.L. Seong, Solubility, Stability, and Avidity of Recombinant Antibody Fragments Expressed in Microorganisms, Front. Microbiol., 11 **(2020)** 10.

[32] M.L. Chiu, D.R. Goulet, A. Teplyakov, G.L. Gilliland, Antibody Structure and Function: The Basis for Engineering Therapeutics, Antibodies (Basel), 8 **(2019)** 55.

[33] T.T. Wu, E.A. Kabat, An analysis of the sequences of the variable regions of Bence Jones proteins and myeloma light chains and their implications for antibody complementarity, J Exp Med, 132 **(1970)** 211-250.

[34] P.J. Conroy, S. Hearty, P. Leonard, R.J. O'Kennedy, Antibody production, design and use for biosensor-based applications, Semin Cell Dev Biol, 20 **(2009)** 10-26.

[35] A.L. Nelson, Antibody fragments, mAbs, 2 **(2010)** 77-83.

[36] R.-M. Lu, Y.-C. Hwang, I.J. Liu, C.-C. Lee, H.-Z. Tsai, H.-J. Li, H.-C. Wu, Development of therapeutic antibodies for the treatment of diseases, Journal of Biomedical Science, 27 **(2020)** 1.

[37] Antibody Society (2020), https://www.antibodysociety.org/resources/approved-antibodies/ (Accessed date: **July 16, 2021**).

[38] B. Wootla, A. Denic, M. Rodriguez, Polyclonal and monoclonal antibodies in clinic, Methods Mol Biol, 1060 **(2014)** 79-110.

[39] G. Köhler, C. Milstein, Continuous cultures of fused cells secreting antibody of predefined specificity. 1975, J Immunol, 174 **(2005)** 2453-2455.

[40] G. Köhler, C. Milstein, Continuous cultures of fused cells secreting antibody of predefined specificity, Nature, 256 **(1975)** 495-497.

[41] M.Z. Siddiqui, Monoclonal antibodies as diagnostics; an appraisal, Indian J Pharm Sci, 72 **(2010)** 12-17.

[42] H.A. Parray, S. Shukla, S. Samal, T. Shrivastava, S. Ahmed, C. Sharma, R. Kumar, Hybridoma technology a versatile method for isolation of monoclonal antibodies, its applicability across species, limitations, advancement and future perspectives, Int Immunopharmacol, 85 **(2020)** 106639-106639.

[43] A. Plückthun, A. Skerra, Expression of functional antibody Fv and Fab fragments in Escherichia coli, Methods in Enzymology, Academic Presspp. 497-515, **1989.**

[44] M. Ho, S. Nagata, I. Pastan, Isolation of anti-CD22 Fv with high affinity by Fv display on human cells, Proc Natl Acad Sci U S A, 103 **(2006)** 9637-9642.

[45] P. Galeffi, A. Lombardi, I. Pietraforte, F. Novelli, M. Di Donato, M. Sperandei, A. Tornambé, R. Fraioli, A. Martayan, P.G. Natali, M. Benevolo, M. Mottolese, F. Ylera, C. Cantale, P. Giacomini, Functional expression of a single-chain antibody to ErbB-2 in plants and cell-free systems, Journal of Translational Medicine, 4 **(2006)** 39.

[46] A.B.H. Choo, R.D. Dunn, K.W. Broady, R.L. Raison, Soluble Expression of a Functional Recombinant Cytolytic Immunotoxin in Insect Cells, Protein expression and purification, 24 **(2002)** 338-347.

[47] L. Montoliu-Gaya, G. Esquerda-Canals, S. Bronsoms, S. Villegas, Production of an anti-Aβ antibody fragment in Pichia pastoris and in vitro and in vivo validation of its therapeutic effect, PLoS One, 12 **(2017)** e0181480.

[48] M. Stech, M. Hust, C. Schulze, S. Dübel, S. Kubick, Cell-free eukaryotic systems for the production, engineering, and modification of scFv antibody fragments, Eng Life Sci, 14 **(2014)** 387-398.

[49] S. Sharma, H. Byrne, R. O'Kennedy, Antibodies and antibody-derived analytical biosensors, Essays in Biochemistry, 60 **(2016)** 9 - 18.

[50] A. Bates, C.A. Power, David vs. Goliath: The Structure, Function, and Clinical Prospects of Antibody Fragments, Antibodies, 8 **(2019)** 28.

[51] J.S. Huston, D. Levinson, M. Mudgett-Hunter, M.S. Tai, J. Novotný, M.N. Margolies, R.J. Ridge, R.E. Bruccoleri, E. Haber, R. Crea, et al., Protein engineering of antibody binding sites: recovery of specific activity in an anti-digoxin single-chain Fv analogue produced in Escherichia coli, Proc Natl Acad Sci U S A, 85 **(1988)** 5879-5883.

[52] K. Alfthan, K. Takkinen, D. Sizmann, H. Söderlund, T.T. Teeri, Properties of a single-chain antibody containing different linker peptides, Protein Engineering, Design and Selection, 8 **(1995)** 725-731.

[53] A.A. Kortt, R.L. Malby, J.B. Caldwell, L.C. Gruen, N. Ivancic, M.C. Lawrence, G.J. Howlett, R.G. Webster, P.J. Hudson, P.M. Colman, Recombinant anti-sialidase single-chain variable fragment antibody. Characterization, formation of dimer and higher-molecular-mass multimers and the solution of the crystal structure of the single-chain variable fragment/sialidase complex, Eur J Biochem, 221 **(1994)** 151-157.

[54] A. Sandomenico, J.P. Sivaccumar, M. Ruvo, Evolution of Escherichia coli Expression System in Producing Antibody Recombinant Fragments, Int. J. Mol. Sci., 21 **(2020)** 6324.

[55] G. Yusakul, S. Sakamoto, B. Pongkitwitoon, H. Tanaka, S. Morimoto, Effect of linker length between variable domains of single chain variable fragment

antibody against daidzin on its reactivity, Biosci Biotechnol Biochem, 80 **(2016)** 1306-1312.

[56] N.E. Long, B.J. Sullivan, H. Ding, S. Doll, M.A. Ryan, C.L. Hitchcock, E.W. Martin, K. Kumar, M.F. Tweedle, T.J. Magliery, Linker engineering in anti-TAG-72 antibody fragments optimizes biophysical properties, serum half-life, and high-specificity tumor imaging, Journal of Biological Chemistry, 293 **(2018)** 9030-9040.

[57] K.S. DEWI, D.S. RETNONINGRUM, C. RIANI, A.M. FUAD, Construction and Periplasmic Expression of the Anti-EGFRvIII ScFv Antibody Gene in Escherichia coli, Scientia Pharmaceutica, 84 **(2016)** 141-152.

[58] X. Hu, R. O'Dwyer, J.G. Wall, Cloning, expression and characterisation of a single-chain Fv antibody fragment against domoic acid in Escherichia coli, J Biotechnol, 120 **(2005)** 38-45.

[59] Y.J. Kim, R. Neelamegam, M.A. Heo, S. Edwardraja, H.J. Paik, S.G. Lee, Improving the productivity of single-chain Fv antibody against c-Met by rearranging the order of its variable domains, J Microbiol Biotechnol, 18 **(2008)** 1186-1190.

[60] D. Gil, A.G. Schrum, Strategies to stabilize compact folding and minimize aggregation of antibody-based fragments, Adv Biosci Biotechnol, 4 **(2013)** 73-84.

[61] F. Li, N. Vijayasankaran, A. Shen, R. Kiss, A. Amanullah, Cell culture processes for monoclonal antibody production, mAbs, 2 **(2010)** 466-479.

[62] O. Spadiut, S. Capone, F. Krainer, A. Glieder, C. Herwig, Microbials for the production of monoclonal antibodies and antibody fragments, Trends in Biotechnology, 32 **(2014)** 54-60.

[63] Z. Li, B.-F. Krippendorff, S. Sharma, A.C. Walz, T. Lavé, D.K. Shah, Influence of molecular size on tissue distribution of antibody fragments, mAbs, 8 **(2016)** 113-119.

[64] R.V. Kholodenko, D.V. Kalinovsky, Doronin, II, E.D. Ponomarev, I.V. Kholodenko, Antibody Fragments as Potential Biopharmaceuticals for Cancer Therapy: Success and Limitations, Curr Med Chem, 26 **(2019)** 396-426.

[65] L. Sanz, Á.M. Cuesta, M. Compte, L. Álvarez-Vallina, Antibody engineering: facing new challenges in cancer therapy, Acta Pharmacologica Sinica, 26 **(2005)** 641-648.

[66] D. Müller, A. Karle, B. Meißburger, I. Höfig, R. Stork, R.E. Kontermann, Improved Pharmacokinetics of Recombinant Bispecific Antibody Molecules by Fusion to Human Serum Albumin*, Journal of Biological Chemistry, 282 **(2007)** 12650-12660.

[67] Y.M. Huang, W. Hu, E. Rustandi, K. Chang, H. Yusuf-Makagiansar, T. Ryll, Maximizing productivity of CHO cell-based fed-batch culture using chemically defined media conditions and typical manufacturing equipment, Biotechnol Prog, 26 **(2010)** 1400-1410.

[68] T. Dammeyer, M. Steinwand, S.-C. Krüger, S. Dübel, M. Hust, K.N. Timmis, Efficient production of soluble recombinant single chain Fv fragments by a Pseudomonas putida strain KT2440 cell factory, Microbial Cell Factories, 10 **(2011)** 11.

[69] A. Lakowitz, R. Krull, R. Biedendieck, Recombinant production of the antibody fragment D1.3 scFv with different Bacillus strains, Microbial cell factories, 16 **(2017)** 14-14.

[70] E. Jordan, M. Hust, A. Roth, R. Biedendieck, T. Schirrmann, D. Jahn, S. Dübel, Production of recombinant antibody fragments in Bacillus megaterium, Microbial Cell Factories, 6 **(2007)** 2.

[71] L. Westers, H. Westers, W.J. Quax, Bacillus subtilis as cell factory for pharmaceutical proteins: a biotechnological approach to optimize the host organism, Biochimica et Biophysica Acta (BBA) - Molecular Cell Research, 1694 **(2004)** 299-310.

[72] G.L. Rosano, E.S. Morales, E.A. Ceccarelli, New tools for recombinant protein production in Escherichia coli: A 5-year update, Protein Sci, 28 **(2019)** 1412-1422.

[73] R. Levy, K. Ahluwalia, D.J. Bohmann, H.M. Giang, L.J. Schwimmer, H. Issafras, N.B. Reddy, C. Chan, A.H. Horwitz, T. Takeuchi, Enhancement of antibody fragment secretion into the Escherichia coli periplasm by co-expression with the peptidyl prolyl isomerase, FkpA, in the cytoplasm, Journal of Immunological Methods, 394 **(2013)** 10-21.

[74] C. Huang, Jr., H. Lin, X. Yang, Industrial production of recombinant therapeutics in Escherichia coli and its recent advancements, Journal of Industrial Microbiology & Biotechnology, 39 **(2012)** 383-399.

[75] K.J. Jeong, S.H. Jang, N. Velmurugan, Recombinant antibodies: engineering and production in yeast and bacterial hosts, Biotechnol J, 6 **(2011)** 16-27.

[76] F.S. Javadian, M. Basafa, A. Behravan, A. Hashemi, Solubility assessment of single-chain antibody fragment against epithelial cell adhesion molecule extracellular domain in four Escherichia coli strains, Journal of Genetic Engineering and Biotechnology, 19 **(2021)** 26.

[77] J.H. Choi, S.Y. Lee, Secretory and extracellular production of recombinant proteins using Escherichia coli, Applied microbiology and biotechnology, 64 **(2004)** 625-635.

[78] V. Akbari, H.M. Sadeghi, A. Jafarian-Dehkordi, D. Abedi, C.P. Chou, Improved biological activity of a single chain antibody fragment against human epidermal growth factor receptor 2 (HER2) expressed in the periplasm of Escherichia coli, Protein expression and purification, 116 **(2015)** 66-74.

[79] N.E. Weisser, J.C. Hall, Applications of single-chain variable fragment antibodies in therapeutics and diagnostics, Biotechnol Adv, 27 **(2009)** 502-520.

[80] G.R.M. Kleiner-Grote, J.M. Risse, K. Friehs, Secretion of recombinant proteins from E. coli, Eng Life Sci, 18 **(2018)** 532-550.

[81] I.M. Kasli, O.R.T. Thomas, T.W. Overton, Use of a design of experiments approach to optimise production of a recombinant antibody fragment in the periplasm of Escherichia coli: selection of signal peptide and optimal growth conditions, AMB Express, 9 **(2019)** 5.

[82] T. Selas Castiñeiras, S.G. Williams, A. Hitchcock, J.A. Cole, D.C. Smith, T.W. Overton, Development of a generic β-lactamase screening system for improved signal peptides for periplasmic targeting of recombinant proteins in Escherichia coli, Scientific Reports, 8 **(2018)** 6986.

[83] K. Mirzadeh, P.J. Shilling, R. Elfageih, A.J. Cumming, H.L. Cui, M. Rennig, M.H.H. Nørholm, D.O. Daley, Increased production of periplasmic proteins in Escherichia coli by directed evolution of the translation initiation region, Microbial Cell Factories, 19 **(2020)** 85.

[84] K. Ukkonen, J. Veijola, A. Vasala, P. Neubauer, Effect of culture medium, host strain and oxygen transfer on recombinant Fab antibody fragment yield and leakage to medium in shaken E. coli cultures, Microbial Cell Factories, 12 **(2013)** 73.

[85] S.K. Gupta, P. Shukla, Microbial platform technology for recombinant antibody fragment production: A review, Critical Reviews in Microbiology, 43 **(2017)** 31-42.

[86] M. Sina, D. Farajzadeh, S. Dastmalchi, Effects of Environmental Factors on Soluble Expression of a Humanized Anti-TNF-α scFv Antibody in Escherichia coli, Adv Pharm Bull, 5 **(2015)** 455-461.

[87] H. Yang, Y. Zhong, J. Wang, Q. Zhang, X. Li, S. Ling, S. Wang, R. Wang, Screening of a ScFv Antibody With High Affinity for Application in Human IFN-γ Immunoassay, Front. Microbiol., 9 **(2018)**.

[88] M. Liu, B. Wang, F. Wang, Z. Yang, D. Gao, C. Zhang, L. Ma, X. Yu, Soluble expression of single-chain variable fragment (scFv) in Escherichia coli using superfolder green fluorescent protein as fusion partner, Applied microbiology and biotechnology, 103 **(2019)** 6071-6079.

[89] D. Esposito, D.K. Chatterjee, Enhancement of soluble protein expression through the use of fusion tags, Curr Opin Biotechnol, 17 **(2006)** 353-358.

[90] H.P. Sørensen, K.K. Mortensen, Soluble expression of recombinant proteins in the cytoplasm of Escherichia coli, Microbial Cell Factories, 4 **(2005)** 1.

[91] J. Lobstein, C.A. Emrich, C. Jeans, M. Faulkner, P. Riggs, M. Berkmen, SHuffle, a novel Escherichia coli protein expression strain capable of correctly folding disulfide bonded proteins in its cytoplasm, Microb Cell Fact, 11 **(2012)** 56.

[92] D. Ritz, J. Lim, C.M. Reynolds, L.B. Poole, J. Beckwith, Conversion of a peroxiredoxin into a disulfide reductase by a triplet repeat expansion, Science, 294 **(2001)** 158-160.

[93] G. Ren, N. Ke, M. Berkmen, Use of the SHuffle Strains in Production of Proteins, Curr Protoc Protein Sci, 85 **(2016)** 5.26.21-25.26.21.

[94] A. Gaciarz, J. Veijola, Y. Uchida, M.J. Saaranen, C. Wang, S. Hörkkö, L.W. Ruddock, Systematic screening of soluble expression ofantibody fragments in the cytoplasm of E. coli, Microbial Cell Factories, 15 **(2016)** 22.

[95] Z. Yildirim, E. Celik, Periplasmic and extracellular production of cellulase from recombinant Escherichia coli cells, J. Chem. Technol. Biotechnol., 92 **(2017)** 319-324.

[96] L. Su, C. Xu, R.W. Woodard, J. Chen, J. Wu, A novel strategy for enhancing extracellular secretion of recombinant proteins in Escherichia coli, Applied microbiology and biotechnology, 97 **(2013)** 6705-6713.

[97] Y. Zhou, Z. Lu, X. Wang, J.N. Selvaraj, G. Zhang, Genetic engineering modification and fermentation optimization for extracellular production of recombinant proteins using Escherichia coli, Applied microbiology and biotechnology, 102 **(2018)** 1545-1556.

[98] G. Zhang, S. Brokx, J.H. Weiner, Extracellular accumulation of recombinant proteins fused to the carrier protein YebF in Escherichia coli, Nature Biotechnology, 24 **(2006)** 100-104.

[99] Z.G. Qian, X.X. Xia, J.H. Choi, S.Y. Lee, Proteome-based identification of fusion partner for high-level extracellular production of recombinant proteins in Escherichia coli, Biotechnol Bioeng, 101 **(2008)** 587-601.

[100] L.A. Fernández, I. Sola, L. Enjuanes, V. de Lorenzo, Specific secretion of active single-chain Fv antibodies into the supernatants of Escherichia coli cultures by use of the hemolysin system, Appl Environ Microbiol, 66 **(2000)** 5024-5029.

[101] A. Nadkarni, L.-L.C. Kelley, C. Momany, Optimization of a mouse recombinant antibody fragment for efficient production from Escherichia coli, Protein expression and purification, 52 **(2007)** 219-229.

[102] S.M. Kipriyanov, G. Moldenhauer, M. Little, High level production of soluble single chain antibodies in small-scale Escherichia coli cultures, Journal of Immunological Methods, 200 **(1997)** 69-77.

[103] J. Schäffner, J. Winter, R. Rudolph, E. Schwarz, Cosecretion of Chaperones and Low-Molecular-Size Medium Additives Increases the Yield of Recombinant Disulfide-Bridged Proteins, Appl Environ Microbiol, 67 **(2001)** 3994-4000.

[104] K. Zarschler, S. Witecy, F. Kapplusch, C. Foerster, H. Stephan, High-yield production of functional soluble single-domain antibodies in the cytoplasm of Escherichia coli, Microbial Cell Factories, 12 **(2013)** 97.

[105] V. Akbari, H.M.M. Sadeghi, A. Jafarian-Dehkordi, C.P. Chou, D. Abedi, Optimization of a single-chain antibody fragment overexpression in Escherichia coli using response surface methodology, Res Pharm Sci, 10 **(2015)** 75-83.

[106] H. Sung, J. Ferlay, R.L. Siegel, M. Laversanne, I. Soerjomataram, A. Jemal, F. Bray, Global Cancer Statistics 2020: GLOBOCAN Estimates of Incidence and Mortality Worldwide for 36 Cancers in 185 Countries, CA Cancer J Clin, 71 **(2021)** 209-249.

[107] A. Perrier, J. Gligorov, G. Lefèvre, M. Boissan, The extracellular domain of Her2 in serum as a biomarker of breast cancer, Lab Invest, 98 **(2018)** 696-707.

[108] I. Rubin, Y. Yarden, The basic biology of HER2, Ann Oncol, 12 Suppl 1 **(2001)** S3-8.

[109] D.F. Hayes, HER2 and Breast Cancer — A Phenomenal Success Story, New England Journal of Medicine, 381 **(2019)** 1284-1286.

[110] B. Altunay, A. Morgenroth, M. Beheshti, A. Vogg, N.C.L. Wong, H.H. Ting, H.J. Biersack, E. Stickeler, F.M. Mottaghy, HER2-directed antibodies, affibodies and nanobodies as drug-delivery vehicles in breast cancer with a specific focus on radioimmunotherapy and radioimmunoimaging, Eur J Nucl Med Mol Imaging, 48 **(2021)** 1371-1389.

[111] G.L. Fiszman, M.A. Jasnis, Molecular Mechanisms of Trastuzumab Resistance in HER2 Overexpressing Breast Cancer, Int J Breast Cancer, 2011 **(2011)** 352182-352182.

[112] E.H. Romond, E.A. Perez, J. Bryant, V.J. Suman, C.E. Geyer, N.E. Davidson, E. Tan-Chiu, S. Martino, S. Paik, P.A. Kaufman, S.M. Swain, T.M. Pisansky, L. Fehrenbacher, L.A. Kutteh, V.G. Vogel, D.W. Visscher, G. Yothers, R.B. Jenkins, A.M. Brown, S.R. Dakhil, E.P. Mamounas, W.L. Lingle, P.M. Klein, J.N. Ingle, N. Wolmark, Trastuzumab plus Adjuvant Chemotherapy for Operable HER2-Positive Breast Cancer, New England Journal of Medicine, 353 **(2005)** 1673-1684.

[113] C. Sheridan, FDA approves pertuzumab, Nature Biotechnology, 30 **(2012)** 570-570.

[114] M.C. Franklin, K.D. Carey, F.F. Vajdos, D.J. Leahy, A.M. de Vos, M.X. Sliwkowski, Insights into ErbB signaling from the structure of the ErbB2-pertuzumab complex, Cancer Cell, 5 **(2004)** 317-328.

[115] D.B. Agus, R.W. Akita, W.D. Fox, G.D. Lewis, B. Higgins, P.I. Pisacane, J.A. Lofgren, C. Tindell, D.P. Evans, K. Maiese, H.I. Scher, M.X. Sliwkowski,

Targeting ligand-activated ErbB2 signaling inhibits breast and prostate tumor growth, Cancer Cell, 2 **(2002)** 127-137.

[116] W. Deng, J. Liu, H. Pan, L. Li, C. Zhou, X. Wang, R. Shu, B. Dong, D. Cao, Q. Li, Z. Wang, A Bispecific Antibody Based on Pertuzumab Fab Has Potent Antitumor Activity, J Immunother, 41 **(2018)** 1-8.

[117] F. Nejatollahi, M. Jaberipour, M. Asgharpour, Triple blockade of HER2 by a cocktail of anti-HER2 scFv antibodies induces high antiproliferative effects in breast cancer cells, Tumour Biol, 35 **(2014)** 7887-7895.

[118] Y. Cao, J.D. Marks, Q. Huang, S.I. Rudnick, C. Xiong, W.N. Hittelman, X. Wen, J.W. Marks, L.H. Cheung, K. Boland, C. Li, G.P. Adams, M.G. Rosenblum, Single-chain antibody-based immunotoxins targeting Her2/neu: design optimization and impact of affinity on antitumor efficacy and off-target toxicity, Mol Cancer Ther, 11 **(2012)** 143-153.

[119] Y. Cao, J.D. Marks, J.W. Marks, L.H. Cheung, S. Kim, M.G. Rosenblum, Construction and Characterization of Novel, Recombinant Immunotoxins Targeting the Her2/neu Oncogene Product: In vitro and In vivo Studies, Cancer Research, 69 **(2009)** 8987.

[120] J.W. Park, K. Hong, D.B. Kirpotin, G. Colbern, R. Shalaby, J. Baselga, Y. Shao, U.B. Nielsen, J.D. Marks, D. Moore, D. Papahadjopoulos, C.C. Benz, Anti-HER2 immunoliposomes: enhanced efficacy attributable to targeted delivery, Clin Cancer Res, 8 **(2002)** 1172-1181.

[121] W.R. Heineman, W.B. Jensen, Leland C. Clark Jr. (1918–2005), Biosensors and Bioelectronics, 21 **(2006)** 1403-1404.

[122] D.A. Skoog, S.R. Crouch, F.J. Holler, Principles of instrumental analysis, Thomson Brooks/Cole, Belmont, CA, **2007**.

[123] D. Kim, A.E. Herr, Protein immobilization techniques for microfluidic assays, Biomicrofluidics, 7 **(2013)** 41501-41501.

[124] R. Ohara, A. Knappik, K. Shimada, C. Frisch, F. Ylera, H. Koga, Antibodies for proteomic research: comparison of traditional immunization with recombinant antibody technology, Proteomics, 6 **(2006)** 2638-2646.

[125] H.R. Hoogenboom, Selecting and screening recombinant antibody libraries, Nature Biotechnology, 23 **(2005)** 1105-1116.

[126] A.K. Trilling, J. Beekwilder, H. Zuilhof, Antibody orientation on biosensor surfaces: a minireview, Analyst, 138 **(2013)** 1619-1627.

[127] D. Saerens, L. Huang, K. Bonroy, S. Muyldermans, Antibody Fragments as Probe in Biosensor Development, Sensors (Basel), 8 **(2008)** 4669-4686.

[128] J.P. Palafox-Hernandez, Z. Tang, Z.E. Hughes, Y. Li, M.T. Swihart, P.N. Prasad, T.R. Walsh, M.R. Knecht, Comparative Study of Materials-Binding Peptide Interactions with Gold and Silver Surfaces and Nanostructures: A Thermodynamic Basis for Biological Selectivity of Inorganic Materials, Chemistry of Materials, 26 **(2014)** 4960-4969.

[129] S.M. Fuchs, R.T. Raines, Polyarginine as a multifunctional fusion tag, Protein Sci, 14 **(2005)** 1538-1544.

[130] T. Ikeda, Y. Hata, K. Ninomiya, Y. Ikura, K. Takeguchi, S. Aoyagi, R. Hirota, A. Kuroda, Oriented immobilization of antibodies on a silicon wafer using Si-tagged protein A, Anal Biochem, 385 **(2009)** 132-137.

[131] J.-B. Tang, X.-F. Sun, H.-M. Yang, B.-G. Zhang, Z.-J. Li, Z.-J. Lin, Z.-Q. Gao, Well-oriented ZZ–PS-tag with high Fc-binding onto polystyrene surface for controlled immobilization of capture antibodies, Analytica Chimica Acta, 776 **(2013)** 74-78.

[132] Y. Kumada, Y. Ishikawa, Y. Fujiwara, R. Takeda, R. Miyamoto, D. Niwa, S. Momose, B. Kang, M. Kishimoto, Efficient refolding and immobilization of PMMA-tag-fused single-chain Fv antibodies for sensitive immunological detection on a PMMA plate, Journal of Immunological Methods, 411 **(2014)** 1-10.

[133] J. Lee, J.H. Chang, Facile and high-efficient immobilization of histidine-tagged multimeric protein G on magnetic nanoparticles, Nanoscale Research Letters, 9 **(2014)** 664.

[134] W. Kusnezow, J.D. Hoheisel, Solid supports for microarray immunoassays, J Mol Recognit, 16 **(2003)** 165-176.

[135] N.G. Welch, J.A. Scoble, B.W. Muir, P.J. Pigram, Orientation and characterization of immobilized antibodies for improved immunoassays (Review), Biointerphases, 12 **(2017)** 02d301.

[136] R. Braun, M. Sarikaya, K. Schulten, Genetically engineered gold-binding polypeptides: structure prediction and molecular dynamics, Journal of Biomaterials Science, Polymer Edition, 13 **(2002)** 747-757.

[137] N.S. Heo, S. Zheng, M. Yang, S.J. Lee, S.Y. Lee, H.-J. Kim, J.Y. Park, C.-S. Lee, T.J. Park, Label-Free Electrochemical Diagnosis of Viral Antigens with Genetically Engineered Fusion Protein, Sensors, 12 **(2012)** 10097-10108.

[138] Y. Kwon, Z. Han, E. Karatan, M. Mrksich, B.K. Kay, Antibody arrays prepared by cutinase-mediated immobilization on self-assembled monolayers, Analytical Chemistry, 76 **(2004)** 5713-5720.

[139] X. Hu, M.J. Hortigüela, S. Robin, H. Lin, Y. Li, A.P. Moran, W. Wang, J.G. Wall, Covalent and Oriented Immobilization of scFv Antibody Fragments via an Engineered Glycan Moiety, Biomacromolecules, 14 **(2013)** 153-159.

[140] A. Mechaly, E. Zahavy, M. Fisher, Development and Implementation of a Single-Chain Fv Antibody for Specific Detection of <i>Bacillus anthracis</i> Spores, Appl Environ Microbiol, 74 **(2008)** 818-822.

[141] X. Hu, L. O’Hara, S. White, E. Magner, M. Kane, J. Gerard Wall, Optimisation of production of a domoic acid-binding scFv antibody fragment in Escherichia coli using molecular chaperones and functional immobilisation on a mesoporous silicate support, Protein expression and purification, 52 **(2007)** 194-201.

[142] A. Carlsson, C. Wingren, J. Ingvarsson, P. Ellmark, B. Baldertorp, M. Fernö, H. Olsson, C.A.K. Borrebaeck, Serum proteome profiling of metastatic breast cancer using recombinant antibody microarrays, European Journal of Cancer, 44 **(2008)** 472-480.

[143] E. Lee, H. Jeon, C. Kang, S. Woo, S. Yum, Y. Kwon, Detection of Metallothionein in Javanese Medaka (Oryzias javanicus), Using a scFv-Immobilized Protein Chip, Sensors (Basel), 18 **(2018)**.

[144] Z. Shen, H. Yan, Y. Zhang, R.L. Mernaugh, X. Zeng, Engineering peptide linkers for scFv immunosensors, Analytical chemistry, 80 **(2008)** 1910-1917.

[145] B. Feng, Y. Dai, L. Wang, N. Tao, S. Huang, H. Zeng, A novel affinity ligand for polystyrene surface from a phage display random library and its application in anti-HIV-1 ELISA system, Biologicals, 37 **(2009)** 48-54.

[146] Y. Kumada, B. Kang, K. Yamakawa, M. Kishimoto, J. Horiuchi, Efficient preparation and site-directed immobilization of VHH antibodies by genetic fusion of poly(methylmethacrylate)-binding peptide (PMMA-Tag), Biotechnol Prog, 31 **(2015)** 1563-1570.

[147] Y. Kumada, S. Murata, Y. Ishikawa, K. Nakatsuka, M. Kishimoto, Screening of PC and PMMA-binding peptides for site-specific immobilization of proteins, Journal of Biotechnology, 160 **(2012)** 222-228.

[148] E. de Juan-Franco, A. Caruz, J.R. Pedrajas, L.M. Lechuga, Site-directed antibody immobilization using a protein A–gold binding domain fusion protein for enhanced SPR immunosensing, Analyst, 138 **(2013)** 2023-2031.

[149] D.F. Keren, Enzyme-linked immunosorbent assay for immunoglobulin G and immunoglobulin A antibodies to Shigella flexneri antigens, Infect Immun, 24 **(1979)** 441-448.

[150] Y. Kumada, M. Nogami, F.M. Hasan, M. Terashima, S. Katoh, Epitope Screening by Use of a Random Peptide-Displayed Phage Library and Polyclonal Antibody-Coupled Liposomes, Journal of Chemical Engineering of Japan, 39 **(2006)** 1195-1199.

[151] Y. Kumada, E. Sasaki, M. Kishimoto, Preparation of scFv-immobilized quartz crystal microbalance sensor by PS-tag-mediated solid-phase refolding, Journal of Bioscience and Bioengineering, 111 **(2011)** 459-464.

[152] J.M. Kogot, D.A. Sarkes, I. Val-Addo, P.M. Pellegrino, D.N. Stratis-Cullum, Increased affinity and solubility of peptides used for direct peptide ELISA on polystyrene surfaces through fusion with a polystyrene-binding peptide tag, Biotechniques, 52 **(2012)** 95-102.

[153] Y. Kumada, Y. Tokunaga, H. Imanaka, K. Imamura, T. Sakiyama, S. Katoh, K. Nakanishi, Screening and characterization of affinity peptide tags specific to polystyrene supports for the orientated immobilization of proteins, Biotechnology progress, 22 **(2006)** 401-405.

[154] Y. Kumada, S. Katoh, H. Imanaka, K. Imamura, K. Nakanishi, Development of a one-step ELISA method using an affinity peptide tag specific to a hydrophilic polystyrene surface, J Biotechnol, 127 **(2007)** 288-299.

[155] Y. Kumada, Y. Shiritani, K. Hamasaki, T. Ohse, M. Kishimoto, High biological activity of a recombinant protein immobilized onto polystyrene, Biotechnol J, 4 **(2009)** 1178-1189.

[156] X. Qiang, K. Sun, L. Xing, Y. Xu, H. Wang, Z. Zhou, J. Zhang, F. Zhang, B. Caliskan, M. Wang, Z. Qiu, Discovery of a polystyrene binding peptide isolated from phage display library and its application in peptide immobilization, Scientific Reports, 7 **(2017)** 2673.

[157] Y. Kumada, Y. Shiritani, K. Hamasaki, A. Nakagawa, E. Sasaki, M. Kishimoto, Novel solid-phase refolding method for preparation of scFv-immobilized polystyrene plates with high-antigen-binding activity, Anal Bioanal Chem, 398 **(2010)** 1295-1303.

[158] A. Liu, Q. Xiong, L. Shen, W. Li, Z. Zeng, C. Li, S. Liu, Y. Liu, G. Han, A sandwich-type ELISA for the detection of Listeria monocytogenes using the well-oriented single chain Fv antibody fragment, Food Control, 79 **(2017)** 156-161.

[159] X.H. Yan, Z.R. Xu, Production of human single-chain variable fragment (scFv) antibody specific for digoxin by ribosome display, Indian J Biochem Biophys, 42 **(2005)** 350-357.

[160] B.R. Miller, S.J. Demarest, A. Lugovskoy, F. Huang, X. Wu, W.B. Snyder, L.J. Croner, N. Wang, A. Amatucci, J.S. Michaelson, S.M. Glaser, Stability engineering of scFvs for the development of bispecific and multivalent antibodies, Protein Eng Des Sel, 23 **(2010)** 549-557.

[161] K. Dudgeon, R. Rouet, I. Kokmeijer, P. Schofield, J. Stolp, D. Langley, D. Stock, D. Christ, General strategy for the generation of human antibody variable domains with increased aggregation resistance, Proceedings of the National Academy of Sciences of the United States of America, 109 **(2012)** 10879-10884.

[162] Y. Cai, J. Zhang, X. Lao, H. Jiang, Y. Yu, Y. Deng, J. Zhong, Y. Liang, L. Xiong, N. Deng, Construction of a disulfide-stabilized diabody against fibroblast growth factor-2 and the inhibition activity in targeting breast cancer, Cancer Sci, 107 **(2016)** 1141-1150.

[163] J.-X. Zhao, L. Yang, Z.-N. Gu, H.-Q. Chen, F.-W. Tian, Y.-Q. Chen, H. Zhang, W. Chen, Stabilization of the single-chain fragment variable by an interdomain disulfide bond and its effect on antibody affinity, Int. J. Mol. Sci., 12 **(2010)** 1-11.

[164] K. Zhang, M.L. Geddie, N. Kohli, T. Kornaga, D.B. Kirpotin, Y. Jiao, R. Rennard, D.C. Drummond, U.B. Nielsen, L. Xu, A.A. Lugovskoy, Comprehensive optimization of a single-chain variable domain antibody fragment as a targeting ligand for a cytotoxic nanoparticle, MAbs, 7 **(2015)** 42-52.

[165] J.I. Austerberry, A. Thistlethwaite, K. Fisher, A.P. Golovanov, A. Pluen, R. Esfandiary, C.F. van der Walle, J. Warwicker, J.P. Derrick, R. Curtis, Arginine to Lysine Mutations Increase the Aggregation Stability of a Single-Chain

Variable Fragment through Unfolded-State Interactions, Biochemistry, 58 **(2019)** 3413-3421.

[166] J. Lee, B.S. Der, C.S. Karamitros, W. Li, N.M. Marshall, O.I. Lungu, A.E. Miklos, J. Xu, T.H. Kang, C.H. Lee, B. Tan, R.A. Hughes, S.T. Jung, G.C. Ippolito, J.J. Gray, Y. Zhang, B. Kuhlman, G. Georgiou, A.D. Ellington, Computer-based Engineering of Thermostabilized Antibody Fragments, AIChE J, 66 **(2020)**.

[167] K.A. Dill, S.B. Ozkan, M.S. Shell, T.R. Weikl, The Protein Folding Problem, Annual Review of Biophysics, 37 **(2008)** 289-316.

[168] B. Kuhlman, D. Baker, Native protein sequences are close to optimal for their structures, Proceedings of the National Academy of Sciences of the United States of America, 97 **(2000)** 10383-10388.

[169] M.I. Hassan, V. Kumar, T.P. Singh, S. Yadav, Structural Model of Human PSA: A Target for Prostate Cancer Therapy, Chemical Biology & Drug Design, 70 **(2007)** 261-267.

[170] F.I. Khan, B. Nizami, R. Anwer, K.R. Gu, K. Bisetty, M.I. Hassan, D.Q. Wei, Structure prediction and functional analyses of a thermostable lipase obtained from Shewanella putrefaciens, J Biomol Struct Dyn, 35 **(2017)** 2123-2135.

[171] M. Bandehpour, S. Ahangarzadeh, F. Yarian, A. Lari, P. Farnia, In silico evaluation of the interactions among two selected single chain variable fragments (scFvs) and ESAT-6 antigen of Mycobacterium tuberculosis, Journal of Theoretical and Computational Chemistry, 16 **(2017)** 1750069.

[172] V.K. Bhardwaj, R. Purohit, Targeting the protein-protein interface pocket of Aurora-A-TPX2 complex: rational drug design and validation, Journal of Biomolecular Structure and Dynamics, 39 **(2021)** 3882-3891.

[173] F.I. Khan, D.Q. Wei, K.R. Gu, M.I. Hassan, S. Tabrez, Current updates on computer aided protein modeling and designing, International journal of biological macromolecules, 85 **(2016)** 48-62.

[174] P. Koehl, M. Levitt, A brighter future for protein structure prediction, Nature Structural Biology, 6 **(1999)** 108-111.

[175] R. Sánchez, A. Šali, Advances in comparative protein-structure modelling, Current Opinion in Structural Biology, 7 **(1997)** 206-214.

[176] https://salilab.org/modeller/, (Accessed date: **July 16, 2021**).

[177] L.A. Kelley, S. Mezulis, C.M. Yates, M.N. Wass, M.J.E. Sternberg, The Phyre2 web portal for protein modeling, prediction and analysis, Nature Protocols, 10 **(2015)** 845.

[178] https://swissmodel.expasy.org/, (Accessed date: **July 16, 2021**).

[179] http://www.robetta.org/, (Accessed date: **July 16, 2021**).

[180] A. Roy, A. Kucukural, Y. Zhang, I-TASSER: a unified platform for automated protein structure and function prediction, Nat Protoc, 5 **(2010)** 725-738.

[181] A. Waterhouse, M. Bertoni, S. Bienert, G. Studer, G. Tauriello, R. Gumienny, F.T. Heer, T.A P. de Beer, C. Rempfer, L. Bordoli, R. Lepore, T. Schwede, SWISS-MODEL: homology modelling of protein structures and complexes, Nucleic Acids Research, 46 **(2018)** W296-W303.

[182] D.B. Kitchen, H. Decornez, J.R. Furr, J. Bajorath, Docking and scoring in virtual screening for drug discovery: methods and applications, Nature Reviews Drug Discovery, 3 **(2004)** 935-949.

[183] S. Shakil, M.A. Kamal, S. Tabrez, A.M. Abuzenadah, A.G.A. Chaudhary, G.A. Damanhouri, Molecular interaction of the antineoplastic drug, methotrexate with human brain acetylcholinesterase: A docking study, CNS and Neurological Disorders - Drug Targets, 11 **(2012)** 142-147.

[184] D. Kozakov, D.R. Hall, B. Xia, K.A. Porter, D. Padhorny, C. Yueh, D. Beglov, S. Vajda, The ClusPro web server for protein-protein docking, Nat Protoc, 12 **(2017)** 255-278.

[185] S.J. de Vries, M. van Dijk, A.M. Bonvin, The HADDOCK web server for data-driven biomolecular docking, Nat Protoc, 5 **(2010)** 883-897.

[186] M. Torchala, I.H. Moal, R.A. Chaleil, J. Fernandez-Recio, P.A. Bates, SwarmDock: a server for flexible protein-protein docking, Bioinformatics, 29 **(2013)** 807-809.

[187] D. Kim, S. Jang, J. Oh, S. Han, S. Park, P. Ghosh, D.K. Rhee, S. Lee, Molecular characterization of single-chain antibody variable fragments (scFv) specific to Pep27 from Streptococcus pneumoniae, Biochem Biophys Res Commun, 501 **(2018)** 718-723.

[188] E.R. Lindahl, Molecular Dynamics Simulations, in: A. Kukol (Ed.) Molecular Modeling of Proteins, Humana Press, Totowa, NJ, pp. 3-23, **2008.**

[189] M. Karplus, J. Kuriyan, Molecular dynamics and protein function, Proceedings of the National Academy of Sciences of the United States of America, 102 **(2005)** 6679.

[190] R. Kumari, R. Kumar, A. Lynn, g_mmpbsa—A GROMACS Tool for High-Throughput MM-PBSA Calculations, Journal of Chemical Information and Modeling, 54 **(2014)** 1951-1962.

[191] J.H. Lakey, E.M. Raggett, Measuring protein—protein interactions, Current Opinion in Structural Biology, 8 **(1998)** 119-123.

[192] B. Friguet, A.F. Chaffotte, L. Djavadi-Ohaniance, M.E. Goldberg, Measurements of the true affinity constant in solution of antigen-antibody complexes by enzyme-linked immunosorbent assay, J Immunol Methods, 77 **(1985)** 305-319.

[193] J.R. Livingstone, Antibody characterization by isothermal titration calorimetry, Nature, 384 **(1996)** 491-492.

[194] P.S. Daugherty, B.L. Iverson, G. Georgiou, Flow cytometric screening of cell-based libraries, J Immunol Methods, 243 **(2000)** 211-227.

[195] C. Hahnefeld, S. Drewianka, F.W. Herberg, Determination of Kinetic Data Using Surface Plasmon Resonance Biosensors, in: J. Decler, U. Reischl (Eds.) Molecular Diagnosis of Infectious Diseases, Humana Press, Totowa, NJ, pp. 299-320, **2004.**

[196] M. Alhajj, A. Farhana, Enzyme Linked Immunosorbent Assay, StatPearls, StatPearls Publishing Copyright © 2021, StatPearls Publishing LLC., Treasure Island (FL), **2021.**

[197] P. Martineau, Affinity Measurements by Competition ELISA, in: R. Kontermann, S. Dübel (Eds.) Antibody Engineering, Springer Berlin Heidelberg, Berlin, Heidelberg, pp. 657-665, **2010.**

[198] J.D. Beatty, B.G. Beatty, W.G. Vlahos, Measurement of monoclonal antibody affinity by non-competitive enzyme immunoassay, Journal of Immunological Methods, 100 **(1987)** 173-179.

[199] P. Tian, Y. Wang, H. Liu, Y. Yang, X. Wu, H. Wei, T. Chen, Preparation and Evaluation of the Fully Humanized Monoclonal Antibody GD-mAb Against Respiratory Syncytial Virus, Frontiers in Cellular and Infection Microbiology, 9 **(2019)**.

[200] R.P. Sparks, J.L. Jenkins, R. Fratti, Use of Surface Plasmon Resonance (SPR) to Determine Binding Affinities and Kinetic Parameters Between Components Important in Fusion Machinery, Methods Mol Biol, 1860 **(2019)** 199-210.

[201] R.B.M. Schasfoort, Chapter 1 Introduction to Surface Plasmon Resonance, Handbook of Surface Plasmon Resonance (2), The Royal Society of Chemistrypp. 1-26, **2017.**

[202] A.C. Fisher, C.H. Haitjema, C. Guarino, E. Celik, C.E. Endicott, C.A. Reading, J.H. Merritt, A.C. Ptak, S. Zhang, M.P. DeLisa, Production of secretory and extracellular N-linked glycoproteins in Escherichia coli, Appl Environ Microbiol, 77 **(2011)** 871-881.

[203] M. Nagae, A. Ikeda, M. Hane, S. Hanashima, K. Kitajima, C. Sato, Y. Yamaguchi, Crystal structure of anti-polysialic acid antibody single chain Fv fragment complexed with octasialic acid: insight into the binding preference for polysialic acid, J Biol Chem, 288 **(2013)** 33784-33796.

[204] J. Sambrook, Russell, D.W., Molecular Cloning: A Laboratory Manual, 3rd ed., Cold Spring Harbor, USA.**2001**.

[205] R.M. Horton, H.D. Hunt, S.N. Ho, J.K. Pullen, L.R. Pease, Engineering hybrid genes without the use of restriction enzymes: gene splicing by overlap extension, Gene, 77 **(1989)** 61-68.

[206] J. Andris-Widhopf, P. Steinberger, R. Fuller, C. Rader, C.F. Barbas, 3rd, Generation of human scFv antibody libraries: PCR amplification and assembly of light- and heavy-chain coding sequences, Cold Spring Harb Protoc, 2011 **(2011)**.

[207] http://biologylabs.utah.edu/jorgensen/wayned/ape/, (Accessed date: **July 16, 2021**).

[208] http://www.snapgene.com/products/snapgene_viewer/, (Accessed date: **July 16, 2021**).

[209] D. Riesenberg, V. Schulz, W.A. Knorre, H.D. Pohl, D. Korz, E.A. Sanders, A. Roß, W.D. Deckwer, High cell density cultivation of Escherichia coli at controlled specific growth rate, Journal of Biotechnology, 20 **(1991)** 17-27.

[210] C. Zhao, L. Wang, D.H. Li, J.J. Li, Y. Ge, T. Liang, Y. Zhu, R. Yu, High-cell-density fermentation of Escherichia coli for expression of a recombinant phenylalanine dehydrogenase mutant and its purification, J. Chem. Technol. Biotechnol., 96 **(2021)** 199-206.

[211] M.M. Bradford, A rapid and sensitive method for the quantitation of microgram quantities of protein utilizing the principle of protein-dye binding, Anal Biochem, 72 **(1976)** 248-254.

[212] U.K. Laemmli, Cleavage of structural proteins during the assembly of the head of bacteriophage T4, Nature, 227 **(1970)** 680-685.

[213] K. Salimi, D.D. Usta, İ. Koçer, E. Çelik, A. Tuncel, Highly selective magnetic affinity purification of histidine-tagged proteins by Ni2+ carrying monodisperse composite microspheres, RSC Advances, 7 **(2017)** 8718-8726.

[214] T. Mahmood, P.-C. Yang, Western blot: technique, theory, and trouble shooting, N Am J Med Sci, 4 **(2012)** 429-434.

[215] B. Voedisch, H. Thie, Size Exclusion Chromatography, in: R. Kontermann, S. Dübel (Eds.) Antibody Engineering, Springer Berlin Heidelberg, Berlin, Heidelberg, pp. 607-612, **2010.**

[216] V. La Verde, P. Dominici, A. Astegno, Determination of Hydrodynamic Radius of Proteins by Size Exclusion Chromatography, Bio-protocol, 7 **(2017)** e2230.

[217] https://www.cytivalifesciences.com/en/us/news-center/benefits-of-automated-protein-purification-10001, (Accessed date: **July 16, 2021**).

[218] G. Hussack, S. Raphael, M.J. Lowden, K.A. Henry, Isolation and characterization of camelid single-domain antibodies against HER2, BMC Research Notes, 11 **(2018)** 866.

[219] A. Sokolowska-Wedzina, G. Chodaczek, J. Chudzian, A. Borek, M. Zakrzewska, J. Otlewski, High-Affinity Internalizing Human scFv-Fc Antibody for Targeting FGFR1-Overexpressing Lung Cancer, Mol Cancer Res, 15 **(2017)** 1040-1050.

[220] E.M. Herold, C. John, B. Weber, S. Kremser, J. Eras, C. Berner, S. Deubler, M. Zacharias, J. Buchner, Determinants of the assembly and function of antibody variable domains, Scientific Reports, 7 **(2017)** 12276.

[221] A. Bujotzek, J. Dunbar, F. Lipsmeier, W. Schäfer, I. Antes, C.M. Deane, G. Georges, Prediction of VH–VL domain orientation for antibody variable domain modeling, Proteins: Structure, Function, and Bioinformatics, 83 **(2015)** 681-695.

[222] M. Klement, C. Liu, B.L. Loo, A.B. Choo, D.S. Ow, D.Y. Lee, Effect of linker flexibility and length on the functionality of a cytotoxic engineered antibody fragment, J Biotechnol, 199 **(2015)** 90-97.

[223] I. Kocer, E.C. Cox, M.P. DeLisa, E. Celik, Effects of variable domain orientation on anti-HER2 single-chain variable fragment antibody expressed in the Escherichia coli cytoplasm, Biotechnol. Prog., 37 **(2021)** 9.

[224] A. Wörn, A.A. Der Maur, D. Escher, A. Honegger, A. Barberis, A. Plückthun, Correlation between in vitro stability and in vivo performance of anti- GCN4 intrabodies as cytoplasmic inhibitors, Journal of Biological Chemistry, 275 **(2000)** 2795-2803.

[225] G.L. Rosano, E.A. Ceccarelli, Recombinant protein expression in Escherichia coli: advances and challenges, Front Microbiol, 5 **(2014)** 172.

[226] M. Fathi-Roudsari, A. Akhavian-Tehrani, N. Maghsoudi, Comparison of Three Escherichia coli Strains in Recombinant Production of Reteplase, Avicenna J Med Biotechnol, 8 **(2016)** 16-22.

[227] H. Safarpour, S.B. Banadkoki, Z. Keshavarzi, M.H. Morowvat, M. Soleimanpour, S. Pourmolaei, F.H. Shirazi, Expression analysis and ATR-FTIR characterization of the secondary structure of recombinant human TNF-α from Escherichia coli SHuffle® T7 Express and BL21 (DE3) cells, International Journal of Biological Macromolecules, 99 **(2017)** 173-178.

[228] E.C. Cox, D.N. Thornlow, M.A. Jones, J.L. Fuller, J.H. Merritt, M.J. Paszek, C.A. Alabi, M.P. DeLisa, Antibody-Mediated Endocytosis of Polysialic Acid Enables Intracellular Delivery and Cytotoxicity of a Glycan-Directed Antibody–Drug Conjugate, Cancer Research, 79 **(2019)** 1810.

[229] A. Vera, N. Gonzalez-Montalban, A. Aris, A. Villaverde, The conformational quality of insoluble recombinant proteins is enhanced at low growth temperatures, Biotechnol Bioeng, 96 **(2007)** 1101-1106.

[230] S.C. Napathorn, M. Kuroki, M. Kuroki, High expression of fusion proteins consisting of a single-chain variable fragment antibody against a tumor-associated antigen and interleukin-2 in Escherichia coli, Anticancer Res, 34 **(2014)** 3937-3946.

[231] T. Ojima-Kato, D. Hashimura, T. Kojima, S. Minabe, H. Nakano, In vitro generation of rabbit anti-Listeria monocytogenes monoclonal antibody using single cell based RT-PCR linked cell-free expression systems, Journal of immunological methods, 427 **(2015)** 58-65.

[232] M. Joachim, J.G. Schäfer, D. Gerlach, P. Czermak, High cell density cultivation of Δgor/ΔtrxB E. coli in a chemically defined minimal medium with an enhanced iron concentration, Process Biochemistry, 73 **(2018)** 1-5.

[233] V. Akbari, H. Mir Mohammad Sadeghi, A. Jafrian-Dehkordi, D. Abedi, C.P. Chou, Functional expression of a single-chain antibody fragment against human epidermal growth factor receptor 2 (HER2) in Escherichia coli, J Ind Microbiol Biotechnol, 41 **(2014)** 947-956.

[234] X. Cao, H. Yu, C. Chen, J. Wei, P. Wang, Expression and characterization of recombinant humanized anti-HER2 single-chain antibody in Pichia pastoris for targeted cancer therapy, Biotechnology letters, 37 **(2015)** 1347-1354.

[235] B.V. Ayyar, M.Z. Atassi, Development of humanized scFv antibody fragment(s) that targets and blocks specific HLA alleles linked to myasthenia gravis, Appl Microbiol Biotechnol, 101 **(2017)** 8165-8179.

[236] A. Schmiedl, J. Zimmermann, J.E. Scherberich, P. Fischer, S. Dübel, Recombinant variants of antibody 138H11 against human gamma-glutamyltransferase for targeting renal cell carcinoma, Human Antibodies, 15 **(2006)** 81-94.

[237] B.V. Ayyar, S. Hearty, R. O'Kennedy, Facile domain rearrangement abrogates expression recalcitrance in a rabbit scFv, Applied microbiology and biotechnology, 99 **(2015)** 2693-2703.

[238] A. Gaciarz, L.W. Ruddock, Complementarity determining regions and frameworks contribute to the disulfide bond independent folding of intrinsically stable scFv, PloS one, 12 **(2017)** e0189964.

[239] S. Yamauchi, Y. Kobashigawa, N. Fukuda, M. Teramoto, Y. Toyota, C. Liu, Y. Ikeguchi, T. Sato, Y. Sato, H. Kimura, T. Masuda, S. Ohtsuki, K. Noi, T. Ogura, H. Morioka, Cyclization of Single-Chain Fv Antibodies Markedly Suppressed Their Characteristic Aggregation Mediated by Inter-Chain VH-VL Interactions, Molecules, 24 **(2019)**.

[240] L. Heinrich, N. Tissot, D.J. Hartmann, R. Cohen, Comparison of the results obtained by ELISA and surface plasmon resonance for the determination of antibody affinity, J Immunol Methods, 352 **(2010)** 13-22.

[241] H. Khalili, S. Brocchini, P.T. Khaw, S.K. Filippov, Comparative thermodynamic analysis in solution of a next generation antibody mimetic to VEGF, RSC Advances, 8 **(2018)** 35787-35793.

[242] H. Khalili, A. Godwin, J.W. Choi, R. Lever, P.T. Khaw, S. Brocchini, Fab-PEG-Fab as a potential antibody mimetic, Bioconjug Chem, 24 **(2013)** 1870-1882.

[243] M. Mohammadi, F. Nejatollahi, A. Sakhteman, N. Zarei, Insilico analysis of three different tag polypeptides with dual roles in scFv antibodies, J Theor Biol, 402 **(2016)** 100-106.

[244] W. Tai, R. Mahato, K. Cheng, The role of HER2 in cancer therapy and targeted drug delivery, J Control Release, 146 **(2010)** 264-275.

[245] C.B.M. Platania, L. Di Paola, G.M. Leggio, G.L. Romano, F. Drago, S. Salomone, C. Bucolo, Molecular features of interaction between VEGFA and anti-angiogenic drugs used in retinal diseases: a computational approach, Frontiers in Pharmacology, 6 **(2015)**.

APPENDICES

Appendix 1: The DNA sequences of the V_L and V_H domains of the anti-HER2 scFv and linkers

V_L:

ATGGATATTCAAATGACCCAAAGCCCGTCTTCTTTAAGCGCGTCTGTCGGTGA
TCGCGTGACCATCACGTGTCGTGCGAGCCAAGATGTTAATACGGCGGTGGCC
TGGTATCAACAAAAACCGGGTAAAGCCCCGAAGCTGTTAATCTACAGCGCCA
GCTTTCTGTACTCTGGCGTCCCGAGCCGCTTTTCTGGCAGCCGCAGCGGTAC
GGACTTCACGCTGACCATTAGCAGCCTGCAGCCGGAGGATTTCGCCACCTAT
TATTGTCAGCAGCACTACACCACCCCGCCAACCTTTGGCCAGGGTACGAAAG
TGGAGATTAAACGCACG

V_H:

GAGGTTCAATTAGTGGAATCTGGCGGTGGTCTGGTGCAGCCAGGCGGTAGCT
TACGTCTGAGCTGTGCAGCGTCTGGCTTCAACATCAAAGATACCTACATTCAT
TGGGTTCGCCAAGCCCCAGGTAAAGGCCTGGAGTGGGTGGCCCGTATCTAT
CCAACCAATGGCTACACGCGTTATGCAGACTCTGTGAAAGGCCGCTTCACCA
TTAGCGCCGACACCTCTAAGAACACCGCATATTTACAGATGAACTCTTTACGC
GCAGAGGACACGGCGGTGTACTACTGCTCTCGTTGGGGCGGTGACGGTTTC
TACGCGATGGACTACTGGGGTCAGGGTACGCTGGTCACGGTCAGCTCT

L1: GGTGGAGGCGGTTCAGGCGGAGGTGGCAGCGGCGGTGGCGGATCG
L2: GGTGGAGGCGGTTCACGTATCATCATCCGAAGGATCCGACGAGGC
L3: GGTGGAGGCGTGCATTGGGATTTCCGTCAGTGGTGGCAGCCGTCC
L4: GGTGGAGGCGTGCGTTCCTGGGAAGAACAGGCGCGTGTGACCACC
L5: CGTATCATCATCCGAAGGATCCGACGA

Appendix 2: Protocols used with commercial kits

Extraction of Plasmid DNA

1. Grow cells overnight in appropriate media and appropriate antibiotics.
2. Pour overnight sample into 1.5 ml tube.
3. Spin sample down at 10,000 rpm for 1 min.
4. Repeat steps 2-3 until all of the sample has been spun down.
5. Resuspend pellet in 250 µl of P1 Buffer.
6. Add 250 µl of P2 Buffer.
7. Mix by inverting four to six times.
8. Add 350 µl of N3 Buffer.
9. Spin sample for 10 minutes at 13000 rpm.
10. Transfer supernatant to a column.
11. Spin column down at 13000 rpm for 1 min.
12. Discard supernatant, DNA is in pellet and add 500 µl of PB buffer.
13. Spin column down at 13000 rpm for 1 min.
14. Discard liquid from bottom column and add 750 µl of PE buffer.
15. Spin column down at 13000 rpm for 1 min.
16. Discard liquid from bottom column and spin the column at 13000 rpm for 1 min again for fully dry.
17. Take column out of flow through tube and put inside of 1.5 ml tube.
18. Add 50 µl of EB Buffer or sterile water.
19. Let the column sit for a minute.
20. Spin column down at 13000 rpm for 1 min to elute DNA.
21. Discard column, plasmid in now in tube.
22. Quantify with nanodrop.

PCR Purification of DNA

1. Add 5 volumes of Buffer PB to 1 volume of PCR sample and mix.
2. Add about 800 µl of this mixture to the column and centrifuge at 13000 rpm for 1 min.
3. Discard flow through and repeat step 2 until all of sample has passed through the column.
4. To wash, add 750 µl of Buffer PE and centrifuge at 13,000 rpm for 1 min.
5. Discard the flow through and centrifuge for an additional 1 min at 13000 rpm.
6. Place column into a clean 1.5 ml tube.
7. To elute DNA, add 50 µl of Buffer EB or H_2O to the center of the column.
8. Quantify with nanodrop.

DNA Extraction from Agarose Gels

1. To a gel-slide, add 900 µl QG buffer and melt at 65°C bath for 0.3-5 min.
2. Add 740 µl of mixture to column, spin 13000 rpm for 1 min, discard supernatant from tube.
3. Add rest of mixture to column, centrifuge for 13000 rpm for 1 min.
4. Add 500 µl QG buffer to wash column, spin 13000 rpm for 1 min, pour off supernatant.
5. Add 740 µl PE wash buffer to column, spin down, elute for 1min at 13000 rpm.
6. Spin down by itself to dry for 1 min at 13000 rpm.
7. Put column in to new tube.
8. To elute DNA, add 50 µl Buffer EB.
9. Quantify with nanodrop.

Calcium Chloride Transformation of Bacteria:

1. Subculture 60 µl from overnight cells into 6 mL of fresh medium.
2. Grow cells at any temp to an OD_{600} of 0.3-0.4.
3. Spin down at 3000g for 10 min.
4. Discard supernatant.

5. Resuspend pellet in 0.6 ml of sterile 100 mM $CaCl_2$.
6. Spin down at 3000g for 10 min.
7. Resuspend pellet in 0.3 ml of sterile 100 mM $CaCl_2$.
8. Aliquot 50 µl into a tube.
9. Add 2 ul of plasmid or 3ul ligation product.
10. Let sit on ice for 30 min.
11. Heat shock by placing in 42°C water bath for 90 sec.
12. Place on ice for 2 min.
13. Add 750 ul SOB medium.
14. Shake at 37°C for 45 min.
15. Spin down at room temp at 3000g for 1 min.
16. Plate on appropriate antibiotics.

Appendix 3: DNA Ladders

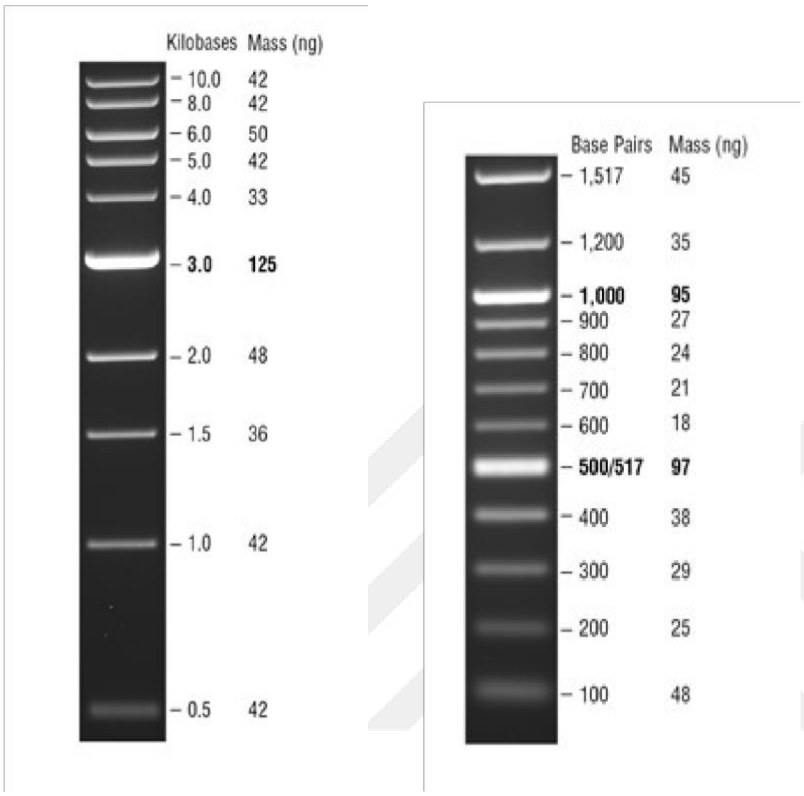

(a) (b)

Figure A3. (a) 1 kb DNA Ladder (b) 100 bp DNA ladder

Appendix 4: Composition of growth media used in experiments

LB

10 g/L tryptone

5 g/L yeast extract

10 g/L NaCl

TB

12 g/L tryptone

24 g/L yeast extract

9.4 g/L K_2HPO_4

2.2 g/L KH_2PO_4

Riesenberg Mineral Medium (RMM) [209]

13.3 g/L KH_2PO_4

4 g/L $(NH_4)_2HPO_4$

1.7 g/L Citric acid

1.2 g/L $MgSO_4.7H_2O$

10 ml/L Trace metal solution

4.5 mg/L Thiamin HCl

27.5 g/L Glucose

Trace Metal Solution: 0.84 g/L EDTA, 0.25 g/L $CoCl_2 \cdot 6H_2O$, 0.15 g/L $CuCl_2 \cdot 2H_2O$, 0.3 g/L H_3BO_3,1.5 g/L $MnCl_2.4H_2O$, 0.25 g/L $Na_2MoO_4.2H_2O$, 0.8 g/L $Zn(CH3COO)_2$. $2H_2O$ and 6 g/L Fe(III) citrate.

MR2 Medium [210]

6.75 g/L KH_2PO_4

2 g/L $(NH_4)_2HPO_4$

0.85 g/L Citric acid

0.7 g/L $MgSO_4.7H_2O$

2.5 ml/L Trace metal solution

20.0 g/L Glucose

Trace Metal Solution: 5 M HCl, 10 g/L $FeSO_4·7H_2O$, 2.25 g/L $ZnSO_4·7H_2O$, 1 g/L $CuSO_4·5H_2O$, 0.5 g/L $MnSO_4·5H_2O$, 0.23 g/L $Na_2B_4O_7·10H_2O$, 2 g/L $CaCl_2·2H_2O$ and 0.1 g/L $(NH_4)_6MO_7O_{24}$.

Appendix 5: Raw data for SPR calculations

Table A5.1. Maximum response units of anti-HER2 scFv-V_LV_H for each concentration

Concentration (nM)	RU-1	RU-2	Average
0.00	4.4	4.2	4.3
1.25	28.0	26.8	27.4
2.50	42.9	45.8	44.4
5.00	61.8	62.9	62.3
10.00	92.4	93.0	92.7
20.00	113.4	114.3	113.9
40.00	122.3	127.5	124.9
80.00	128.6	129.0	128.8

Table A5.2. Maximum response units of anti-HER2 scFv-V_HV_L for each concentration

Concentration (nM)	RU-1	RU-2	Average
0.00	3.6	4.9	4.3
0.625	14.8	15.0	14.9
1.25	25.8	25.6	25.7
2.50	41.0	43.4	42.2
5.00	63.1	64.4	63.8
10.00	83.5	85.6	84.6
20.00	101.2	105.5	103.3
40.00	109.7	109.5	109.6
80.00	116.8	122.0	119.4

Appendix 6: Raw data for K_d calculations with ELISA

Table A6.1. Absorbance measured at 450 nm in the ELISA

Concentration (nM)	**A1**	**A2**	**Aaverage**	**$[scFv]_f$**
50	0.052	0.053	0.053	0.00000
25	0.058	0.054	0.056	0.00088
12.5	0.057	0.072	0.064	0.00288
6.25	0.065	0.070	0.067	0.00369
3.125	0.079	0.082	0.081	0.00705
1.5625	0.139	0.136	0.137	0.02133
0.78125	0.360	0.371	0.366	0.07905
0.390625	0.799	0.799	0.799	0.18849
0.195313	1.073	1.121	1.097	0.26367
0.097656	1.330	1.303	1.316	0.31915
0.048828	1.362	1.436	1.399	0.34000
0	1.560	1.476	1.518	0.37014

Appendix 7: A sample determination of scFv concentration at half the maximum absorbance by an online curve fitting program

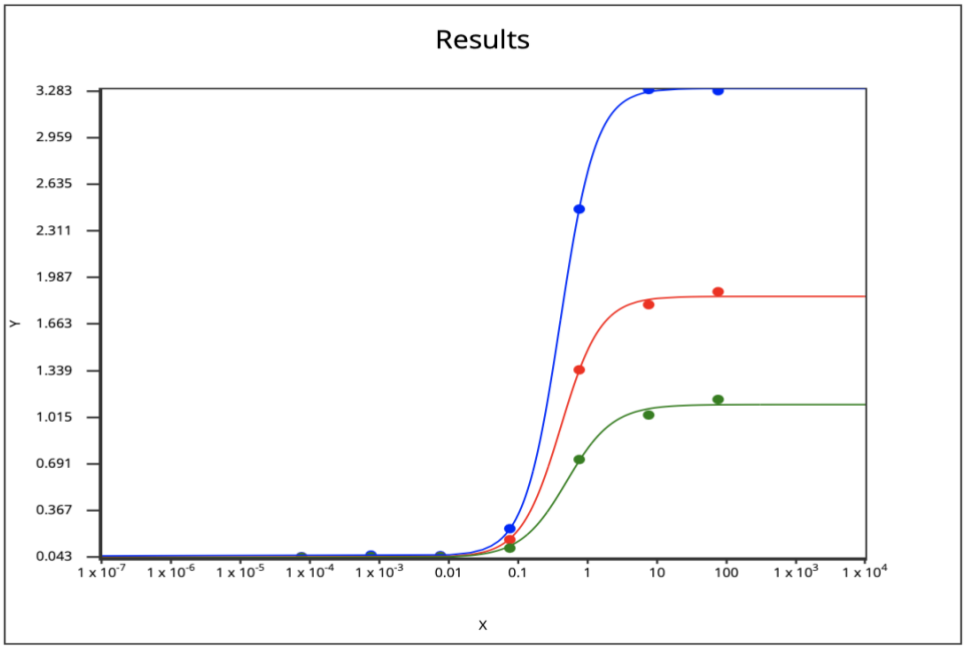

Parameter	Value
Inflection Point	0.3936
Equation	$Y = 0.0532 + \dfrac{3.2907 - 0.0532}{1 + \left(\dfrac{X}{0.3936}\right)^{-1.6727}}$
Equation Form	$Y = \text{Min} + \dfrac{\text{Max} - \text{Min}}{1 + \left(\dfrac{X}{\text{Inflection Point}}\right)^{\text{Hill coefficient}}}$

Inflection Point Regression Calculator [Data 1]

X	Y
0.386	1.645
Enter x to calculate y	Enter y to calculate x

*(https://www.aatbio.com)

Appendix 8: Publications related to the thesis

Koçer İ, Cox EC, DeLisa MP, Çelik E., Effects of variable domain orientation on anti-HER2 single chain variable fragment antibody expressed in the *Escherichia coli* cytoplasm. Biotechnology Progress, 37, p.9, 2021.

Appendix 9: Presentations related to the thesis

Koçer İ., Şahinbaş D., Cilasun S., Çelik E., 5-7/03/2020. Production of ScFv Antibody Fragments and Their Applications. International Biotechnology Congress (BIOTürkiye-2020), İstanbul, Türkiye, Abstract Book, P39 (oral presentation).